


Research Article

A New Geological Map of the Marginal Basins of Eastern Papua New Guinea: Implications for Crustal Accretion and Mineral Endowment at Arc–Continent Collisions

Philipp A. Brandl¹ ,¹ Mark D. Hannington,^{1,2} Anna Krätschell,¹ Sven Petersen,¹ Alan T. Baxter,² Margaret S. Stewart,^{2,3} Christopher Galley,^{2,4} Justin Emberley,² and Sylvia G. Sander^{1,5}

¹GEOMAR Helmholtz Centre for Ocean Research Kiel, Kiel, 24148, Germany

²Department of Earth and Environmental Sciences, University of Ottawa, Ottawa, Ontario, K1N 6N5, Canada

³Department of Earth and Environmental Sciences, Mount Royal University, Calgary, Alberta, T3E 6K6, Canada

⁴Department of Earth Sciences, Memorial University of Newfoundland, St. John's, Newfoundland and Labrador, A1B 3X5, Canada

⁵Faculty of Mathematics and Natural Sciences, Christian-Albrechts-Universität zu Kiel, Christian-Albrechts-Platz, Kiel, 24118, Germany

Correspondence should be addressed to Philipp A. Brandl; pbrandl@geomar.de

Received 17 April 2024; Published 15 November 2024

Academic Editor: Aleksandr S. Stepanov

Copyright © 2024. Philipp A. Brandl et al. Exclusive Licensee GeoScienceWorld. Distributed under a Creative Commons Attribution License (CC BY 4.0).

Accretion of island arc terranes is a fundamental process of crustal growth and the formation of new continents. Convergent margin tectonics, both compressional and extensional, in accretionary orogens also control the origin and distribution of their contained mineral resources, including many of the world's important Cu and Au deposits. However, the details of crustal growth and accretion are often lost because of deformation and selective preservation during subduction. The Melanesian Borderland, which includes the offshore regions of eastern Papua New Guinea and the Solomon Islands, contains several active and relict arc and backarc systems that have formed in response to more than 50 Ma of subduction and complex plate tectonic adjustments. The composite terrane is a region of some of the fastest growing crust on Earth and also spectacular mineral endowment, including three of the top ten porphyry Cu and epithermal Au deposits in the world. However, more than 80% of the belt is submerged, and so little is known about its geological evolution and makeup. Here, we present the first detailed geological map of the region in one map sheet, including the marginal deep ocean basins. The map identifies and groups the key lithostratigraphic formations and correlates associated tectonic events across the belt. The final compilation is presented at 1:1,000,000 scale, which is sufficient to allow quantitative analysis of crustal growth and accretion during ocean–continent collision throughout the region. The map shows the diversity of assemblages in accreting terranes that may eventually become part of a growing continent and highlights their complex formation and structural relationships. Because so much of that history has occurred offshore, the new map presents the first complete picture of the geology of the region in the critical period leading up to its eventual incorporation in the Australian continent.

1. INTRODUCTION

The record of crustal growth in ancient continental landmasses is often obscured or completely erased by the plate tectonic cycle. Numerous studies have investigated the processes of growth at island arcs as potential analogues of

the growth of continental crust [1, 2]. However, because island arcs are mostly submarine, the study of their subaerial parts provides only a partial view of the architecture of the original marginal basins that may survive closure and become part of the continent. The precursors of continental crust are also thought to be much thicker (>40

km) than modern oceanic island arcs. This raises questions about the processes involved in the growth of continental crust in marginal basins during and after collision. Most models of crustal growth of the continents have a very low resolution; in increments spanning hundreds of millions of years (e.g. [3]) and with little certainty about the processes operating at much shorter time scales. Evidence from modern subduction zones suggest that there may be significant additions in just a few millions of years, but very little is known about the volumes being added by different processes (e.g. [4, 5]).

The marginal basins of eastern Papua New Guinea and the Solomon Islands offer a unique opportunity to study crustal growth at a globally significant ocean–continent collision. The region formed in response to complex plate tectonic adjustments following the breakup of Australian Gondwana in the Mesozoic and subduction initiation at the Indo-Australian margin in the Eocene (~45 Ma; e.g. [6–8]). A second major reorganization occurred at 25 Ma, when the New Guinean passive margin collided in the west with the East Philippines–Halmahera–South Caroline arc system and when the collision between the Melanesian Arc and the Ontong Java Plateau (OJP) began in the east [6]. This collision initiated a subduction reversal and the simultaneous closure of some basins and opening of others (e.g. [6, 8]). The collision produced three marginal basins (Woodlark, Solomon, and Bismarck seas) surrounded by active volcanic arcs (West Bismarck, New Britain, Bougainville, and Solomons), forearc sedimentary basins (New Ireland Basin) and a number of smaller foreland basins (Sepik and Trobriand) bordered by major deformation zones of the Papuan Peninsula and the Manus-Kilinaulau Trench (Figure 1). Some of the basins include trapped ocean floor, some are products of backarc spreading, and some are formed by rifting arc crust and dispersal of the fragments. Since the most recent reorganization at ~5 Ma [6], the region resembles a large left-lateral deformation zone between the Indo-Australian and Pacific Plates and is the epicenter of some of the fastest growing crust on Earth. The interconnected basins are characterized by a distinctive geology, with crustal thickening and thinning due to multiple opposing subduction zones and microplate rotation. This article focuses on the formation-level geology of the different lithotectonic assemblages and the record of the pre-, syn-, and post-collisional crustal growth and destruction that will eventually lead to its amalgamation with Australia.

Importantly, we can compare the submerged portions of the region with the better-known geology of the adjacent terrestrial terranes. This presents a unique opportunity to study the formation of continental lithosphere where the original geological and geophysical evidence is still preserved and where ancestral structures and different crustal types (and their contained mineral deposits) are still present. Among other distinctive features of the region is the young age of its significant mineral endowment. It is one of the world's most productive copper provinces, hosting several of the youngest porphyry Cu deposits in the world such as Grasberg, Porgera, Frieda River, and Ok Tedi on

New Guinea and the Panguna deposit on Bougainville, as well as the world's largest alkalic-type epithermal Au deposit on the island of Lihir. In their review of the regional mineral deposits, Holm et al. [9] pointed out that in approximately 20 Ma, when the OJP eventually collides with the Australian continent, these deposits will become part of a major new metallogenic province along northeast Australia.

To study the region further, we have compiled a new 1:1,000,000 geological map of the active marginal basins at a resolution sufficient to allow quantitative analysis of crustal growth and accretion. The new map underpins a time-stratigraphic correlation of tectonic events and depositional events across the region, including coincident arc volcanism, rifting, and ore formation. The modern architecture provides clues to key questions such as the origin of structures that control magmatism and hydrothermal activity. Where and when these structures emerge are important questions for understanding the metallogeny of older orogenic belts; in particular, how the structures can switch from extensional to compressional, producing different mineral deposit types within the same broad orogeny. The kinematics that result in multiple mineralizing events in the same place in relatively brief episodes relative to the age of the craton are widely accepted as a major cause of regional mineral endowment.

2. REGIONAL GEOLOGY

The Western Melanesian Archipelago, including Papua New Guinea and its surroundings, is one of the most geodynamically complex regions globally (Figure 1), resulting from long-lived tectonic adjustments along the margins of the Pacific and Indo-Australian plates [4, 6, 7, 10–16]. Baldwin et al. [4] summarize the history of the region in a recent review: the geodynamic evolution of the margin involved microplate formation and rotation, lithospheric rupture to form backarc basins, arc–continent collision, orogenesis, ophiolite obduction, and exhumation of metamorphic rocks. The marginal basins are dominated by the long-lived Pacific Plate (>180 Ma old at this location) and the largest and thickest oceanic plateau on Earth (the 33 km thick OJP; [17]).

The “recent” geological history of Papua New Guinea started with the breakup of Gondwana and widespread rifting in the Permian and Early Triassic [7]. The northern margin of New Guinea developed as an active margin in the Triassic and subsequent rifting in the Jurassic generated promontories of extended continental crust separated by embayments of oceanic crust, including the former Owen Stanley oceanic basin [7, 16], remnants of which are preserved as ophiolites in the Papuan Ultramafic Belt (PUB; e.g. [18]). In the Late Jurassic and Early Cretaceous, New Guinea became a passive margin and thermal subsidence resulted in the widespread deposition of clastic sediments and carbonates [7, 16].

In the Late Cretaceous and Early Paleogene, renewed rifting and ultimately seafloor spreading led to opening of the Coral Sea and Tasman Sea basins (e.g. [13, 19]; Figure 2). Evidence for intraoceanic arc magmatism at

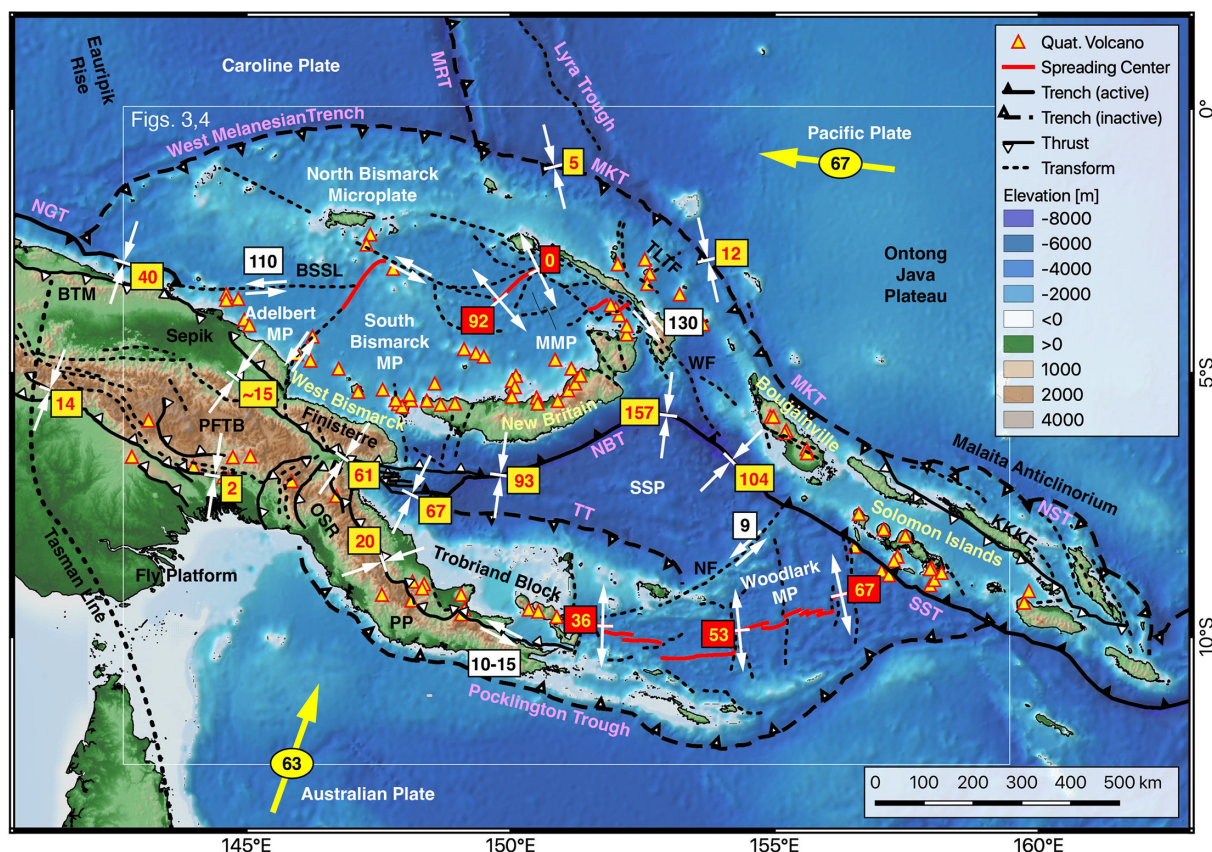


FIGURE 1: Morpho-tectonic map of eastern Papua New Guinea and the Solomon Islands. White labels denote tectonic plates, light yellow to active magmatic arcs, and light purple to troughs and trenches. Numbers denote relative plate motions and are given in mm a^{-1} for convergence (yellow box), divergence (red box), and transfer (white box). Abbreviations: BSSL – Bismarck Sea Seismic Lineation, BTM – Bewani–Torricelli Mountains, KKKF – Kia-Kaipito-Korigole Fault zone, MKT – Manus-Kilinauilau Trench, MMP – Manus Microplate, MP – Microplate, MRT – Mussau Ridge and Trench, NBT – New Britain Trench, NF – Nubara Fault, NGT – New Guinea Trench, NST – North Solomon Trench, OSR – Owen Stanley Ranges, PFTB – Papuan Fold and Thrust Belt, PP – Papuan Peninsula, SSP – Solomon Sea Plate, SST – South Solomon Trench, TLTF – Tabar-Lihir-Tanga-Feni island chain, TT – Trobriand Trough, WF – Weitin Fault.

that time is preserved in the Bewani–Torricelli and the Gauthier terranes (e.g. [10, 20]). A major plate reorganization occurred at ~ 45 Ma when the Indian and Australian plates started to move jointly and the rate of northward drift of the Australian Plate increased [6]. This event triggered convergence between the Indo-Australian and Pacific plates and resulted in the obduction of ophiolites and the initiation of the Melanesian Arc system [6, 7].

In the Late Eocene and Early Oligocene, the Solomon Sea Plate (28–39 Ma: [21]) and the Caroline Plate (25–36 Ma: [8]) formed by seafloor spreading in a backarc environment [6, 7]. Since the Late Oligocene, the accretion of arc terranes to New Guinea started in the west of the island and is continuing until today, forming the New Guinea Mobile Belt (e.g. [7]). Late Eocene to Oligocene plate construction occurred from 25 Ma, when New Britain was situated along the Manus-Kilinauilau Trench at the intersection of the South Caroline and Melanesian arcs [22].

In the Latest Oligocene and Early Miocene, the oceanic OJP entered the Manus-Kilinauilau subduction zone (e.g. [23, 24]). The OJP formed by flood basalt magmatism in the South Pacific in the Aptian (Early Cretaceous, ~ 120 Ma)

at $34\text{--}42^\circ\text{S}$ [25] and travelled $>7,000$ km before encountering the Manus-Kilinauilau Trench at ~ 25 Ma (e.g. [6]). Resistance to subduction and contemporaneous accretion of the South Caroline Arc (e.g. Sepik, Halmahera, and Gauthier terranes) to the New Guinea Mobile Belt triggered subduction reversal and terminated seafloor spreading in the Caroline and Solomon seas and the Rennell Trough [8, 21, 26]. A new subduction zone initiated along a suture that is now preserved as the Moresby-Aure-Pocklington Trough (northward-dipping slab: e.g. [9]). The associated arc magmatism formed the Maramuni Arc of New Guinea and the Papuan Peninsula that is now host to world-class mineral deposits ranging in age from 6 to 12 Ma [9, 27].

Collision of the New Guinea Mobile Belt (including the Maramuni Arc) with the Australian continental margin at ~ 12 Ma caused subduction to jump northward to the modern New Britain and South Solomon trenches (e.g. [9]; Figure 2). Subduction initiated in the east at 12 Ma and propagated westward from 8 to 9 Ma, resulting in renewed arc magmatism along the West Bismarck, New Britain, Bougainville, and Solomon arcs (e.g. [9, 12, 15, 28]). Several major structures oblique to the New Britain Trench localized the emplacement of mineralized Miocene

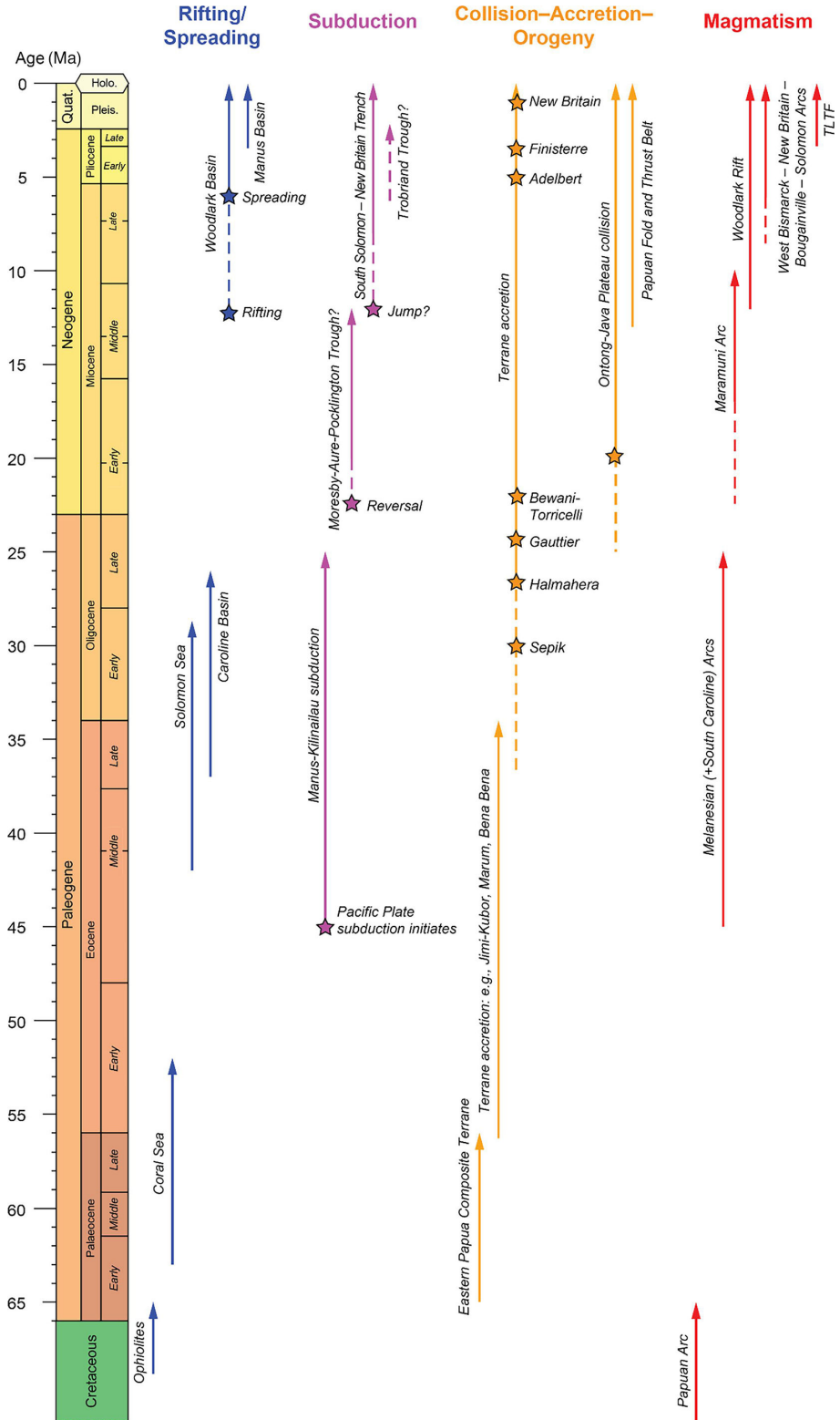


FIGURE 2: Overview of major tectonic events in eastern PNG. Stars denote the timing or start of a specific tectonic event, whereas lines depict the duration of a tectonic event (dashed if precise timing is less well constrained).

intrusions in New Britain, New Ireland, and Manus Island early in the history of the northward subduction [29]. At the same time, open ocean seafloor spreading initiated in the eastern Woodlark Basin and subsequently propagated

westward (e.g. [30, 31]). At about 4 Ma, a new phase of collision between the OJP and the Solomon Arc resulted in accretion and the formation of the Malaita accretionary prism [23]. Contemporaneous accretion of the Adelbert and

Finisterre terranes to the New Guinea Mobile Belt resulted in complex adjustments in the regional geodynamics and a breakout of microplates (e.g. [9, 32]). Accretion converted the former subduction zone west of the modern New Britain Trench to a suture zone and the style of magmatism along the associated West Bismarck Arc changed from subduction related to collisional [28]. The suture is now occupied by the Ramu-Markham Fault, a seismically active midcrustal detachment [33]. West of the Woodlark Basin, microplate rotation has caused exhumation of the world's youngest known (ultra-) high pressure rocks (2–8 Ma old: [4]). Here, the Australian–Woodlark plate boundary also transitions from divergence and seafloor spreading in the Woodlark Basin to convergence at the Papuan Peninsula. Deformation is dominated by extension near the tip of the Papuan Peninsula, oblique-sinistral slip faulting, and eventually convergence [4].

The Australian Plate is moving north-northeast relative to the Pacific Plate [34, 35], and the northern margin of the plate is actively deforming [36]. The boundary zone is dominated by westward convergence of the Pacific Plate at 70 mm a^{-1} [6, 37–42]. As a result, the OJP continues to converge on the North Solomon Trench at an oblique angle at a rate of 100 mm a^{-1} [43]. Within the last 5 Ma breakup of the Bismarck Plate into a northern and southern microplate created the space for the Manus backarc basin and associated spreading centers (e.g. [44]). Widespread crustal extension resulted in the westward propagation of the Woodlark Spreading Center, rifting in advance of the seafloor spreading and related volcanism that affected large areas of the eastern Papuan Peninsula and the Trobriand Platform and resulted in the exhumation of high-grade metamorphic rocks in the metamorphic core complexes of the D'Entrecasteaux Islands and the Dayman Dome (e.g. [14, 41, 45]). Ongoing oblique convergence between the Indo-Australian and Pacific plates are the cause of continuing subduction along the New Britain and San Cristobal trenches (e.g. [7]), large strike-slip faulting (e.g. the Weitin Fault moving $>130 \text{ mm a}^{-1}$: [46]), and active orogeny in the New Guinean highlands [4].

Recent volcanism initiated along the Tabar-Lihir-Tanga-Feni island chain in the New Ireland at 3.7 Ma [47]. The volcanoes lie offshore and about 400 km above the subducting Solomon Sea Plate. They comprise a series of uplifted Pliocene to Holocene stratovolcanoes that have a shoshonitic, K-enriched alkaline geochemical signature interpreted as reflecting partial melting of subduction-modified mantle material [32].

As a result of the complex and long geodynamic history, this region is uniquely endowed with some of the youngest and richest mineral deposits of their type (e.g. [9, 22, 32, 48]), including world-class porphyry, epithermal, and skarn deposits (Grasberg, Ladolam, Ertsberg, Panguna, and Porgera). Recently, potential or proven seafloor massive sulfide deposits in the Bismarck Sea [49] and the Woodlark Basin have also attracted attention (e.g. [50]). Extensive onshore and offshore exploration for hydrocarbons has focused on the shelf platforms and marine sedimentary basins (e.g. [51, 52]).

In this study, we present a seamless geological map of the region where the established onshore and offshore geology does not stop at the shoreline, as is often the case. The map underpins a quantitative analysis of the makeup of the complex orogenic belt and marginal seas of the arc-continent collision. The result is a modern tectonic and lithostratigraphic model that can be compared to other diverse metallogenic belts from the Western US to complex orogenic systems around the Pacific rim and elsewhere [22] including the Paleozoic fold belts of Eastern Australia, Mesozoic terrane accretion of the North American Cordillera, and Paleoproterozoic and Archean greenstone belts.

3. MATERIALS AND METHODS

3.1. Onshore–Offshore Geological Mapping

Remote sensing on land and offshore use different techniques for on-land and submerged areas, but the resulting terrain models and geophysical data sets can provide a seamless coverage at kilometer-scale resolution (full coverage) to tens of meters on land (e.g. by radar topography from air or space) and offshore (e.g. and by satellite altimetry and ship-based multibeam echosounder at sea). Geophysical data, such as magnetics and gravimetry, provide similar onshore–offshore coverage. These data have guided the creation of geological maps of the oceans at a range of scales and resolution. Advances in remote predictive mapping workflows and an increasing availability of offshore data have encouraged a new generation of seafloor geological maps at local (e.g. [32, 49, 53, 54]) and regional scale [55]. Here, we adapted the methods used by Stewart et al. [55] for the Lau Basin to the marginal seas of PNG and the Solomon Islands and prepared the first geological map compilation at a scale of 1:1,000,000 integrating onshore and offshore areas and correlating assemblage- and formation-level geological units across the entire region.

The marginal seas of PNG and the Solomon Islands have been targeted by numerous research cruises since the late 1960s and extensive geophysical and sampling data provided the basis for the recognition of geological formations and for the development of an internally consistent legend. The extrapolation of geological formations offshore was guided by ship-based multibeam, magnetics, gravity, seismic reflection and refraction, and geological sampling, including drilling. Where the coverage or resolution of these data types is low, mapping of geological formations was guided by remotely acquired geophysical data, such as satellite altimetry and the derived vertical gravity gradient (VGG) [56, 57], to recognize geological units and structures, and confidently extrapolate them. Publicly available geological maps were used to complement remote predictive mapping offshore (full list provided in Table S1 in the online Supplementary Material 1). Most of these maps include a higher level of detail than could be represented in what could be fused into

the regional scale map and therefore were integrated in a simplified version only. Cross-correlation between similar lithostratigraphic units of distinct areas also guided the regional-scale mapping process.

3.2. Data Sources

We compiled all publicly available geophysical data and multibeam bathymetry to guide remote predictive mapping of the offshore areas. Our digital terrain model integrates the global GMRT models (GMRT grid version 3.4 of July 2017: [58]) and ASTER GDEM data [59] for terrestrial areas.

A significant proportion of the map area is covered by ship-based multibeam echosounder data (Figure 3). A complete list of ship-based multibeam bathymetric data integrated into the digital terrain model used for remote predictive mapping is provided in Table S2 in the Supplementary Material 1. In total about 400,000 km² of the map area are covered by ship-based multibeam data, compared to 650,000 km² in a similar-sized area of the Lau Basin mapped by Stewart et al. [55]. Large areas of our map have been covered by geophysical studies conducted for the South Pacific Applied Geoscience Commission (SOPAC), including in the New Ireland [60], Manus, and Woodlark basins [61]. The most comprehensive collection exists for the Woodlark Basin and integrates >60 individual cruises by scientific and/or commercial entities in Australia, the USA, and Japan. These cruises collected extensive hydroacoustic data, including multibeam bathymetry, acoustic backscatter, and/or sidescan imagery plus other geophysical data such as magnetics, gravity, and/or subbottom profiling. The geophysical data from fifty-nine individual research cruises are synthesized in a data report of ODP leg 180 [62]. Additionally, we compiled hydroacoustic data from seven RV Sonne cruises: SO68 in the Manus Basin [63], SO94, SO133, and SO166 in the New Ireland and eastern Manus basins [64–66], SO203 in the Woodlark Basin [67], SO216 in the eastern Manus Basin [68], and SO252 off New Britain [69].

Several areas of the study, such as the Manus and Woodlark basins, are comprehensively covered with sidescan sonar images, ship-based multibeam bathymetry, gravity, and/or magnetic data (e.g. SeaMARC II and HAWAII-MR1 surveys: [62, 70]). Additionally, Nautilus Minerals Inc. carried out extensive commercial surveys in the eastern Manus Basin (including the Solwara vent sites) and the Woodlark Basin (e.g. with the Fugro Solstice in 2009). The French submersible “Nautile” was deployed during the MANAUTE cruise in 2000. Remotely operated vehicles (ROVs) and autonomous underwater vehicles (AUVs) that were used to survey and sample the active spreading centers, included ROV Jason-2 and AUV ABE both of Woods Hole Oceanographic Institution (Magellan-06 cruise), the German ROV Quest from Marum/University of Bremen (SO216), and GEOMAR’s AUV Abyss (SO203).

Satellite-derived, 1-minute resolution Bouguer gravity anomaly data were produced for this study to reveal

density variations in the subsurface. Bouguer anomaly data are produced from free-air gravity anomaly data but are filtered to remove any signal dependence from the seafloor’s bathymetry. The Bouguer anomaly dataset was derived from the Sandwell et al. [56] V31.1 gravity model, where the gravity signal due to the seawater–seafloor interface was removed from the model’s free-air anomaly data using its bathymetry surface model. The seawater–seafloor interface was modeled as a three-dimensional triangular irregular network, whose signal was calculated using Memorial University’s FOGO forward modeling program assuming a seawater density of 1.03 g cm⁻³ [71] and seafloor density of 2.89 g cm⁻³ [72].

These data were supplemented by continuous coverage of satellite-derived gravity gradient, following the method of Stewart et al. [55]. Recent advances in data quantity and quality and data reduction and modelling techniques of satellite-derived gravity (e.g. CryoSat-1 and Jason-1 satellite missions) allow geological features larger than ~5 km² (or taller than 1–2 km in the case of individual seamounts) to be mapped in detail. With these improvements, tectonic structures such as the fabric of the seafloor originating from seafloor spreading, with a typical wavelength of 2–12 km, can be mapped in deep ocean basins and under thick sediment cover [56, 73]. Our integration of the gravity anomaly and the VGG data and the related geological interpretation followed the method described in Stewart et al. [55].

Magnetic data were used at two different resolutions in this study. The global Earth magnetic anomaly grid at 2 arc-minute resolution version 3 (EMAG2v3: [74]) was used through the map area. Regional-scale studies within individual marginal basins were also compiled to identify magnetic anomalies (e.g. polarity reversals) resulting from seafloor spreading. These data were gathered for the Woodlark Basin [62, 75], the Manus Basin [44], Solomon Sea [8, 76], Caroline Basin [8, 77], and Coral Sea Basin [16, 19, 26]. Magnetic lineations and derivative age information guided the age dating of oceanic- and backarc-type lithostratigraphic assemblages. The integration of magnetic data into the mapping process is outlined in Stewart et al. [55].

The centroid moment tensor (CMT) data are from the open-source Global Centroid Moment Tensor project (www.globalcmt.org; accessed October 2018) [78, 79]. The database contains moment tensors mostly for earthquakes with $M_w > 5.0$ with calculated values for the strike, dip, and rake of the two focal planes and an estimate for the focal depth. The CMT was constructed using the ArcBeachball tool (v2.2) in ArcMap (v10.6). Earthquakes with depths of >30 km were excluded. The CMTs are classified based on the ternary diagram of Frohlich [80].

In the 1970s, numerous seismic surveys began to investigate the crustal structure and the complex tectonics of the Indonesian and Papua New Guinean region (e.g. [81]). However, most exploration activities focused on the lithostratigraphy and hydrocarbon potential of shelf platforms and marine sedimentary basins. The results of most of these surveys are proprietary and unpublished due

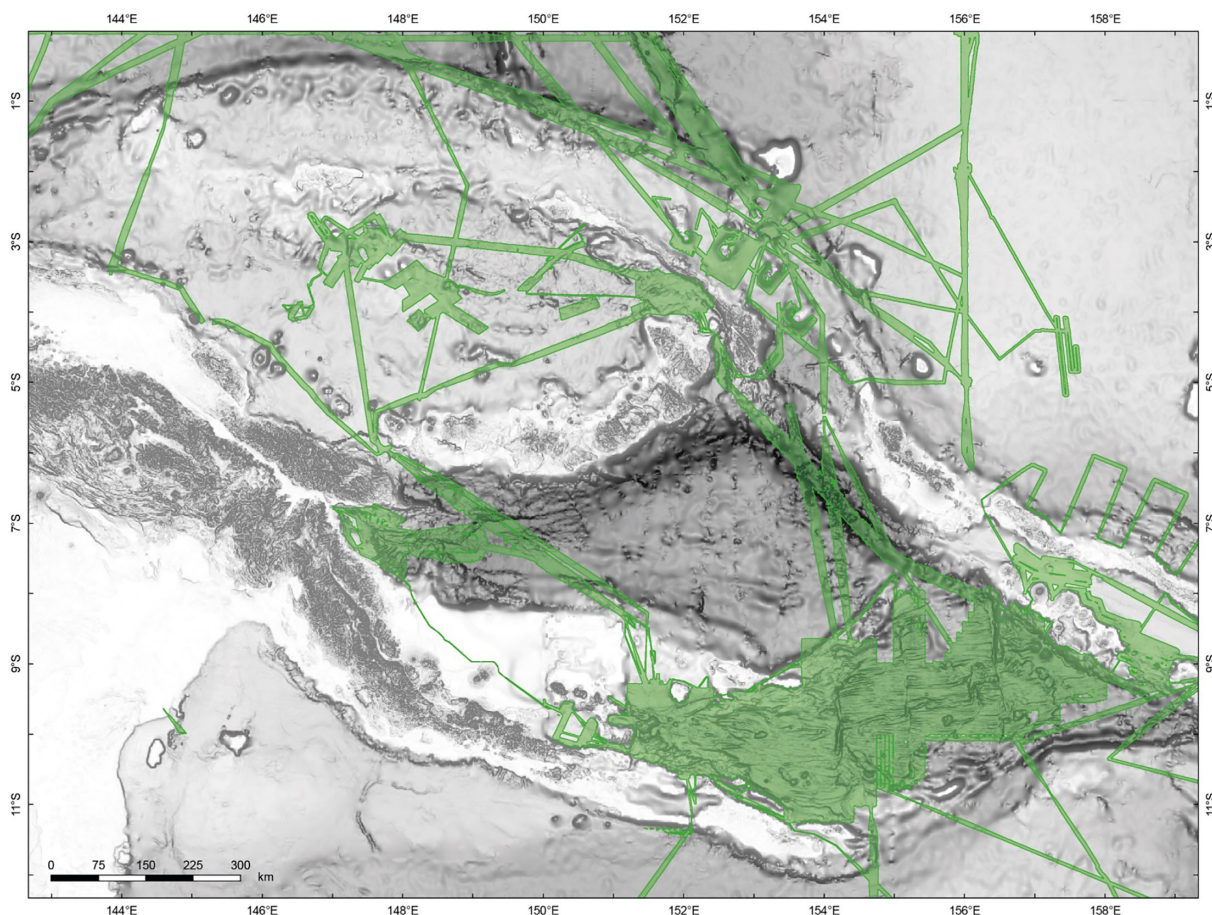


FIGURE 3: Relief map of the map area with green shaded areas representing areas with ship-based MBES data available for this study (list of individual cruises included in Table S2, the online Supplementary Material 1).

to commercial interests. However, significant seismic data are available for the New Ireland Basin. A compilation of seismic profiles for this area was presented by Brandl et al. [32] and included studies of Ravenne et al. [82], Exon & Tiffin [60], Exon & Marlow [83], and Gennerich [84] among others. Other well-imaged regions include the Gulf of Papua and the northwestern Coral Sea Basin [16, 85], the Trobriand Platform is reasonably well studied through seismic surveys (e.g. [86, 87]), the Solomon Islands (e.g. [24]) including the Central Solomon and Shortland basins (e.g. [88, 89]), and the Solomon Arc-OJP collision zone with the Malaita accretionary prism (e.g. [43, 90]). However, other areas remain poorly understood including some of the most complex structures such as the Mussau Trench and Lyra Basin [81, 91, 92] and the western Bismarck Sea with the New Guinea Basin and Willaumez Rise [81, 93].

In areas with the most data, critical ground truthing of geological formations is possible through direct seafloor observation and sampling. Extensive visual observations have been made by towed cameras, ROV, AUV and, less commonly, by human-occupied submersibles, in particular along the active spreading centers in the Manus and Woodlark basins. Sampling by dredging, coring, camera-guided grabs, and ROV also is an essential step in confirming the identification of different geological

formation. Extensive rock sampling was conducted using drilling, dredges, camera-guided grab systems, and sediment coring. Data for more than 800 rock samples have been compiled for this study and all sites are illustrated in Figure 4.

3.3. Methodology

Geological maps are created by gathering units with similar properties, age, and/or origin and sorting them into stratigraphic order in such a way that the geological history of an area can be reconstructed, including the sequence of depositional events, the composition of the substrate, and its deformation. The spatial relationships of different rock units, their stratigraphic order, and structural features are directly linked to processes of crustal accretion that can be recorded in the geological maps. Using spatial data and area–age relationships from geological maps, precise models of crustal growth can be derived. The geological map (Figure 5 and full-scale map sheet in the online Supplementary Material 1) presented in this article was constructed using the legends developed for the land areas and for other marginal basins that have been mapped offshore [32, 53–55]. The construction of the offshore legend was based on the standard lithostratigraphic classification scheme of the

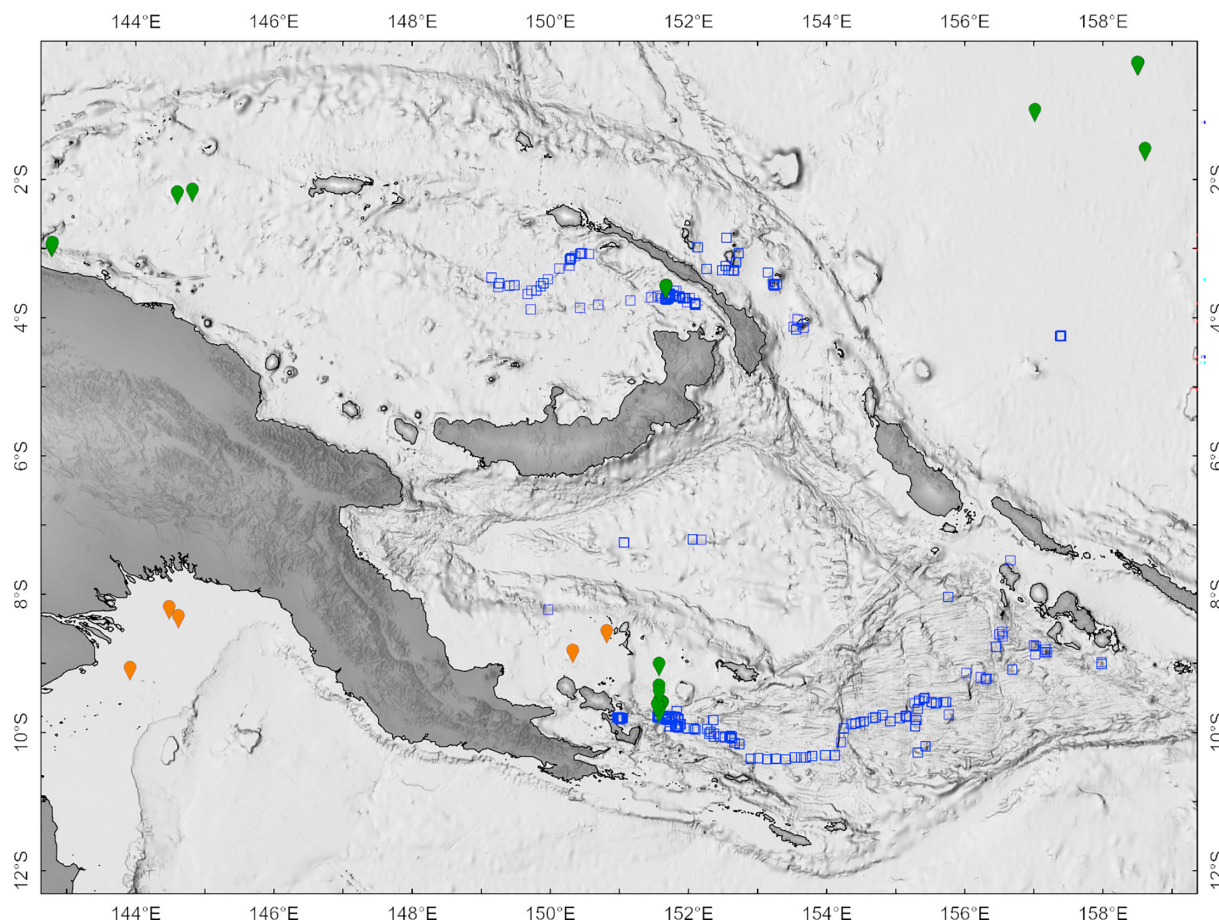


FIGURE 4: Map illustrating all locations of seafloor samples compiled for this study. Blue squares indicate samples collected from the seafloor by dredging, grabbing, or submersible, green markers indicate locations of DSDP-ODP-IODP drill sites, and orange markers additional drill sites.

International Commission on Stratigraphy [94, 95]. As on land, geological units were identified as formation types and grouped in increasing stratigraphic rank into assemblages. On this basis, individual units could be correlated across the entire map area. The onshore formations were created by integrating the formations of published geological maps (online Supplementary Table S1) and the merging of similar units through cross-correlating lithology and stratigraphy to match the lower level of detail mapped offshore.

The offshore formations were created by gathering different types of crust into mappable units with similar properties, age, and origin and sorting different types of crust into distinct packages, taking into consideration the crust type composition and thickness, where known, sequence of depositional events, and tectonic fabric and structure. Contacts between formations are based on inferred stratigraphic relationships, discontinuities in high-precision digital elevation models supported by acoustic backscatter, other geophysical data (magnetics and gravity), and direct seafloor observations where available. The geological legend used in this study is described below and is a combination of legends from

onshore geological maps and new conventions established for geological mapping offshore.

The remote predictive mapping approach of Stewart et al. [55] was used to extrapolate formations and structures from training areas, including on land, to areas with less data. In areas where offshore data are sparse, the extrapolation of geological formations requires knowledge from training areas where the particular formations can be discerned with a high degree of confidence through available data. In this study, we used training areas in the eastern Manus Basin [49, 96], the Tabar-Lihir-Tanga-Feni (TLTF) island chain [32], the Woodlark Basin [4, 30, 31], and extensive coastal geological maps.

The final digitized map consists of 697 polygons grouped into seventy different formations. Surface areas of the mapped formations were calculated using the “Calculate Geometry” tool of ArcGIS® in Lambert cylindrical equal-area projection (cf. [55]). At 1:1,000,000, the average spatial resolution of the mapped formations is 3,603 km² per polygon (excluding individual volcanoes). This resolution is at least twenty times higher than the offshore areas depicted in the current Geological Map of the World at 1:35,000,000 scale [97]. The average number of polygons

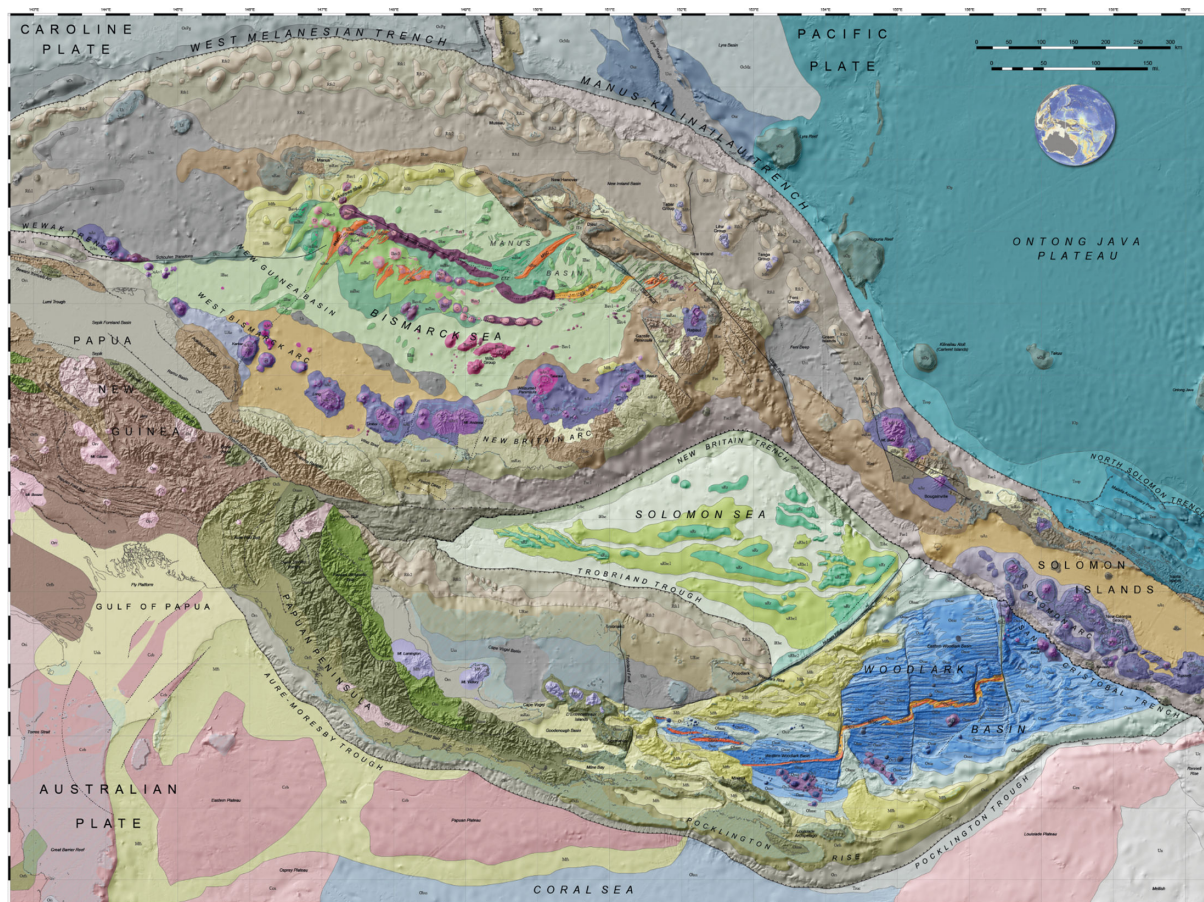


FIGURE 5: Reduced version of the 1:1,000,000-scale geological map of eastern Papua New Guinea and the Solomon Islands at the formation level. The corresponding legend with formation abbreviations is included in Table 1. The complete map sheet with marginal notes is provided at the original scale in the online Supplementary Material 1 (M1).

per formation type, ~10, provides a statistically meaningful basis for spatial analysis at the final scale, following the criteria of Peucker-Ehrenbrink & Miller [98, 99].

4. RESULTS AND DISCUSSION

4.1. A New Geological Map of the Marginal Basins of Eastern Papua New Guinea

We identify the marginal seas of Papua New Guinea and the Solomon Islands (MSPS) as a subprovince of the larger Northern Australian Margin (NAM). Twenty-two of the thirty-five assemblages identified in this study are assigned to the MSPS. The NAM comprises two major subdomains: one dominated by fragments of continental crust (southern New Guinea and Coral Sea region) and the other dominated by oceanic and backarc crust, island arc crust, and accreted terranes. The fragments of mainly extended continental crust in the first subdomain formed through rifting of the Australian margin in the Mesozoic, whereas the oceanic terranes of the other subdomain formed in a convergent setting mainly since the Eocene [7]. The NAM is distinct from regions to the north, where Cretaceous oceanic crust and large igneous province of

the OJP dominate, and the southwest, where the Australian craton prevails. It is, however, continuous to the west (island arcs of Southeast Asia; cf. [6]) and the east (north-west Indo-Australian margin [55]). The MSPS subprovince comprises eleven different assemblage types (Table 1). Each assemblage consists of one or more mapped formations that are grouped in terms of their origin, lithology, inferred age, and tectonic and structural regime (e.g. an arc or a backarc spreading center and all associated geological units), taking into account available geophysical and geological data, sampling, and seafloor observations in the map area. The formations within an assemblage are thus correlatable and similar to established lithostratigraphic units in many ancient volcanic terranes on land.

Details on the classification of mapped formations are described in [55]. Formations are the lowest rank in Table 1, defined by spatially and/or temporally distinct lithostratigraphic units. They are the basis for the 1:1,000,000 geological map shown in Figure 5 and reproduced as a full-scale map sheet included in the online Supplementary Material 1 (M1). Formations may be further subdivided into members where high-resolution ship-based multibeam and/or acoustic backscatter data are available. These include, for example, sedimentary units such as

TABLE 1: Organizational chart of mapped formations in the marginal seas of PNG and the Solomon Islands.

Subprovince	Assemblage type	Assemblage name(s)	Formation(s)
Australian Plate	Continental crust and orogenic belts	Carpenteria, Fly, Torres Strait	Orogenic folded basement rocks (Orfb), undivided volcanics (Orv), intrusive complex (Ori), pre- or syn-collisional sedimentary succession (Orfs)
	Other continental formations	Fly, Louisiade, Osprey, Papuan Plateau, Torres Strait	Continental crustal block (Ccb), extended continental crust (Ccx), continental crustal block (Ccb)
	Undivided shelf formations	Torres Strait, Fly	Undivided sedimentary succession of the shelf (Ush)
	Rifted margins	Osprey, Papuan Plateau	Rift sedimentary succession (Mfs)
	Trench	Louisiane, Coral Sea	Undivided crust in the trench (Truc)
	Oceanic crust and spreading centers	Coral Sea, Mellish	Ocean basin sedimentary succession (Obs)
	Other undivided crust	Mellish, Rennell	Unassigned extended crust (Ux), unassigned crust (Uc)
Bismarck Sea Basin	Rifted margins	Manus	Undivided crustal block (Mfb), undivided rifted margin crust (Mfc)
	Active arc	West Bismarck, Manus-Willaumez	Inner arc volcano (uAv2), upper intra-arc sedimentary succession (uAs), undivided arc crust (UAc)
	Arc-backarc transition	Manus-Willaumez	Lower transitional arc-backarc crust (lTc), ridge at the arc-backarc transition (uTr)
	Backarc volcanoes	Manus, Manus-Willaumez, West Bismarck	Conical volcano (Bav1), shield volcano (Bav2), dome volcano (Bav3), fissure volcano (Bav4), volcanic field (Bavf)
	Backarc rifts and spreading centers	Manus-Willaumez, New Britain	Axial backarc crust (uBac), axial backarc volcanic ridge (uBar), proximal backarc crust (mBac), proximal volcanic or tectonic ridge (mBar), backarc rift flank (mBaf), distal backarc crust (lBac), distal volcanic or tectonic ridge (lBar)
	Deformation zones	Manus-Willaumez	Leaky transform (Dz1), deformation zone (Dz2)
	Other undivided crust	West Bismarck	Unassigned ridge (Ur)
Caroline Plate	Trench	Caroline	Oceanic crust on the trench outer slope (Troc)
	Oceanic crust and spreading centers	Caroline	Undivided oceanic crust paleogene (OcPg)
	Other oceanic formations	Caroline	Intraplate seamount (uOs)
Melanesian Island Arc	Continental crust and orogenic belts	Solomon	High-grade metamorphic rocks (Orme)
	Rifted margins	New Britain, New Ireland Basin	Undivided crustal block (Mfb), rift volcano (Mfv)
	Active arc	New Britain, Solomon, West Bismarck	Arc front volcano (uAv1), inner-arc volcano (uAv2), upper arc crust (uAc), upper intra-arc sedimentary succession (uAs), lower arc crust (lAc)
	Relict arc	Adelbert-Finisterre, Manus, Manus-Willaumez, New Britain, New Guinea Basin, New Ireland Basin, Solomon, Trobriand	Upper relict arc crust (uRac), upper relict arc sedimentary succession (uRas), middle relict arc crust (mRac), middle relict arc sediment (mRas), lower relict arc crust (lRac), undivided relict arc crust (URac)
	Backarc volcanoes	New Britain, West Bismarck	Conical volcano (Bav1)
	Backarc rifts and spreading centers	West Bismarck	Distal backarc crust (lBac)

(Continued)

TABLE 1: Continued

Subprovince	Assemblage type	Assemblage name(s)	Formation(s)
	Active forearc	New Britain, New Britain Forearc, New Ireland Basin, San Cristobal Forearc	Forearc crust (Fac1), forearc crustal block (Fac2), forearc sedimentary succession (Fas)
	Relict forearc	Manus, New Guinea Basin, New Ireland Basin, Trobriand	Relict forearc crust (Rfc1), relict forearc crustal block (Rfc2), relict forearc sedimentary succession (Rfs1), tectonized relict forearc sedimentary succession (Rfs2)
	Trench	Malaita, New Guinea Basin, Rennell, San Cristobal Forearc	Accretionary complex (Trac), accretionary complex basement (Trab), accretionary complex ridge (Trar), backarc crust on the outer trench slope (Trbc), undivided crust in the trench (Truc)
	Deformation zones	Manus-Willaumez, New Ireland Basin, West Bismarck	Leaky transform (Dz1), deformation zone (Dz2)
	Other undivided crust	New Guinea Basin, Trobriand	Unassigned ridge (Ur), unassigned sedimentary succession (Uss)
New Guinea	Continental crust and orogenic belts	Bewani–Torricelli, Eastern Fold Belt, Fly, New Guinea Mobile Belt, Owen Stanley, Papuan Fold and Thrust Belt, Papuan Ultramafic Belt, Pocklington Rise, Sepik–Ramu, Trobriand, Woodlark	High-grade metamorphic rocks (Orme), ophiolite (Oro), postcollisional sedimentary succession (Ors), intrusive complex (Ori), pre- or syn-collisional sedimentary succession (Orfs), orogenic folded basement rocks (Orfb), undivided volcanics (Orv)
	Rifted margins	Owen Stanley, Pocklington Rise, Trobriand, Woodlark	Rift volcano (Mfv), rift sedimentary succession (Mfs)
	Relict arc	Bewani–Torricelli, New Guinea Mobile Belt, Trobriand	Middle relict arc sediment (mRas), lower relict arc crust (lRac)
	Active forearc	Bewani–Torricelli	Forearc crust (Fac1), forearc crustal block (Fac2)
Pacific Plate	Relict arc	Mussau	Undivided relict arc crust (URac)
	Active forearc	Mussau	Forearc crust (Fac1)
	trench	Mussau	Oceanic crust on the trench outer slope (Troc)
	Oceanic crust and spreading centers	Lyra, Mussau	Undivided oceanic crust mesozoic (OcMz)
	Other oceanic formations	Lyra, Mussau	Undivided oceanic ridge (Our)
	Other undivided crust	Lyra	Unassigned sedimentary succession (Uss)
Pacific Plate - Ontong Java Plateau	Trench	Ontong Java	Oceanic plateau crust in the trench (Trop)
	Other oceanic formations	Ontong Java	Oceanic plateau (IOP), oceanic plateau edifice (uOp)
Solomon Sea Basin	Relict backarc	Solomon Sea	Relict backarc ridge (uRr), upper relict backarc crust (uRbc1), lower relict backarc crust (lRbc)
	Trench	Solomon Sea	Backarc crust on the outer trench slope
Woodlark Basin	Rifted margins	Woodlark	Undivided crustal block (Mfb), undivided rifted margin crust (Mfc)
	Active arc	Woodlark	Upper arc crust (uAc), arc front volcano (uAv1)
	Relict backarc	Woodlark	Tectonized relict backarc crust (uRbc2)
	Active forearc	Woodlark	Forearc crustal block (Fac2)
	Trench	Woodlark	Undivided crust in the trench (Truc)
	Oceanic crust and spreading centers	Woodlark	Axial neovolcanic zone (Onvz), inner rift valley floor (Onvi), proximal oceanic crust (Onac), proximal oceanic volcanic ridge (Onar), distal oceanic crust (Ooac), distal oceanic volcanic ridge (Ooar), ocean basin margin crust (Obmc)

(Continued)

TABLE 1: Continued

Subprovince	Assemblage type	Assemblage name(s)	Formation(s)
	Oceanic volcanoes	Woodlark	Conical volcano (Ov1), shield volcano (Ov2), dome volcano (Ov3), volcanic field - oceanic (Ovf)
	Deformation zones	Woodlark	Deformation zone (Dz2)

carbonate sequences, talus fields (e.g. breccia deposits), or individual flow sequences which are mappable at 1:100,000 to 1:200,000 scale [55]. Member-level mapping has been done in the training areas, such as along the Tabar-Lihir-Tanga-Feni island chain [32], and was an important step in defining the formations in the 1:1,000,000 map. However, individual members are typically not mappable at the 1:1,000,000 scale and so are not included in Table 1 (cf. [55]).

4.2. Mapped Formations

By comparing mapped formations in well-studied training areas to similar features in areas where they have not been sampled or directly observed, we have been able to identify seventy formation types (Table 1). Sediments have been mapped where they accumulated to an assumed thickness of greater 500 m (including carbonate platforms, Cp). A thickness of 500 m or less (equivalent to ~5% of the width of the smallest polygons, excluding individual volcanoes, at 1:1,000,000 scale) have been ignored to emphasize bedrock lithology (cf. [55]). Quantitative data on the different formation types and individual formations are summarized in Tables 2 and 3.

4.2.1. Volcanoes

More than 1000 discrete volcanoes are identified in the volcano layer (Table 4). They include: (1) syn-collisional volcanoes (Orv), (2) rift volcanoes (Mfv), (3) active arc front (uAv1) and inner arc volcanoes (uAv2), (4) backarc volcanoes (Bav1-4), and (5) oceanic volcanoes (Ov1-3). The classification of these volcanoes and larger volcanic fields follows Stewart et al. [55] and thus only a brief summary is provided here. In the 1:1,000,000 compilation, only volcanoes >1 km in diameter were included. Volcanic fields (e.g. in the backarc: Bavf) typically occur only around the largest volcanoes or distinct clusters of individual volcanoes. Based on the morphology of the volcanic edifice, volcanoes were classified as conical, shield, dome, or fissure volcanoes. In the backarc, these volcano classes were labeled Bav1-4, whereas in oceanic assemblages only conical, shield, and dome volcanoes were identified (Ov1-3: Table 4). Arc volcanoes are either classified as arc front volcano (uAv1) when aligned along the volcanic front or as inner arc volcano (uAv2) when positioned behind the arc front. Syn-collisional volcano (Orv) refers to a volcanic edifice located within an active orogenic belt and is built on older metamorphosed basement rocks. A type example is Mt. Bosavi located on a major crustal lineament at the margin of the Papuan Fold and Thrust Belt (PFTB) (e.g. [100]). Rift volcanoes (Mfv) are genetically linked to

the extension and rifting of preexisting (arc) crust. One example is Mt. Lamington on the Papuan Peninsula that erupts medium- to high-K andesites as well as silica-undersaturated trachybasalts [101]. Several volcanic or tectonic features of undetermined origin were mapped as intra-plate seamounts (uOs) or undivided oceanic ridge (Our) based on their general shape (circular vs. elongated) and geological setting.

4.2.2. Carbonate Platform

The global reefs database of the United Nations Environment Program World Conservation Monitoring Centre (UNEP-WCMC) was used in its updated version 1.3 (released in 2015) to map warm-water coral reefs [102]. Areas of very high reef density and/or shallow marine areas (<125 m and thus within the photic zone) that were enclosed by barrier reefs were identified as recent carbonate platforms. Examples for large carbonate platforms and reef complexes in the map area include the Great Barrier Reef offshore Australia and the Trobriand Platform (e.g. [103]).

4.2.3. Continental Crust and Orogenic Belts

Continental crust and orogenic belts are subdivided into folded and metamorphosed basement rocks (Orfb) and high-grade metamorphic rocks (Orme) that are commonly exhumed by orogenic processes. Examples are the rocks of the Papuan Fold Belt (Orfb) and the Owen Stanley metamorphics (Orme) that include eclogites and blueschist-facies rocks, example in the core complexes of the D'Entrecasteaux Islands (e.g. [41, 104, 105]). Ophiolites (Oro) represent obducted fragments of oceanic and/or backarc crust (e.g. the PUB). The mapped continental crust and orogenic belts also include pre- and syn-collisional sedimentary rocks (Orfs) that differ from their post-collisional counterparts in intraorogenic and/or foreland basins (e.g. molasses-type: Ors) in that they are folded and/or metamorphosed. Thick (>500 m) successions of undivided sediments that belong to a continental shelf (Ush) are grouped into undivided shelf formations (e.g. sediments of the Fly Platform). Other continental formations include coherent but largely submerged blocks of undivided continental crust (Ccb; e.g. Eastern and Papuan plateaux) and isolated, submerged blocks of extended but otherwise undivided continental crust (Ccx; e.g. Osprey and Louisiade plateaux). Syn- or post-collisional intrusive complexes (Ori) are also common in these formations and may include exposed older intrusions.

TABLE 2: Quantitative data on formation types.

Formation type	Total area (km ²)	% of total area	# of polygons	Area/polygon (km ²)	Onshore area (km ²)	Offshore area (km ²)
Carbonate platforms	109,082	N/A	N/A	N/A	N/A	N/A
Continental crust and orogenic belts	318,614	12.7	32	9957	221,929	96,685
Other continental formations	211,163	8.4	9	23,463	90	211,073
Undivided shelf formations	53,300	2.1	1	53,300	16,769	36,530
Rifted margins	153,802	6.1	48	3204	210	153,593
Active arc	126,048	5.0	34	3707	21,678	104,370
Relict arc	228,284	9.1	63	3624	81,254	147,029
Arc-backarc transition	5130	0.2	47	109		5130
Backarc volcanoes/volcanic field (Bavf)	2319	0.1	13	178		2319
Backarc rifts and spreading centers	126,551	5.0	110	1150	108	126,443
Relict backarc	107,233	4.3	32	3351		107,233
Active forearc	94,022	3.7	16	5876	453	93,570
Relict forearc	201,438	8.0	67	3007	1663	199,775
Trench	100,732	4.0	23	4380	2254	98,477
Oceanic crust and spreading centers	231,346	9.2	142	1629		231,346
Oceanic volcanoes/volcanic field (Ovf)	2702	0.1	4	676		2702
Other oceanic formations	404,205	16.1	27	14,971	18	404,187
Deformation zones	11,838	0.5	14	846	4	11,833
Other undivided crust	132,437	5.3	15	8829	54	132,383
Volcanoes	37,608	N/A	1049	36	21,767	15,841
Seamounts and mounds	14,209	N/A	14	1015	All offshore	

4.2.4. Rifted Margin Crust

Rifted margins are formed by extensive periods of crustal extension in response to continental rifting and breakup. Mapped formations include rift sedimentary successions where sediments have accumulated in rift-related basins to a thickness greater 500 m (Mfs), undivided rifted margin crust that can be distinguished from adjacent formations (Mfc) and undivided crustal blocks (Mfb) that represent coherent blocks of rifted but otherwise undivided crust that can be distinguished from adjacent formations. Examples are the sediments accumulated in the Aure-Moresby Trough, the Milne Bay, or the Goodenough basins (all Mfs), the extended/rifted crust of the Woodlark and Pocklington rises (Mfc) and the individual ridges and crustal blocks contained in those (Mfb).

4.2.5. Active Arc Crust

Active arc crust is subdivided into upper and lower formations following the definition of Stewart et al. [55]. Upper arc crust is exposed in the West Bismarck, the New

Britain, and the Solomon arcs. Lower arc crust (lAc) is exposed, for example, in the New Georgia Group of the Solomon Arc. In addition, intraarc sedimentary successions (>500 m) were mapped (uAs; e.g. the Shortland and Russell basins of the Solomon Islands). Crust associated with an active arc but without any clear relationship to upper or lower arc crust is designated as undivided arc crust (UAc).

4.2.6. Relict Arc Crust

Relict arc crust is subdivided into upper (uRac), middle (mRac), and lower (lRac) formations. All three formed during an early phase of arc magmatism unrelated to the currently active arcs. Most of these formations are found along the Melanesian, Maramuni, and Trobriand arcs. Examples include the Kimbe volcanics of New Britain or the Bougainville group (both uRac: [106–108]), the Nengmutka volcanics of the Gazelle Peninsula (mRac; [108]), and the Jaulu (New Ireland) and Baining volcanics (New Britain: lRac; [108–110]). Relict arc crust that cannot be identified as upper, middle, or lower units is designated undivided relict-arc crust (URac). During

TABLE 3: Quantitative data on individual formations.

Formation	Legend abbreviation	Area (km ²)	# of polygons	Average polygon area (km ²)	Area on land (km ²)	Area offshore (km ²)
Volcanic field	Bavf	2319	13	178		2319
Continental crustal block	Ccb	142,198	7	20,314	90	142,108
Extended continental crust	Ccx	68,965	2	34,482		68,965
Leaky transform	Dz1	7112	4	1778	4	7108
Deformation zone	Dz2	4726	10	473		4726
Forearc crust	Fac1	72,853	5	14,571	28	72,824
Forearc crustal block	Fac2	16,066	9	1785	425	15,641
Forearc sedimentary succession	Fas	5104	2	2552		5104
Lower arc crust	lAc	10,032	1	10,032	0	10,032
Distal backarc crust	lBac	84,294	4	21,073	108	84,186
Distal volcanic or tectonic ridge	lBar	5529	47	118		5529
Oceanic plateau	lOp	371,913	1	371,913		371,913
Lower relict arc crust	lRac	109,416	16	6838	39,557	69,859
Lower relict backarc crust	lRbc	52,137	1	52,137		52,137
Lower transitional arc-backarc crust	lTc	4252	3	1417		4252
Proximal backarc crust	mBac	15,593	7	2228		15,593
Backarc rift flank	mBaf	14,361	3	4787		14,361
Proximal volcanic or tectonic ridge	mBar	1220	18	68		1220
Undivided crustal block	Mfb	29,790	37	805	171	29,619
Undivided rifted margin crust	Mfc	30,455	7	4351	3	30,452
Rift sedimentary succession	Mfs	93,557	4	23,389	36	93,522
Middle relict arc crust	mRac	2703	4	676	1747	956
Middle relict arc sediment	mRas	52,270	13	4021	29,139	23,131
Ocean basin margin crust	Obmc	32,927	6	5488		32,927
Ocean basin sedimentary succession	Obss	39,969	1	39,969		39,969
Undivided oceanic crust Mesozoic	OcMz	37,218	2	18,609		37,218
Undivided oceanic crust Paleogene	OcPg	32,576	1	32,576		32,576
Proximal oceanic crust	Onac	13,034	16	815		13,034
Proximal oceanic volcanic ridge	Onar	23,847	34	701		23,847
Inner rift valley floor	Onvi	1620	1	1620		1620
Axial neovolcanic zone	Onvz	1765	12	147		1765
Distal oceanic crust	Ooac	25,704	7	3672		25,704

(Continued)

TABLE 3: Continued

Formation	Legend abbreviation	Area (km ²)	# of polygons	Average polygon area (km ²)	Area on land (km ²)	Area offshore (km ²)
Distal oceanic volcanic ridge	Ooar	22,687	62	366		22,687
Orogenic folded basement rocks	Orfb	78,727	3	26,242	76,440	2286
Pre- or syn-collisional sedimentary succession	Orfs	74,320	3	24,773	32,731	41,589
Intrusive complex	Ori	16,328	9	1814	13,021	3307
High-grade metamorphic rocks	Orme	47,929	8	5991	40,316	7612
Ophiolite	Oro	20,354	4	5089	16,542	3812
Postcollisional sedimentary succession	Ors	80,957	5	16,191	42,879	38,078
Undivided oceanic ridge	Our	18,084	12	1507		18,084
Volcanic field - oceanic	Ovf	2702	4	676		2702
Relict forearc crust	Rfc1	49,532	3	16,511		49,532
Relict forearc crustal block	Rfc2	61,261	60	1021	1663	59,598
Relict forearc sedimentary succession	Rfs1	69,111	3	23,037		69,111
Tectonized relict forearc sedimentary succession	Rfs2	21,534	1	21,534		21,534
Accretionary complex	Trac	11,196	2	5598		11,196
Accretionary complex ridge	Trar	14,060	11	1278	2254	11,806
Backarc crust on the outer trench slope	Trbc	16,191	2	8096		16,191
Oceanic crust on the trench outer slope	Troc	22,021	2	11,011		22,021
Oceanic plateau crust in the trench	Trop	24,586	1	24,586		24,586
Undivided crust in the trench	Truc	12,677	5	2535		12,677
Upper arc crust	uAc	57,351	30	1912	21,606	35,744
Undivided arc crust	UAc	3547	1	3547		3547
Upper intra-arc sedimentary succession	uAs	55,119	2	27,559	72	55,047
Axial backarc crust	uBac	1232	4	308		1232
Axial backarc volcanic ridge	uBar	4323	27	160		4323
Unassigned crust	Uc	5602	1	5602		5602
Oceanic plateau edifice	uOp	12,195	13	938	18	12,177
Intraplate seamount	uOs	2013	1	2013		2013
Upper relict arc crust	uRac	19,502	19	1026	4672	14,830
Undivided relict arc crust	URac	36,273	2	18,136	1305	34,968
Upper relict arc sedimentary succession	uRas	8121	9	902	4835	3286

(Continued)

TABLE 3: Continued

Formation	Legend abbreviation	Area (km ²)	# of polygons	Average polygon area (km ²)	Area on land (km ²)	Area offshore (km ²)
Upper relict backarc crust	uRbc1	36,040	5	7208		36,040
Tectonized relict backarc crust	uRbc2	2025	1	2025		2025
Relict backarc ridge	uRr	17,031	25	681		17,031
Unassigned ridge	Ur	11,323	9	1258	19	11,303
Undivided sedimentary succession of the shelf	Ush	53,300	1	53,300	16,769	36,530
Unassigned sedimentary succession	Uss	93,281	4	23,320	34	93,246
Ridge at the arc–backarc transition	uTr	879	44	20		879
Unassigned extended crust	Ux	22,232	1	22,232		22,232
Totals		2,511,165	697		346,485	2,164,680

phases of magmatic quiescence and/or tectonic activity, volcanoclastic sediments and/or carbonates were deposited that can be grouped into upper (uRas), middle (mRas), and (lower) relict arc sedimentary successions (lRas). The Yalam and Lelet limestones of New Britain and New Ireland [108–110] are type examples of middle relict arc sedimentary successions (mRas).

4.2.7. Transitional Arc–Backarc Crust

Crust in the arc–backarc transition is formed by extension of arc crust and concomitant intrusion by magmas formed by decompression melting in a backarc environment. This formation includes volcanic or tectonic ridges in a zone of arc rifting (uTr) and extended arc or backarc crust that surrounds these ridges (lTc). The geological processes generating this specific type of crust have been intensely studied in the Havre Trough north of New Zealand (e.g. [111]). Both, the Havre Trough and parts of the Manus Basin are places where backarc crust is not continuous throughout the entire basin (cf. [49, 111]), and transitional crust occurs in the areas between rifting of the arc and active spreading.

4.2.8. Backarc Rift and Spreading Center Crust

The different backarc crust formations are assigned according to their position relative to an active backarc spreading center, following the approach of Stewart et al. [55]. The crust is divided into axial, proximal, and distal backarc crust (uBac, mBac, and lBac) and crust formed on the flank of the rift valley (mBaf). The upper and middle (axial and proximal) backarc crust is often free of sediment; lower (distal) backarc crust is often covered by volcanoclastic material. The crust at active backarc spreading centers is characterized by discrete or coalesced ridge-parallel volcanic and tectonic features. Following Stewart et al. [55], these are designated axial (or “upper,” uBar) when

located within the neovolcanic zone, proximal (or “middle,” mBar) when outside the neovolcanic zone but within the rift valley, and distal (or “lower,” lBar) when located outside the rift valley. The more distal formations have a characteristic off-axis fabric similar to that of mid-ocean ridges (cf. [112]).

4.2.9. Relict Backarc Crust

Relict backarc crust includes crust that originated from a backarc spreading center but is now located outside an identifiable region of active backarc formation [55]. Relict backarc crust is subdivided into upper (uRbc) and lower (lRbc) formations where the stratigraphic relationships can be determined (e.g. upper crust formed on lower crust exposed by rifting). Where undeformed, the upper relict backarc crust is designated uRbc1; tectonized upper relict backarc crust is designated uRbc2. Relict ridges (uRr) have been mapped as separate formations even though their origin is uncertain [55].

4.2.10. Active Forearc Crust

Large areas between the trench and the active arc are designated “active” forearc crust, including crust and sediments of the forearc slope (Fac1) and uplifted, commonly tectonized blocks (Fac2). Sediments that accumulated to more than 500 m thickness in a forearc basin of an active subduction zone are mapped as a distinct formation (Fas).

4.2.11. Relict Forearc Crust

The relict forearc crust includes mostly undivided formations of an inactive forearc. They include crust exposed on the relict forearc slope (Rfc1) and uplifted, commonly tectonized blocks of relict forearc crust (Rfc2). This type of crust can be found along the inactive West Melanesian Trench and the Trobriand Trough, and along the Tabar-Lihir-Tanga-Feni island chain. Sedimentary successions in subbasins of the relict forearc are divided into undeformed

TABLE 4: Quantitative data on volcano types.

Formation	Legend abbreviation	Area (km ²)	N
Conical (oceanic) volcano	Ov1	806.5	36
Shield (oceanic) volcano	Ov2	93.9	2
Dome (oceanic) volcano	Ov3	1043.6	299
Arc front volcano	uAv1	12778.3	79
Inner arc volcano	uAv2	1694.1	10
Conical (backarc) volcano	Bav1	1000.3	78
Shield (backarc) volcano	Bav2	2307.9	5
Dome (backarc) volcano	Bav3	3420.0	421
Fissure (backarc) volcano	Bav4	617.8	85
Rift volcano	Mfv	6435.9	20
Undivided volcanics	Orv	7409.2	14
	SUM	37607.5	1049

sediments (Rfs1) and those that have been strongly disturbed by tectonic processes (Rfs2). The New Ireland Basin is a type example of a relict forearc sedimentary succession.

4.2.12. Trench Crust

Different formations in the active or relict trenches are subdivided into accretionary complexes on the inner slope wall (Tra) and nonaccretionary crust on the outer slope, which can include deformed relict backarc (Trbc), oceanic (Troc), oceanic plateau (Trop), and undivided (Truc) crust. Examples are the Solomon Sea Plate crust (Trbc) in the New Britain Trench, Caroline Plate crust (Troc) in the West Melanesian Trench, OJP crust (Trop) in the Manus-Kilinau Trench, and the undivided crust (Truc) in the inactive Pocklington Trough. Accretionary complexes are further subdivided into the accretionary wedge (Trac) that may include sediments (>500 m), obducted crust, and/or volcanic features of the subducting plate and into accretionary complex ridges (Trar) that represent tectonized (uplifted) portions of the accretionary wedge. Both formations can be found in the Malaita accretionary prism of the Solomon Islands.

4.2.13. Oceanic Crust and Spreading Centers

The marginal seas of Papua New Guinea and the Solomon Islands encompass large areas of oceanic crust and spreading centers. Mapped formation in the young oceanic Woodlark Basin includes the axial volcanic zone that marks the active spreading center (Onvz) and the inner rift valley floor (Onvi) that includes crust in the axial or median rift valley bound by active, inward dipping faults. Elongate volcanic edifices or coalesced ridges adjacent to an active spreading center (and younger than magnetic chron 2A) have been designated proximal oceanic volcanic ridges (Onar) and ordinary oceanic crust of the same age as proximal oceanic crust (Onac). Similar crust that is older than magnetic chron 2A is designated distal oceanic crust (Ooar and Ooac, respectively). Mixed crust at the margin of an oceanic basin adjacent to and/or including rifted

continental, arc-related, or oceanic plateau crust has been designated “ocean basin margin crust” (Obmc). Sediments that accumulated on oceanic crust to >500 m thickness (e.g. in the Coral Sea Basin) are mapped as an ocean basin sedimentary succession (Obss). Other undivided oceanic crust (Oc) has been subdivided according to its age of formation (Mz: Mesozoic, Pg: Paleogene).

4.2.14. Other Oceanic Formations

Other oceanic formations include seamounts, ridges, and plateaux either of intraplate or unknown origin. Intraplate seamounts on oceanic crust (uOs) can be volcanic or tectonic edifices of undetermined origin. Elongated volcanic or tectonic edifices are designated undivided oceanic ridges (Our). Flat-topped volcanic edifices that are clearly built on oceanic plateau crust are termed oceanic plateau edifice (uOp), and the underlying oceanic plateau crust and rise are designated oceanic plateau (IOp). These formations can be found at the margins or on the Cretaceous OJP.

4.2.15. Deformation Zones

Several major deformation zones are mapped in the Bismarck Sea (e.g. Schouten and Willaumez transforms: e.g. [44, 70, 113]) and the Woodlark Basin area (Trobriand and Nubara faults: e.g. [45, 114]). We identified these features as geological formations because they include significant amounts of deformed crust of uncertain origin. In some cases, lava flows have erupted through the crust, for example, along a leaky transform (Dz1) such as the Willaumez Transform. Elsewhere, they are interpreted as simple high-strain zones along one or more large-scale transcurrent faults (Dz2). Examples include the crust within the Djaul Fault in the eastern Manus Basin, the Schouten Transform in the New Guinea Basin, and the Nubara Fault between the Solomon Sea and the Woodlark Basin.

4.2.16. Other Undivided Crust

Some obvious morphological features or sedimentary successions that could not be assigned to a particular origin

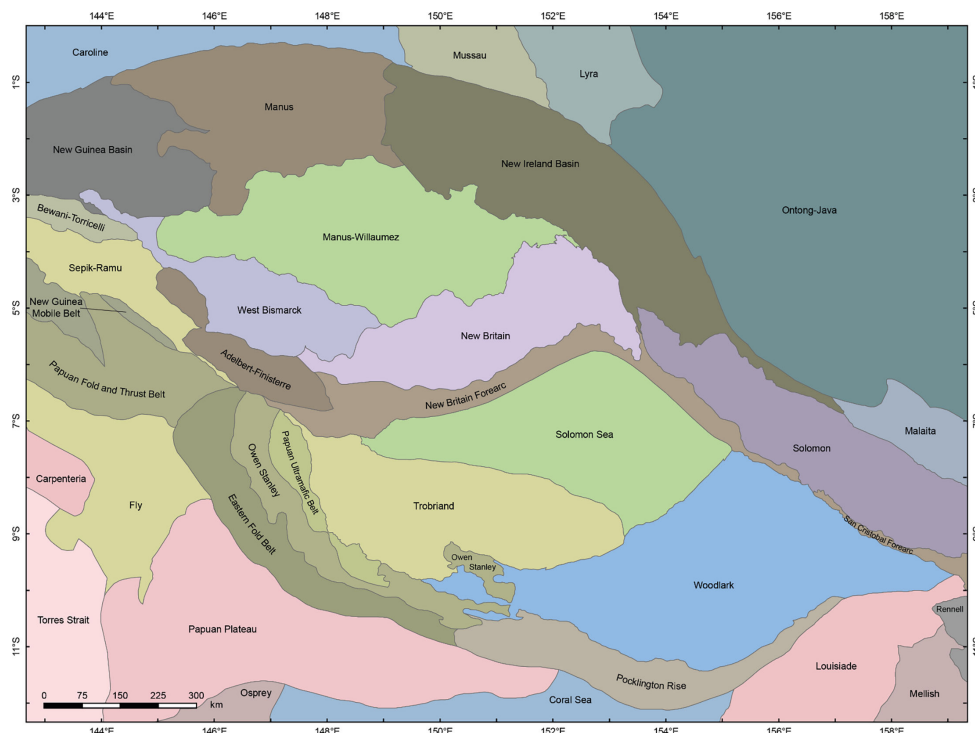


FIGURE 6: Assemblage map and assigned assemblage names of the marginal seas of PNG and the Solomon Islands.

have been grouped into other undivided crust. For elongate volcanic or tectonic features of undetermined origin, we use the term “unassigned ridge” (Ur; e.g. some ridges in the western New Guinea Basin). For more general crust that can be distinguished from adjacent formations but for which the origin is uncertain, we use the general term “unassigned crust” (Uc; e.g. the Rennell Rise described by Seton et al. [26]). If the crust has been extended, the term “unassigned extended crust” has been used (Ux); an example of this type of formation is the crust embedded between the Louisiade Plateau and the Rennell Rise. Sediments that accumulated in a basin of uncertain origin have been mapped as “unassigned sedimentary succession” (Uss; e.g. the western New Guinea Basin).

4.3. Assemblages, Assemblage Types, and Bounding Structures

Following standard lithostratigraphic classification, formations can be grouped into lithotectonic assemblages (Figure 6) using the criteria outlined in [55]. Each assemblage consists of one or more geological formations that are grouped in terms of their origin, lithology, inferred age, and tectonic and structural regime (e.g. an arc or a backarc spreading center and all associated geological units). The lithologies belonging to different assemblages may be very similar or even identical. However, the assemblages are almost always in fault or depositional contact with each other and, in some cases, may be separated by major unconformities. The major bounding structures of the assemblages are highlighted in Figure 4, and their relationship to the regional seismicity, VGG,

Bouguer gravity anomalies, and magnetic anomalies is shown in Figure 7. Assigned names for the different offshore assemblages are based on major tectonic or geographic features they contain. The assemblages (or terranes) on land have been variably interpreted as allochthonous fragments of lithosphere that were successively accreted onto the continental margin.

We have grouped the mapped formations into eleven different assemblage types: (1) oceanic, (2) intraplate, (3) active arc, (4) backarc rifts and spreading centers, (5) relict backarc basin, (6) relict arc, (7) forearc, (8) relict forearc, (9) orogenic and ophiolitic, (10) continental, shelf, and platform, and (11) undivided crust. The locations of the thirty-five assemblages and the assigned names are shown in Figure 6 and described in detail below.

4.3.1. Oceanic Assemblages

The oldest oceanic assemblage in the region is the Coral Sea. It includes the lower slopes of the rifted margins and the oceanic crust in the Coral Sea Basin. The basin formed by rifting in the Late Cretaceous [16] followed by seafloor spreading in the Paleocene and Early Eocene (63, 52 Ma: [19]). It comprises the two formations: ocean basin sedimentary succession (Obs) and undivided crust in the trench (Truc; Figure 5). The ~10 km thick oceanic igneous crust is covered by Eocene to Holocene sediments. The sedimentary sequence consists of detrital clay and deep marine biogenic and pelagic sediments and reaches 1 km thickness in the central basin and up to 2 km thickness at its margins (see [85]). The location of the relict Coral Sea spreading center can be mapped in VGG [73].

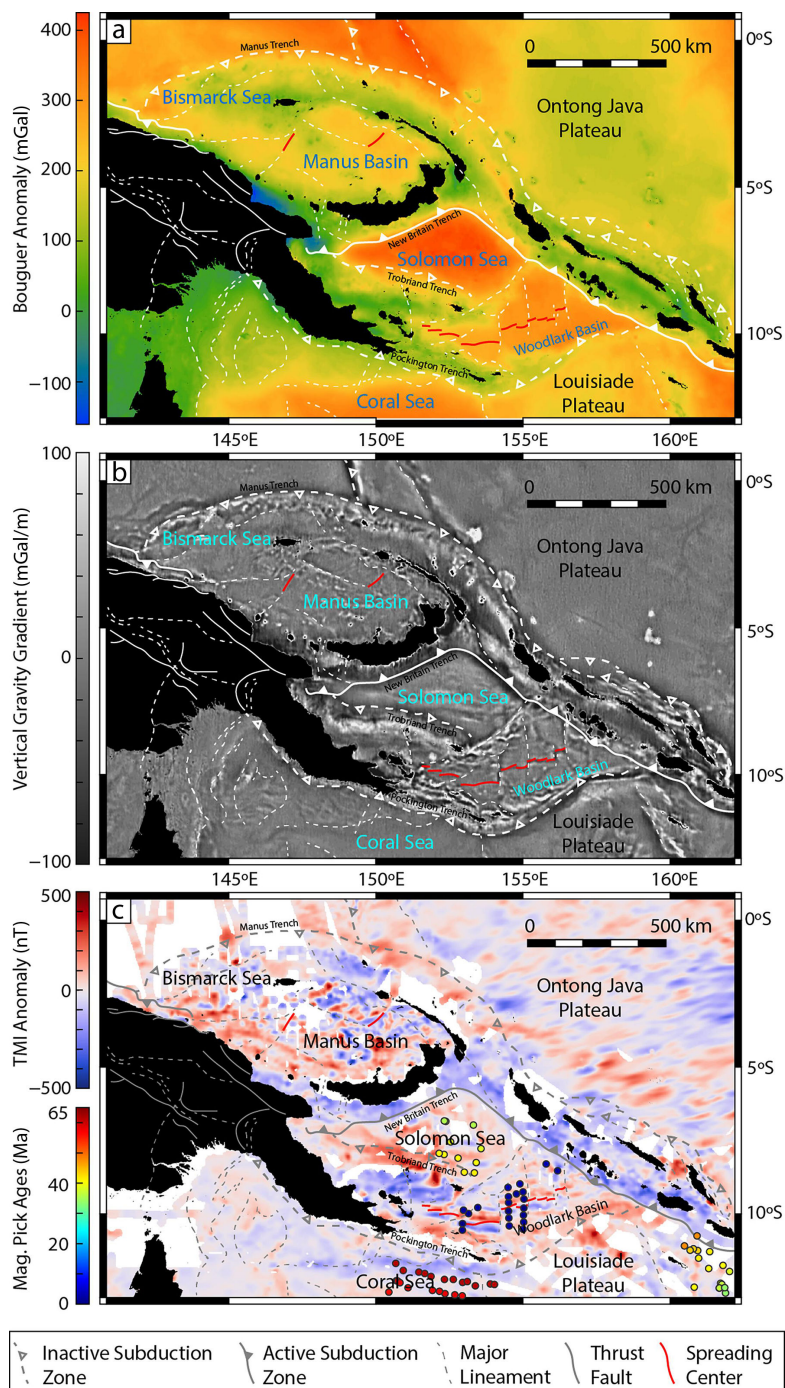


FIGURE 7: Maps of the gravity and magnetic data covering the study region. (a) Bouguer anomaly gravity map; (b) VGG map from [73]; (c) EMAG2-V3 magnetic map [74], and chron picks from [184]. In each figure, land is shown in black, with structural features such as active/inactive subduction zones, major lineaments, and thrust faults lined in white/gray and spreading centers in red.

The Caroline assemblage represents an oceanic sequence beginning with the formation of oceanic crust in a potentially backarc-like environment in the Oligocene (25, 36 Ma: [8, 77]). Crustal accretion took place by spreading along the West Caroline and Kilsgaard troughs; carbonate and hemipelagic sedimentation prevails since. The assemblage encompasses the Caroline Plate and the Eauripik Rise (Figure 1). It comprises the formations undivided oceanic crust of Paleogene age (OcPg), oceanic

crust on the trench outer slope (Troc), and intraplate seamounts (uOs) of unclear origin. The assemblage is bounded in the west and northwest by the Ayu Trough and the Palau and Yap trenches [115]. In the north, the suggested boundary of the assemblage is the Sorol Trough, a rift that separated the West Caroline Rise from the Caroline Island Ridge and was active between 7 and 17 Ma [116]. This may have been facilitated by interaction with the proposed Manus hotspot (cf. [8]). The Eauripik Rise may

have a similar origin. To the south, the assemblage is bound by the active New Guinea Trench and the inactive West Melanesian (Manus) Trench. Today, the West Melanesian Trench acts as a translithospheric strike-slip fault, and sediments in the Trench are undeformed [117]. To the east, the Caroline assemblage borders on the Mussau assemblage.

The Mussau assemblage defined here closely follows the “Mussau terrain” of Hamilton [81]. It comprises the formations undivided relict-arc crust (URac), forearc crust (Fac1), oceanic crust on the trench outer slope (Troc), undivided oceanic crust of Mesozoic age (OcMz), and undivided oceanic ridge (Our). The assemblage is bound in the west by the 7 km deep Mussau Trench, in the north and east by the Lyra Trough, and in the south by the Manus-Kilinailau Trench. East of the intersection with the Mussau Trench, sediments in the Manus-Kilinailau Trench are deformed as a result of active oblique convergence [117]. The rate of convergence increases from $\sim 5 \text{ mm a}^{-1}$ in the vicinity of the Mussau Trench to $10\text{--}12 \text{ mm a}^{-1}$ close to the TLTF island chain [36, 118]. Underthrusting of the Caroline Plate under the Mussau terrain (as part of the Pacific Plate) is indicated by a steeply dipping Benioff Zone [81, 91]. The Mussau Ridge is assumed to represent the corresponding arc [117]. In the inner trench wall, altered oceanic basalts and serpentinites are exposed [119] and according to magnetic lineations, the crust of the Mussau terrain is the same age as that of the Caroline Plate and thus may represent a detached fragment of it [120]. The Mussau Trench is interpreted as a young ($<1 \text{ Ma}$) incipient subduction zone that forms along a preexisting oceanic fracture zone [120]. Our preliminary interpretation of the Mussau Ridge as undivided relict arc crust is thus uncertain and urgently requires ground truthing.

The Woodlark assemblage includes the rift basins west of the propagating Woodlark Spreading Center, the rifted margins of the Pocklington Rise as well as those of the Woodlark Rise south of the Nubara Fault and the young ($<6 \text{ Ma}$) oceanic crust of the Woodlark Basin that is being subducted in the east along the San Cristobal and New Britain trenches. It comprises a total of twenty individual formations of eight different assemblage types (Table 1). The individual rift basins (the largest being the Goodenough Basin) and the rifted margins are assumed to be similar to crust of the adjacent Trobriand and Pocklington assemblages but covered by Late Miocene and Plio-Pleistocene sediments. A detailed description of the geology of the Goodenough Basin can be found in Fitz & Mann [87]. Well-studied fragments of the extended margin located within the Woodlark Basin include Moresby Seamount (fault rocks, meta-gabbro, and meta-dolerite: [121]) and Cheshire Seamount (altered andesitic to rhyolitic breccias: [50]). Rifting of the Woodlark Basin started $\sim 2 \text{ Ma}$ prior to the initiation of seafloor spreading in the eastern basin at the end of the Miocene (6 Ma: [31, 75]). Seafloor spreading propagated episodically westward (and is still actively propagating) at an average rate of 140 mm a^{-1} since 3.5 Ma [75]. Currently, the basin opens at rates of 36 mm a^{-1} in the west and 67 mm a^{-1} in the east. Oceanic crust formed at spreading segments 1 and 2 ($<1.9 \text{ Ma}$) make up the

shallower western basin, whereas older (up to 6 Ma) crust formed at segments 3, 4, and the subducted segment 5 make up the eastern basin. South of the Woodlark Spreading Center, several oceanic volcanoes are grouped into volcanic fields, but their origin (intraplate or related to the Woodlark Spreading Center?) remains uncertain. In the east, the Simbo and Ghizo ridges as well as the Kana Keoki and Coleman seamounts show evidence for rare subduction-related volcanism on the subducting plate. Here, medium-K calc-alkaline melts and island arc tholeiitic melts are mixing with N-MORB melts of the Woodlark Spreading Center to form andesites and dacites; this is thought to be a result from the transfer of mantle material through slab windows created by the subduction of the spreading center [122].

4.3.2. Intraplate Assemblages

The Lyra assemblage includes the Lyra Basin that is bound by the Lyra Trough in the west, the Manus-Kilinailau Trench in the south, and the OJP in the east. Its northern boundary is so far undefined. The crust of the Lyra Basin is composed of thickened mid-Cretaceous oceanic crust (OcMz) that is smoothly increasing in thickness toward the OJP (from 11 to 20 km: [123]). The crust may have formed initially in a ridge-like setting related to emplacement of the OJP [124] that was later modified by magmatic underplating when the crust passed over the Rarotongan hotspot about 65 Ma ago [92, 125]. Alternatively, the crust of the Lyra Basin may be downfaulted blocks of the OJP [91]. The 6 km deep Lyra Trough is considered to be an inactive graben or Paleogene subduction zone that is now filled by 1 km of sediments (Uss; [81]). Up to 2 km, high fault scarps are observed at its eastern flank and these extensional faults may have acted as pathways for the ascent of alkalic melts [92]. Currently, it remains unclear whether the Lyra Reef represents a seamount that formed along with the eruption of the OJP or formed later collision-induced volcanism (“Stewart Arch”: [126]; see OJP for further details).

The OJP assemblage is a Cretaceous large igneous province with a mean age of 122 Ma [25, 127]. It is similar in size to western Europe, bound by the Lyra, Pigafetta, East Mariana and Nauru basins [124], and the North Solomon Trench in the south. It comprises oceanic plateau crust (IOp) and edifices (uOp) as well as oceanic crust in the trench (Trop). The leading edge of the OJP has been accreted to the overriding plate to form the Malaita accretionary prism (alternate name: Malaita Anticlinorium). The crustal thickness is in the range of 30–35 km [123] and as much as 36–42 km underneath the main plateau [128]. Post-plateau volcanism has been dated at 90, 65 and possibly 44, 34, and 20–25 Ma ([92, 126]; the 90 Ma age may be an analytical artifact [124]). The 65 Ma age of alkaline volcanism is thought to have been induced by interaction of the OJP lithospheric root with the Rarotongan hotspot [125]. Younger (20, 44 Ma) alkaline volcanism along the Stewart Arch may have been caused by partial melting of the OJP lithospheric mantle associated with the collision of the OJP with the Solomon Arc [126]. Postvolcanic sequences of the OJP assemblage include pelagic sediments and carbonate platforms/reef

complexes. The Lyra Reef, Nuguria Reef, Kilinailau Atoll (Carteret or Tulun Islands), Takuu Islands, and the Ontong Java Reef together make up the Stewart Arch [126].

The Malaita assemblage is wedged between the North Solomon Trench and the Kia-Kaipito-Korigole fault zone between Santa Isabel and Choiseul islands that marks the old Vitiaz Trench—OJP suture [23, 24, 129]. The assemblage comprises accretionary complex crust (Trac) and ridges (Trar) which are exposed on the islands of Santa Isabel, Malaita, Maramasike, and Ulawa. It represents an accreted terrane of the Pacific Ontong Java large igneous province. It has a thick igneous basement dominated by OJP basalts (120, 123 Ma; potentially ~120 and ~90 Ma on Santa Isabel) and Cretaceous to Pliocene pelagic sediments; 44 Ma old alkali basalts and 34 Ma old alnoites are intercalated [23]. The Malaita assemblage likely formed in the Pliocene due to collision of the OJP with the Solomon Arc and 30% crustal shortening [23, 89]. There is evidence for incipient subduction along the newly formed North Solomon Trench (e.g. [90]).

4.3.3. Active Arc Assemblages

The Solomon assemblage extends from the island of Bougainville (exclusive of Buka) in the northwest to the island of Makira in the southeast. Its northeastern boundary is the Kia-Kaipito-Korigole fault zone (see Malaita assemblage), and in the southwest, the assemblage is bound by the New Britain and San Cristobal forearc assemblages. The Solomon assemblage comprises lower and upper arc crust (lAc and uAc) as well as arc front volcanoes (uAv1) and an upper intraarc sedimentary succession (uAs; Figure 5). It spans a long and complex history as evidenced by studies of zircon xenocrysts [129]. On the islands of Guadalcanal and Choiseul, MORB-like basement with an age of 92 ± 20 Ma is exposed, and on Makira, the igneous basement is of mixed MORB- and OIB character with ages of >90 and ~ 30 Ma [23]. A first phase of arc magmatism may be recorded in 63–71 Ma old zircons that predate the opening of the Coral Sea between 62 and 52 Ma [129]. Arc magmatism related to subduction along the Manus-Kilinailau Trench was widespread across the Solomon Islands for the time period 39 to ~ 20 Ma with possible arc inception at 46 Ma [23, 129]. This Eocene to lowermost Miocene arc basement is exposed on Bougainville, the Shortland islands, Santa Isabel south of the Kia-Kaipito-Korigole fault zone, San Jorge, and the Floridas Group. Collision with the Ontong Java ceased subduction along the Manus-Kilinailau Trench and shut off arc magmatism across the whole region until the Mid-Miocene. At around 12 Ma, subduction stopped along the Pocklington-Aure Trough and subsequently initiated along the New Britain and San Cristobal (alternate name: South Solomon) trenches that are also presently active [12, 130]. Arc magmatism resumed on Bougainville and resumed and/or initiated in the New Georgia Group. In a setting unique to the Solomon island arc, arc magmatism crosses the active plate boundary and feeds volcanic systems on the incoming and actively subducting Woodlark Plate (see Woodlark assemblage). Due to subduction of the spreading center, the

forearc region of the Solomon Arc is experiencing accelerated uplift (e.g. [131]) and forearc volcanism is unusually active close to the trench (Kavachi Seamount: e.g. [132]). Large sedimentary basins (uAs) occupy the area between Bougainville, the Malaita accretionary prism, and the New Georgia Group (e.g. Shortland Basin and Central Solomon intraarc basin/Russell Basin: [88, 89]).

The West Bismarck assemblage includes all volcanic centers of the West Bismarck Arc as well as the seafloor surrounding them. It comprises upper arc crust (uAc) and arc front and inner arc volcanoes (uAv1, uAv2; Figure 5). Here, we count the westernmost volcanic centers of New Britain (Cape Gloucester, Langila, Aimaga, Tangi, and Gloucester) as part of the West Bismarck Arc (cf. [28, 133]). Several volcanic centers are located northwest of the Schouten Transform and include the islands of Wokeo, Koil, and Wei [113]. Manam and Boisa are two volcanic islands that are possibly built on submerged crust belonging to the Adelbert Terrane. Karkar sits on the margin of this crustal fragment along the West Bismarck fault zone [15, 134]. In the southeast, the volcanic islands of Umboi, Sakar, and Ritter are emerging from shelf areas of the New Britain Terrane. The nature of the igneous crust surrounding the central West Bismarck Arc volcanoes is obscured by thick sediment cover [134]. It may be stretched older arc lithosphere or backarc crust that formed in a phase of backarc spreading that predated current crustal accretion along the western spreading ridges (cf. [134]). The age of West Bismarck Arc inception is unclear, but in the Early Pliocene subduction transitioned into collision resulting in the accretion of the Adelbert and Finisterre terranes at 3.0–3.7 Ma. The collision progressed eastward and reached the eastern end of the West Bismarck Arc at 1.0–1.5 Ma [28]. Today, magmatism is still driven by dehydration of the remnant slab but progressive stages of collision reduce the geochemical expression of slab-derived components [28]. Volcaniclastic sedimentation from eruption-fed turbidites or volcanic sector collapse (e.g. historic 1888 collapse of Ritter: [135]) forms the most recent submarine strata (uAs) of the West Bismarck assemblage.

The New Britain assemblage encompasses the island of New Britain with the exception of the westernmost volcanic centers (see West Bismarck assemblage) and the surrounding extended shelf area. It comprises upper, middle, and lower relict arc crust (lRac, mRac, and uRac) and sedimentary successions (mRas and uRas) as well as upper arc crust (uAc), arc front and inner arc volcanoes (uAv1 and uAv2), axial backarc volcanic ridges (uBar) and conical backarc volcanoes (Bav1), and undivided crustal blocks (Mfb). We refer to the crustal block of New Britain as the New Britain Terrane, as distinct from the Adelbert and Finisterre terranes. Currently, the terrane is still separated from the Finisterre(-Huon) Terrane by the more than 1,000 m deep Vitiaz Strait. However, with ongoing subduction of the Solomon Sea Plate, New Britain is expected to also collide with mainland PNG. The geological history of New Britain started in the Eocene with the Baining volcanics formed by arc magmatism related to subduction along the Manus-Kilinailau Trench (strata equivalent to the Jaulu volcanics

of New Ireland and the Atamo volcanics of Bougainville: [32]). In the Early Miocene, arc magmatism ceased and sedimentation prevailed (mRas and uRas). With subduction initiation along the modern San Cristobal and New Britain trenches, arc magmatism emerged on the Gazelle Peninsula in the Late Miocene (Nengmutka volcanics) and propagated westward (Kapiura beds). The modern New Britain Arc is geochemically controlled by input from the subducting Solomon Sea slab prior to collision (as opposed to the West Bismarck Arc) and the variable depth above the slab [136–138].

4.3.4. Backarc Rift and Spreading Center Assemblages

The Manus-Willaumez assemblage occupies most of the area of the Bismarck Sea. It extends from the New Guinea Basin and Manus assemblage in the north to the West Bismarck and New Britain arcs in the south and southwest. It comprises nineteen individual formations that mainly belong to the arc-backarc transition (ITc and uTr), to backarc rifts and spreading centers (e.g. uBac, uBar, and Bav1-4) and to deformation zones (Dz1-2). In the east, the assemblage is invading the New Ireland assemblage as a result of the eastward propagation of seafloor spreading related to the opening of the Manus backarc basin (Manus Spreading Center and Southeast Rifts). The Manus-Willaumez assemblage formed by complex tectonics along the Bismarck Sea Seismic Lineament that consists of a number of strike-slip faults (e.g. Schouten transform and Djaul transform), leaky transforms (e.g. Willaumez Transform, Extensional Transfer Zone, and Southern Rifts), and spreading centers, some of which open in a wedge-shaped manner (e.g. Manus Spreading Center). Backarc spreading initiated at ~3.5 Ma [70]. The Willaumez Rise separates the Manus-Willaumez assemblage into eastern and western sections. Whereas the eastern (Manus Basin) is clearly produced by backarc rifting and spreading, less is known about the nature and origin of the basement in the west. One possibility is that the crust of the western basin originated during an earlier phase of backarc formation as evident from thick stratified sediment cover (not mapped; [134, 139]). The Willaumez Rise appears to be a long-lived translithospheric tectonic transfer zone that provides the pathways for a diverse range of magmas (cf. [134, 139]). At its northwestern end, the Willaumez Rise connects to the Schouten Transform and the West Bismarck fault zone through a complex system of individual spreading ridges and structurally controlled volcanic centers (“Western Spreading Ridges” of Lee & Ruellan [134]). Along its central segment, the Willaumez Rise is characterized by tectonic ridges, individual volcanic centers, and numerous spreading ridges. In the south of the Manus-Willaumez assemblage, volcanism of the Witu Islands is related to recent subduction along the New Britain Trench [136, 138]. Volcanism along the St. Andrews Strait islands may differ from backarc magmatism (see Manus assemblage).

4.3.5. Relict Backarc Basin Assemblages

The Solomon Sea assemblage is enclosed by the active New Britain Trench in the northwest and northeast, the Nubara strike-slip fault in the southeast, and the inactive Trobriand Trough in the southwest. It comprises lower and upper relict backarc crust (IRbc and uRbc1), relict backarc ridges (uRr), and backarc crust on the trench outer slope (Trbc). The Solomon Sea formed as a backarc basin relative to subduction along the Manus-Kilinailau Trench at 28–34 Ma [76], 28–39 Ma [21], or 35–42 Ma [8]. Even though several E-W trending tectonic features are recognizable, none of them represents the extinct spreading center [8]. Prior to subduction, the Solomon Sea Plate may have had an extent similar in size to the Caroline Plate (~1,000 km across: [8]). Since then, pelagic and clastic sedimentation has prevailed (not mapped). Today, seafloor of the western Solomon Sea is intensely deformed as a result of collision and accretion of the Finisterre-Huon block with mainland New Guinea (e.g. 149° Embayment: [140–142]). In the east subduction, erosion at the New Britain Trench is dominant.

4.3.6. Relict Arc Assemblages

The Bewani-Torricelli assemblage (alternate name: North Sepik Complex) includes the accreted Bewani-Torricelli Arc and associated crustal fragments that form a prominent E-W striking mountain range between the Wewak Trench and the Sepik-Ramu Basins. It comprises high-grade metamorphics (Orme), lower relict arc crust (IRac), forearc crust, and crustal blocks (Fac1, Fac2). The arc assemblage started to form in the Upper Cretaceous and thus earlier than the adjacent Adelbert, Finisterre, and New Britain terranes but shares a common evolution as an intra-oceanic island arc during the Eocene and Oligocene [20]. In the Early to Middle Miocene, the Bewani-Torricelli Arc was accreted to the northern margin of the Australian Craton, but significant lateral transport along the landward continuation of the sinistral Schouten Transform is indicated by the rotation of the individual crustal blocks [20].

The New Guinea Mobile Belt assemblage includes various subterranean terranes that have been accreted onto the Australian Craton during the Cenozoic. The assemblage extends from the Sepik-Ramu Basin in the north to the PFTB in the south and east. It comprises lower relict arc crust (IRac), high-grade metamorphic rocks (Orme), ophiolites (Oro), intrusive complexes (Ori), and collision-related undivided volcanic edifices (Orv). The largest individual complex of the assemblage is the South Sepik complex, which comprises arc volcanic, ultramafic, metamorphic, dioritic intrusive, and sedimentary rocks that formed by arc-continent collision in the Eocene [14]. Following Davies [14], we group the Cretaceous (~110 Ma) moderate- to high-grade metamorphic rocks of the Prince Alexander Range with this assemblage. Exposed lithologies include amphibolite gneiss, orthogneiss, and mica schists [14]. Mafic and ultramafic bodies include the April ultramafics (peridotite and plutonics) in the Sepik region and the 3–4 km thick incomplete ophiolite sequence

of the Marum complex in the Bismarck Range south of the Ramu-Markham valley [18]. Both complexes may have formed in the Late Cretaceous or Eocene and were most likely emplaced during the Oligocene [18]. Large bodies of granodiorite intruded the southeastern part of the Sepik Terrane in the Miocene and extend eastward into the Jimi-Kubor Terrane (see PFTB assemblage; [14]). These intrusions are related to magmatism of the Maramuni Arc formed by subduction along the Pocklington Trough [9].

In this study, the Adelbert–Finisterre assemblage includes the two distinct Adelbert and Finisterre subterrane that collided with mainland PNG in the Late Pliocene [28]. Collision started in the west about 3.7 Ma ago and propagated southeastward [143]. As a result, the western New Britain Trench was converted from a subduction zone to a thrust (Ramu-Markham Fault: [15, 143]). The Adelbert–Finisterre assemblage is bound in the west by the Sepik–Ramu assemblage and in the south with the assemblages making up the Papuan Peninsula. In the east, the assemblage is bound by the New Britain and New Britain Forearc assemblages, whereas in the north the offshore area is occupied by the West Bismarck assemblage. The Adelbert–Finisterre assemblage comprises lower relict arc crust (lRac) and middle relict arc sediments (mRas). It shows close similarities to the other Melanesian arc terranes further east (i.e. New Britain, New Ireland, and Bougainville). The Sarawaget beds form the lowermost lithostratigraphic unit of the assemblage and represent an Eocene to Early Miocene clastic apron that formed from the contemporaneous Finisterre volcanics [143]. From the Middle Miocene to the Early Pleistocene, deep water turbidites dominated the clastic sequence that is interpreted as the accretionary wedge above the former subduction zone. Pleistocene–Holocene terrestrial sediments (molasse) form the Leron formation [143]. The northern parts of the assemblage are unconformably overlain by the Miocene Gowop limestone that correlates with other major limestone units of New Britain (Yalam limestone), New Ireland (Lelet limestone), and Bougainville (Keriaka limestone).

The Manus assemblage extends from the Manus (alternate name: West Melanesian) Trench in the north to the Manus backarc basin (Manus–Willaumez assemblage) in the south and is of Eocene to the recent age. In the west, it is bounded by the New Guinea Basin, and in the east, it transitions into the New Ireland assemblage. The assemblage is subaerially exposed on Manus Island only. It comprises lower and upper relict arc crust (lRac and uRac), middle relict arc sediments (mRas), relict forearc crust, crustal blocks, and sedimentary successions (Rfc1, Rfc2, and Rfs1), undivided rifted margin crust and crustal blocks (Mfc and Mfb) as well as conical backarc volcanoes (Bav1). Lithologically, the Manus and New Ireland assemblages are similar with the difference that lithospheric extension is restricted to the southeastern New Ireland Basin. Several Quaternary volcanic centers are known in the area, concentrated on western Manus Island (Likum volcanics) and on the islands in the St. Andrews Strait. Here, Quaternary bimodal (basaltic–rhyolitic) volcanism resulted in the emergence of several islands (Baluan, Fedarb

islands, Tuluman, Lou, Pam Lin, and Pam Mandian). The cause of volcanism on these islands remains inconclusive but an origin related to a hotspot has been proposed [144]. Alternatively, the volcanism may be related to the Willaumez Rise that represents a major lineament and potentially extending from Manus Island across the Bismarck Sea to the Willaumez Peninsula.

The Trobriand assemblage extends from the inactive Trobriand subduction zone (termed Trobriand Trough) in the north and the Nubara Fault in the east, to the PUB and Owen Stanley Metamorphic Belt in the south and west. The assemblage consists of the relict Trobriand forearc high (relict forearc crust and crustal blocks: Rfc1, Rfc1; now covered by the Quaternary Trobriand carbonate platform), major sedimentary basins (Uss, Ors, and mRas; e.g. Cape Vogel Basin, foreland basin of the PUB), and recent volcanism related to rifting (Mfv; e.g. Mt. Victory). Subaerial outcrops are restricted to Woodlark Island and several other islands and atolls such as the Trobriand island group and the Egum Atoll. The origin of the igneous basement of the Trobriand assemblage is still inconclusive, but a genetic relationship to the PUB (see Owen Stanley assemblage) is most likely. Ages for the Trobriand basement (54–59 Ma to possibly 66 Ma: [145, 146]) agree with the suggested Maastrichtian formation age (66–72 Ma) for the PUB and its emplacement age (~58 Ma: [14, 147]). The Late Paleocene Cape Vogel boninites formed in the time period between the formation and emplacement of the PUB and by melting of a highly refractory mantle source in a subduction-related setting (e.g. [148]). Volcanic rocks exposed on Woodlark Island (Loluai volcanics) are likely of Eocene age and may correspond to the Kutu volcanics of the Milne Terrane (Owen Stanley assemblage; [149]). The Eocene to Oligocene history of the assemblage is unclear until subsidence resulted in basin formation in the Late Oligocene to Early Miocene [86, 87]. The Cape Vogel Basin (with the four subbasins Buna, Tufi, Trobriand, and Goodenough) resulted from rifting and developed into a forearc basin (relative to the Trobriand Trough) with clastic and volcanoclastic sediments providing evidence for arc volcanism in the area at ~16 Ma [146]. The basin was filled until 11 Ma and submerged due to regional uplift associated with the waning of subduction along the Pocklington–Aure Trough (see Holm et al. [9] for a discussion on the competing Pocklington vs. Trobriand subduction models). At 8.4 Ma, the southern Goodenough subbasin was reactivated as a result of subsidence related to incipient rifting in advance of the propagating Woodlark Spreading Center (see Woodlark assemblage). The total thickness of sedimentary strata of the Trobriand assemblage is <5 km [87]. The basin is subject to current exploration for hydrocarbons.

The Pocklington Rise assemblage extends eastward and offshore from the southeastern tip of the Papuan Peninsula. In the north, the assemblage is bound by the rifted margins of the Woodlark Basin. In the south, it includes the relict Pocklington forearc but is separated from the Pocklington Trough, Coral Sea Basin, and Papua Plateau by the inactive (relict) Pocklington–Aure subduction zone. It comprises

metamorphic rocks or variable grade (Orme; greenschist to blueschist and eclogite facies), pre- or syn-collisional (Orfs), postcollisional (Ors), and rift-related sedimentary successions. The assemblage is mostly submarine, with subaerial outcrops limited to Misima Island, the islands of the Deboyne Group and the Louisiade Archipelago, and Rossel Island. The geology of these islands indicates an eastward (offshore) continuation of the PUB (Deboyne Group) and the Owen Stanley Metamorphic Belt (mainly greenschist-facies with eclogite-facies rocks exposed on Misima Island: [150]). The dominant lithology is the Calvados schist that consists of volcanic and volcanoclastic protoliths of the Mesozoic metamorphosed to greenschist-facies in the Middle Miocene; locally, these rocks are intruded or covered by late Miocene mafic to intermediate volcanics of the Panarora group [150].

4.3.7. Forearc Assemblages

The New Britain Forearc assemblage includes the area between the shelf of the Huon Peninsula, New Britain, New Ireland, and Bougainville and the plate boundary along the New Britain Trench. It comprises forearc crust, crustal blocks, and sedimentary succession (Fac1, Fac2, and Fas). In the west, close to the collision zone between the Finisterre Terrane and the Trobriand Platform (i.e. area north of the Solomon Sea triple junction of Whitmore et al. [140]), the forearc is dominated by accretion, faulting, and possible thrusting, and the trench is filled with sediment [141]. The prominent submarine Markham Canyon marks the basal thrust fault of the New Britain accretionary wedge [151]. This fault also marks the plate boundary between the Trobriand Block/Solomon Sea Plate on one side and the Finisterre Terrane/South Bismarck Microplate on the other. Further to the east, the forearc is being eroded and no sediment is preserved in the New Britain Trench [141]. Between the islands of New Ireland and Bougainville, the translithospheric Weitin Fault cuts through the forearc and connects with the New Britain Trench.

The San Cristobal forearc assemblage occupies the area between the San Cristobal (alternate name: South Solomon) Trench and the Solomon island arc. It is separated from the New Britain forearc by the Simbo Ridge (see Woodlark assemblage for details on this feature). It comprises forearc crust and crustal blocks and undivided crust in the trench (Fac1, Fac2, and Truc). Currently, the area of the forearc adjacent to the subducting Woodlark Spreading Center experiences uplift of up to 7.5 mm a^{-1} [131]. The basement is exposed in the New Georgia Group on the outer arc islands of Tetepare, Rendova, and Ranongga and consists of Miocene to Pliocene volcanics (brecciated basalt, pillows, tuffs, and hyaloclastites). The basement is overlain by 800–1,600 m of predominantly clastic sediments including turbidites and Pleistocene shallow marine carbonates [131].

4.3.8. Relict Forearc Assemblages

The New Ireland Basin assemblage extends from the New Ireland escarpment against the Manus backarc basin to the Manus-Kilinaillau Trench and from Mussau to Buka Island. Lithologically, the assemblage consists of Eocene

to Oligocene arc-related rocks (IRac and uRac), Miocene platform carbonates, and Upper Miocene to recent arc- and rifting-related igneous and volcanoclastic rocks (mRas, uRas; Mfv; [32, 110]). Most of these rocks were deposited in the sedimentary New Ireland Basin that started to form as a forearc basin in the Eocene (Rfc2, Rfs1, Rfs2; e.g. [152]). Offshore, the assemblage consists of an up to 7 km-thick sedimentary sequence that is underlain by ~12 km of oceanic igneous crust that formed 100–120 Ma ago. The igneous basement is thus similar in type, thickness, and age to the oceanic basement identified in the Solomon Islands (see Brandl et al. [32]; “South Solomon MORB terrain” of [23]). Currently, the New Ireland Basin assemblage is influenced by lithospheric extension, leading to the development of new depositional centers such as the Feni Deep and <3.6 Ma alkaline volcanism along the Tabar-Lihir-Tanga-Feni island chain [32].

4.3.9. Orogenic and Ophiolitic Assemblages

The Sepik–Ramu assemblage occupies the area between the New Guinea Mobile Belt and the accreted arc terranes of the Bewani–Torricelli Mountains and Adelbert and Finisterre ranges. In the northeast, where the Sepik River connects to the sea, the assemblage is bounded by the Bismarck Sea (West Bismarck and Manus–Willaumez assemblages). The assemblage represents a Neogene, predominantly clastic (with some minor carbonate at its base) postcollisional sedimentary succession (Ors) that is potentially underlain by the Marum ophiolite [12].

The PFTB extends from west to east across the full length of New Guinea. Its northern boundary against the New Guinea Mobile Belt is marked by translithospheric fault zones, and its southern boundary is formed by major fault zones along which the PFTB is thrust onto the Fly Platform. In the northeast, the Jimi-Kubor Terrane represents a distinct geological unit that we group here into the PFTB Assemblage. The Jimi-Kubor Terrane is composed of Mesozoic sedimentary rocks overlying basement of metamorphosed Permian sediments. Igneous rocks of the sequence include arc-related Middle Triassic granodiorites (~240 Ma) and rift-related intrusives and volcanics of Late Triassic age (~220 Ma: [14]). Parts of the Jimi-Kubor Terrane are metamorphosed to greenschist facies and intruded by Jurassic granitoids (Orme, Ori; Bena Bena metamorphics: [14]). Most of the PFTB, however, represents a sedimentary sequence that has been folded and (thrust) faulted (Orfb). Rifting of the Australian margin in the Late Triassic to Middle Jurassic was followed by siliciclastic sedimentation through the Late Jurassic and Cretaceous and carbonate formation from Eocene to the Middle Miocene. The development of the fold and thrust belt was accompanied by molasse-type sedimentation and volcanic activity starting in the Late Miocene as a result of collision between the Australian Craton and the Melanesian Arc (Orv). Uplift related to the opening of the Coral Sea in the Paleocene led to the erosion of parts of the Cretaceous sequence [14, 85]. The structure of the PFTB is controlled by sinistral strike-slip faulting and southward-directed

fold-thrust belts, with the latter producing strongly folded imbricated thrust sheets [85].

The Eastern Fold Belt assemblage includes the Aure-Moresby Fold and Thrust Belt and occupies the area between the Owen Stanley Metamorphic Belt and the relict subduction zone of the Pocklington-Aure Trough (alternate name: Pocklington and Aure-Moresby troughs). It comprises pre-, syn- and post-collisional sedimentary successions (Orfs and Ors), intrusive complexes (Ori), and undivided but collision-related volcanics (Orv). The assemblage is bound by the PFTB in the northwest, the Fly Platform in the west, and the Papuan Plateau in the southwest and south. Eastward, the Eastern Fold Belt assemblage merges with the largely submarine Pocklington Rise assemblage (see below). Rotation of the Woodlark Microplate leads to a reversal in the stress field along the Papuan Peninsula that also affects the Eastern Fold Belt assemblage [85]. In the southern section, adjacent to the Papuan Plateau, transtension is the dominant tectonic stress, whereas further west and northwest, transpression prevails. As a result, the Pocklington Trough represents today a passive margin, whereas its wester continuation along the Aure-Moresby Trough is an active thrust fault [85]. Rotation of the Woodlark Microplate is also responsible for the major tectonic boundary between the Aure-Moresby and the PFTB. The corresponding Aure-Moresby foreland basin occupies the eastern part of the Fly Platform and covers the basal thrust fault that is only imaged in seismic profiles [85]. Lithologically, the Aure-Moresby Fold and Thrust Belt is composed of Late Oligocene to Pliocene clastic sediments (Ors and Orfs; [14]). Further to the southeast, the Eastern Fold Belt (Poreporena Complex) comprises Paleocene to Eocene and possibly Oligocene siliceous sediments and minor serpentinite that are interpreted as an accretionary prism above the NE-dipping subduction zone of the Pocklington-Aure Trough [14]. Locally, the sediments are intruded by Oligocene gabbro, and both sediments and gabbro are partly metamorphosed to low greenschist facies [14]. Here, we also include the Sadowa Complex near Port Moresby as part of the Eastern Fold Belt assemblage. This complex consists of gabbroic rocks that likely correlate with the Milne Terrane volcanics [149].

The Owen Stanley assemblage includes two subterrains: the Owen Stanley Metamorphic Belt and the Milne Terrane. The assemblage forms the central mountain range of the Papuan Peninsula and generally represents a variably metamorphosed subduction mélangé (Orme; sediments and basalts: [105]) with minor intrusive complexes (Ori) and volcanics related to the Woodlark rifting (Mfv). Whereas the PUB is considered to represent obducted relicts of the overriding plate, the Owen Stanley metamorphics are considered to be part of the lower plate that have been metamorphosed from greenschist- to blueschist- and partly to eclogite-amphibolite-facies conditions [105, 153]. The Owen Stanley metamorphics are generally subdivided into a metasedimentary (Kagi metamorphics) and a metabasaltic (Emo metamorphics) suite [149]. The high-grade metamorphic rocks (eclogite-amphibolite-facies) are

generally exposed as metamorphic core complexes with coesite-bearing eclogite as the highest metamorphic grade preserved on Goodenough and Fergusson Island [41]. Other major metamorphic core complexes (blueschist-facies) are exposed in the Prevost Range of Normanby Island (together with Goodenough and Fergusson Island forming the D'Entrecasteaux Islands west of the propagating Woodlark Spreading Center) and the Dayman Dome (alternate name: Suckling-Dayman Massif) of the Milne Terrane (e.g. [14, 41, 45]). The Milne Terrane is the easternmost part of the Owen Stanley assemblage occupying the southeastern part of the Papuan Peninsula. It is interpreted as a sliver of Australian (Coral Sea?) crust uplifted by subduction-related underplating [149]. The main lithostratigraphic units are the 3–4 km thick sequence of the probably Cretaceous Goropu metabasalts of lower metamorphic grade exposed in the Dayman Dome and Eocene Kutu volcanics (included in Orme). These volcanic rocks may correspond to the Lolui volcanics of Woodlark Island [149].

The PUB assemblage represents the easternmost of a series of ophiolites in PNG (e.g. April Ultramafics in the New Guinea Mobile Belt and the Marum Ophiolite northeast of the Jimi-Kubor Terrane: [18, 154]). The PUB assemblage is the largest ophiolite in PNG and is exposed for 400 km strike length along the NE flank of the Owen Stanley Range [155]. The PUB assemblage includes 4–8 km of peridotite, ~4 km of gabbroic rocks, and 4–6 km of basalt and boninites (Oro; [155]). Crust of the PUB initially formed in the Owen Stanley oceanic basin during the Cretaceous (66–72 Ma: [14, 16]) and thus earlier than the Paleocene-Eocene Coral Sea. Obduction of the PUB is likely to have resulted from arc–continent collision synchronous with the opening of the Coral Sea (~58 Ma: [147]). Locally subduction-related Early Eocene tonalites and arc andesites occur in the northern PUB [18]. The PUB together with the late Cretaceous Emo metamorphics (here part of the Owen Stanley assemblage), the Late Paleocene Cape Vogel boninites, and the Early Eocene arc rocks may belong collectively to a sequence that represents the initiation of subduction along the northeast Australian margin in the Late Cretaceous and Early Paleogene (cf. [156]).

4.3.10. Continental, Shelf, and Platform Assemblages

The Fly Platform assemblage represents a part of the Papuan Basin and extends from the Papuan and Eastern fold belts to the continental shelf of the Papuan Plateau, Torres Strait, and Carpenteria. The Papuan Thrust as well as a series of other north dipping thrust faults separate the Fly Platform from the PFTB. However, the northernmost part of the Fly Platform is dominated by an inverted graben structure (basement-involved anticline) and uplifted Oligocene-Miocene carbonates (Ush; [14, 85]). The large Pleistocene Bosavi volcanic complex (Orv) most likely took advantage of the structural pathways related to the Darai uplift [14]. The basement of the Fly Platform represents a part of the Australian Craton and is composed of Permian metasedimentary rocks (Orfb), intruded by Early Triassic arc-related granodiorites (Ori; [157]). Mid- to Late-Triassic

syn-rift bimodal intrusives, volcanics, and sediments mark the transition to a sedimentary sequence [14]. Continuous but episodic subsidence led to the formation of a 5 km (onshore) to 10 km (offshore) thick sequence of terrigenous and shallow marine sediments [11, 14, 85]. Initially, the Papuan Basin developed as a passive margin sequence (~500 m thickness) from the Eocene to the Early Oligocene. In the Late Oligocene, the onset of terrane accretion and collision (along with subduction initiation along the Pocklington-Aure Trough and emerging magmatism along the Maramuni Arc) transformed the Papuan Basin into a foreland basin with increased sedimentation rates (~125 m Ma⁻¹; [11]).

The Carpenteria assemblage represents Australian continental crust that is composed of a Proterozoic basement (mostly west of the Tasman Line), covered by Paleozoic fold belts (Orfb; [16]).

The Torres Strait assemblage includes the Australian shelf (Ush) with the Great Barrier Reef and the eastern half of the Cape York Peninsula of onland Australia. The assemblage represents Phanerozoic continental basement (Ccb) with granitic inliers (Ori) and is bound in the north and west by the Paleozoic fold belts (Orfs) of the Carpenteria assemblage. The lineament between these two assemblages marks the boundary of the Australian Craton and is named Tasman Line (Figure 1; e.g. [4]).

The Papuan Plateau assemblage includes the Papua and Eastern plateaus, their surrounding rift basins as well as the Aure-Moresby Trough representing the western continuation of the relict Pocklington subduction zone. The two plateaus represent submerged fragments of continental lithosphere (Ccb) that rifted off the Australian margin. The timing of rifting, indicated by sediments in the adjacent rift basins, may have initiated locally in the Triassic and was more widespread in the Jurassic [16]. The sedimentary strata in the rift basins (Mfs) reflects several distinct extensional phases in the Jurassic, Cretaceous, and Paleocene [16]. Both plateaus represent continental basement capped by syn- and post-rift sediments.

The Louisiade assemblage includes the Louisiade Plateau and the Pocklington Trough (Truc) in the north of the plateau. In the west, south, and east, the Louisiade assemblage is bound by the Coral Sea Basin, the Louisiade Trough (not shown), separating the Louisiade Plateau from the Mellish assemblage (Ux), and the Rennell Ridge (Uc). The 190 km wide and 4,000 m deep Louisiade Trough formed by rifting and seafloor spreading synchronous with the opening of the Coral Sea (58–61 Ma; [19]). This assemblage is considered to represent a submerged fragment of extended continental Australian lithosphere (Ccx) similar to that of the Mellish Rise [26]. Up to 500 m of sediments (pelagic ooze and drowned reefs) covers the basement. An ophiolite similar in composition and age to the PUB has been recently discovered at the northern margin of the plateau [158].

The Osprey assemblage occupies the Osprey Basin (or Osprey embayment) and represents hyperextended continental crust related to passive margin formation along the Coral Sea Basin in the Paleocene (Ccx; [11, 16]).

The nature and origin of the Mellish assemblage remains inconclusive. It most likely represents a fragment of submerged continental lithosphere (Ux) that rifted off the Australian margin during the Cretaceous to Paleocene opening of the Tasman and Coral Sea [26]. Seismic profiles indicate similarities to the continental Kenn and Queensland plateaux (see [26]).

4.3.11. Undivided Crust

The Rennell assemblage, after Seton et al. [26], occupies the area of the Rennell Rise. Subaerial outcrops along the 200 by 70 km ridge structure are limited to the Rennell and Bellona Islands and the shallow Indispensable Reef complex (not shown). The sequence is capped by an up to 500 m-thick reef complex. Its origin is unclear and possible scenarios include an arc-related origin, a rifted fragment of Australian lithosphere, and uplifted Cretaceous oceanic crust [26]. It is thus mapped as unassigned crust (Uc).

Finally, the New Guinea Basin assemblages in the northwest of the map area is bound by the Manus Trench in the north and west and by the Wewak Trench in the southwest that represents the part of the New Guinea Trench east of its intersection with the West Melanesian Trench (Figure 1). In the south, the New Guinea Basin assemblages is cut off by the Schouten Transform (part of the Bismarck Sea Seismic Lineation [BSSL]; [113]). Its eastern boundary is poorly constrained due to the lack of ship-based bathymetry but was identified here by decreasing water depths toward the Manus Assemblage and a change in the VGG that is indicative of changes in crustal structure. The nature of the crust in the New Guinea Basin is currently unclear, but the (igneous) seafloor is covered by thick layers of stratified sediments (Uss; [139]). Bathymetric highs have been mapped as unassigned ridges (Ur) since their nature remains inconclusive. Toward the West Melanesian Trench, mapped formations include relict forearc crust and crustal blocks as well as sedimentary successions (Rfc1, Rfc2, Rfs1). The basin may represent a fragment of Paleogene oceanic or backarc crust (e.g. detached fragment of the Caroline Plate or backarc basin relative to the Oligocene Caroline Arc), backarc crust that predates seafloor spreading along the Pliocene to recent Willaumez Spreading Center, or tectonically stretched and thinned arc or forearc lithosphere.

4.4. Interpretation and Analysis

Quantitative assessment of crustal growth in many terranes has been possible from the analysis of regional geological maps [98], although highly variable preservations means that the mapped assemblages do not always reflect the distribution of different crust types at the time of their formation. Nonuniform preservation and tectonic erosion, in particular, obscure the history of terrane accretion and the volumes added. Modern analogues provide the evidence of the early architecture, including ancestral structures that likely played a role in terrane accretion and mineral endowment.

The geological map of the marginal seas of eastern Papua New Guinea and the Solomon Islands is a window into an early accretionary orogen that was the focus of long-lived subduction with alternating extensional and compressional regimes. A range of distinctive geological domains is present, including island arcs, backarc basins, accretionary wedges, continental fragments, clastic sedimentary basins, and overprinting magmatic belts similar to some ancient greenstone terranes. The main assemblages are broadly divided into continental margin basement (paleo-arc and sedimentary basins) and active rifts (rift volcanism, active arc, backarc basin) assembled during three main episodes of accretion: the paleo-arc (~25 Ma early Manus-Kilinau Trench and the original Melanesian Arc), a subduction reversal and accretion of the Maramuni Arc (~10 Ma), and renewed subduction at the New Britain Trench, with widespread rifting (<5 Ma). The tectonic events are well correlated across the region, including major mineralizing events that reflect rapid transition from collision, to inversion and renewed subduction [9, 32].

The present-day geology is almost entirely submarine (86% by area). The continental freeboard is only 346,485 km²; the offshore terrane to a water depth of 1,000 m covers 359,659 km², and the areas deeper than 1,000 m cover 1,805,020 km². The offshore areas are characterized by highly diverse crustal types compared to already accreted terranes. They include rifted arc crust (Mfb), forearc crust (Fac), relict forearc crust (Rfc1, Rfc2), proximal and distal backarc crust (mBac, lBac), backarc volcanic fields (mBaf), relict backarc crust (lRbc, uRbc), undivided relict arc crust (URac), intra-arc sedimentary basins (uAs) and unassigned sediments (Uss), and in the Woodlark Basin, oceanic crust (Onar, Ooac, Obmc). The major formations are about equally distributed by area among continental crust and orogenic belts (13%), volcanic arc crust (14%), forearc crust (12%), trench formations (4%), backarc basin crust (10%), and oceanic crust including the OJP (25%). The largest areas of nonoceanic crust are the relict arcs (228,000 km²), forearc successions (295,000 km²), rift-related sedimentary successions (93,000 km²), and backarc basin (129,000 km²) (Tables 2 and 3). On land, the dominant crust is folded basement, pre- and syn-collisional sedimentary successions, metamorphic rocks, ophiolite crust (Orfb, Orfs, Orme, Ors, Oro, respectively), and lesser relict arc crust (lRac and mRas). One formation, Orfb, is found only on land.

Active volcanic arcs (uAc formations of the Solomon Arc and West Bismarck Arc) and relict arcs (Rac formations of New Britain and New Ireland) occur both on land and offshore. The backarc crust (uBac, mBac, and lBac and associated volcanic formations uBaf) and the intra-arc sedimentary successions (uAs, Uss) are exclusively marine and occupy 12% of the map area (Tabs. 2 and 3). Although ocean crust and backarc basin crust occupies more than 35% of the map area, little of this crust is expected to be preserved on the emerging landmass (see discussion). As a result, the current landmass includes only 16,500 km² of

ophiolitic (oceanic) crust, representing less than 5% of the land-based assemblages.

In magmatically robust intra-oceanic arc-backarc systems, typically there are large numbers of active spreading centers and crustal growth is mainly from seafloor spreading. In the Lau Basin, for example, there are at least seven active spreading centers [55], but there are only two in the marginal basins of eastern PNG (Bismarck Sea and Woodlark Basin: Table 5). Seafloor spreading in the Lau Basin is distributed among many short segments (average length of 225 km) compared to 700 km for the Bismarck Sea spreading centers (Willaumez and Manus) and 650 km for the Woodlark Spreading Center. Spreading rates in the Bismarck Sea and Woodlark Basin average of 46 and 52 mm a⁻¹, which is similar to the individual spreading centers of the Lau Basin, but overall crustal accretion is nearly 50% greater in the Lau Basin (0.095 km² a⁻¹ compared to 0.066 km² a⁻¹ in PNG: Table 5) because there are three times as many spreading centers. Instead, the marginal basins of eastern PNG are dominated by trenches (about three times the global average relative to other boundary types: [35]). The predominance of trench boundaries is consistent with the massive additions to the crust resulting from multiple subduction zones in this region (e.g. [4]).

4.4.1. Volcanoes

Discrete volcanic cones account for about 10% of the area of volcanic crust. These are distributed among (1) syn-collisional volcanoes (Orv), (2) rift volcanoes (Mfv), (3) active arc front (uAv1) and inner arc volcanoes (uAv2), (4) backarc basin volcanoes (Bav1-4), and (5) oceanic volcanoes (Ov1-3). The largest are the arc (front and inner arc) volcanoes, covering 14,500 km², the rift volcanoes, covering 6,400 km², and the syn-collisional volcanoes, covering 7,400 km². Together they account for 75% of the volcano formations by area but only 10% of the total number of volcanic cones that were mapped (1,049 cones: Table 4). The relatively small number of volcanoes contrasts with the Lau Basin, where more than 3,000 discrete volcanoes were mapped in a similar-sized area (e.g. [55]). The difference is most likely explained by the extensive fragmentation and thus "leaky" nature of the arc and backarc crust in the Lau Basin that is reflected in a large number of leaky fault zones, rifts and spreading centers, and intraplate volcanoes [55].

4.4.2. Successor Basins

A major difference between intraoceanic and continental margin subduction zones is the prevalence of sedimentary basins. A range of different postcollisional sedimentary successions account for nearly 30% of the map area. The major offshore basins include sediment-filled rifts, active and relict forearc sedimentary successions, and postcollisional sediment accumulation. Molasse-type sediments (Ors) in foreland basins cover 81,000 km². The major successor basins are: (1) the Eastern Papuan and Aure-Moresby Fold and Thrust Belt with 1.5 km of marine sediment extending onshore and offshore [14, 85]; (2) the Sepik-

TABLE 5: Spreading and accretion rates of marginal basins in eastern PNG and the Solomon Islands.

Location	Spreading rate (mm a ⁻¹)	Type	Length (km)	Average full spreading rate (mm a ⁻¹)	Crustal accretion (km ² Ma ⁻¹)
Western Melanesia					
Woodlark	36–67	Oceanic	650	52	33,800
Bismarck Sea	0–92	Backarc	700	46	32,200
Lau Basin					
NELSC	42	Backarc	150	42	6300
FRSC	18	Backarc	250	18	4500
ELSC-VFR	69	Backarc	400	69	27,600
CLSC-LETZ	110	Backarc	200	110	22,000
MTJ	30	Backarc	175	30	5250
RR-NWLSC	90	Backarc	250	90	22,500
Futuna	40	Backarc	170	40	6800

NELSC – North-East Lau Spreading Center, FRSC – Fonualei Rift and Spreading Center, ELSC-VFR – Eastern Lau Spreading Center-Valu Fa Ridge, CLSC-LETZ – Central Lau Spreading Center-Lau Extensional Transform Zone, MTJ – Mangatolu Triple Junction, RR-NWLSC – Rochambeau Rifts-North-West Lau Spreading Center.

Ramu Basin, which has flooded the West Bismarck arc and backarc system and shed debris into the New Guinea Basin [28]; (3) sediment from the Ramu-Markham Fault, which is mainly fluvial debris from the Finisterre Ranges shed into the Markham Canyon, Finsch Deep, and Huon Basin [140]; (4) sediment from the Weitin Fault system, which may be entering the Feni Deep. The larger basins are indicated by prominent negative VGG anomalies despite the shallow water depths (Figure 8). They formed immediately after the termination of subduction-related volcanism, and several are now characterized by young rift-related alkaline volcanoes (New Ireland and West Bismarck). Some of these basins are highly prospective for oil and gas (e.g. [159]).

4.4.3. Regional Structures

The assemblages that make up the marginal basins of easternmost PNG, including the oceanic domains (Woodlark Basin), volcanic arcs (New Britain), actively rifting backarc basins (Bismarck Sea), relict backarc basins (Solomon Sea), forearc sedimentary basins (New Ireland, Manus, and New Guinea basins), and smaller successor basins (Trobriand and West Bismarck) are mostly bound by crustal-scale faults and therefore are distinct microplates. This contrasts with many intra-oceanic arc-backarc terranes where the principal assemblage boundaries are active spreading centers. The number and sizes of microplates reflect the regional scale stress regime, with syn- to post-collisional microplate rotation being a leading cause of basin opening and locally extreme extension and exhumation (e.g. Moresby Detachment). The largest structures include (1) active and former subduction-zone faults, (2) rift zones, and (3) crustal-scale strike-slip faults with well-defined geophysical expression. The currently active and former subduction-zone faults include the Manus-Kilinau, North Solomon, and New Britain trenches, the Aure-Moresby and Pocklington troughs, and the now

inactive Trobriand Trough, Ramu-Markham (thrust) Fault, and Wewak Trough. These structures are characterized by strong gravimetric contrasts (e.g. rapid changes in the Bouguer Anomaly or VGG across these structures) over short distances (Figures 7(a) and 7(b)). Active spreading centers and rift zones (Bismarck Sea spreading centers and Woodlark Spreading Center) are characterized by positive Bouguer Anomalies, pronounced contrasts in the VGG and axisymmetric magnetic lineations (Figure 7). Crustal-scale strike-slip faults and associated deformation zones (Weitin, Djaul and Nubara faults, Willaumez and Schouten transforms) are characterized by a high contrast in the VGG and contrasting TMI Anomalies when within oceanic/backarc crust (Figures 7(b) and 7(c)).

CMTs, calculated for large ($M_w > 5$), shallow (<30 km) seismic events were used to classify the major structures in the map region. The major active tectonic structures are indicated by current seismicity (Figure 8) and include destructive (thrusts/nappes and subduction zones), constructive (spreading centers and rifts), and conservative (strike-slip and transform) plate boundaries. The majority of the compressive shallow seismic events occur along the active subduction zones of the New Guinea, Wewak, New Britain, and San Cristobal trenches. The majority of the transcurrent shallow seismic events are focused along the BSSL which includes the Schouten, Willaumez, and Djaul transforms. The majority of the left-lateral focal planes of the CMTs align with the orientation of the BSSL, suggesting that there is predominantly left-lateral movement along this structure. Transcurrent shallow seismic events are also concentrated along the Weitin Fault, which connects the Manus backarc rift to the New Britain Trench through the island of New Ireland [36, 39, 46, 160–164]. Extensional shallow seismic events are found in the Solomon Sea, most likely controlled by plate flexure as the Solomon Sea Plate enters the New Britain Trench. Extensional shallow seismic

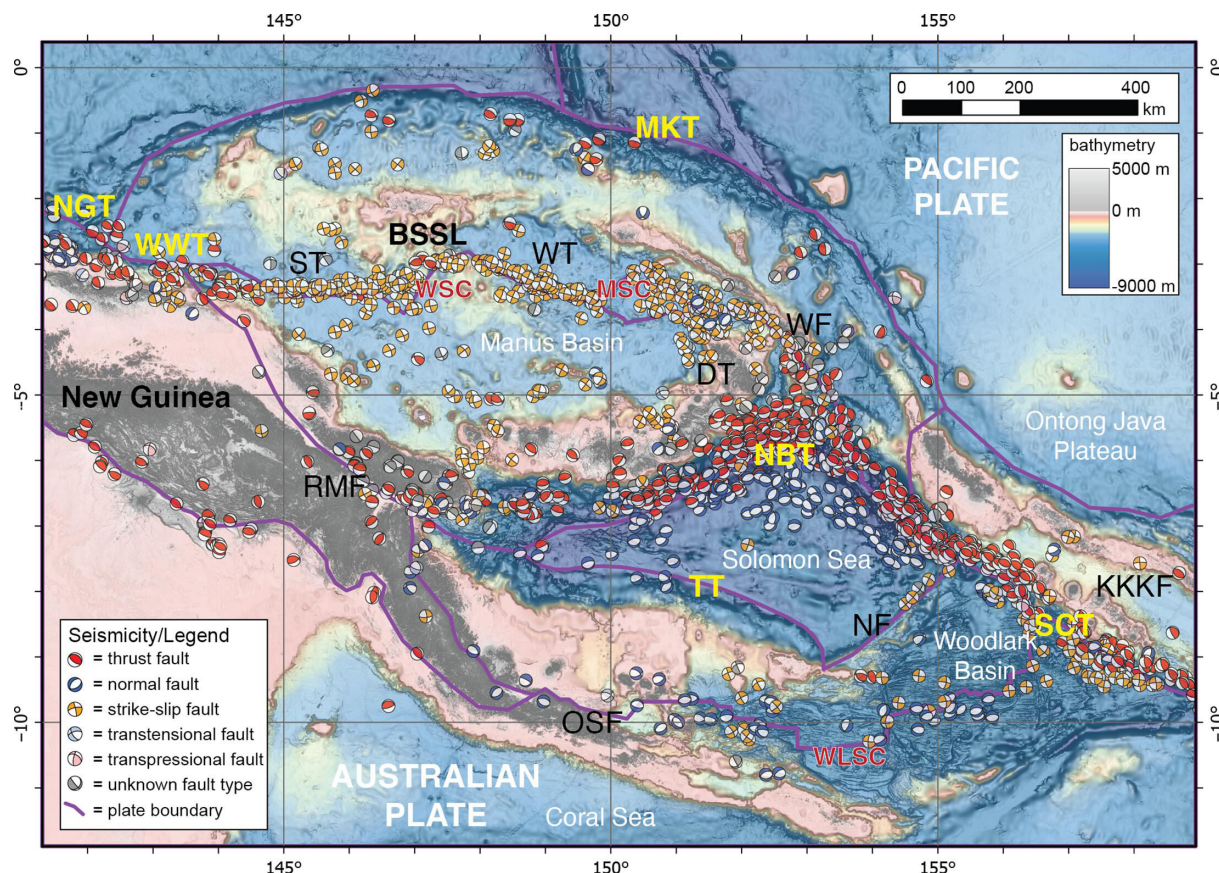


FIGURE 8: Regional bathymetric map overlain by CMT data from the open-source Global Centroid Moment Tensor (GCMT) project [78, 79]. The CMTs are classified based on the ternary diagram of Frohlich [80]. Earthquakes with depths of >30 km were excluded. The CMTs were constructed using the ArcBeachball tool (v2.2) in ArcMap (v10.6). Fault zones/Transforms (black): BSSL – Bismarck Sea Seismic Lineation with ST – Schouten Transform, WT – Willaumez Transform, DT – Djaul Transform, WF – Weitin Fault; RMF – Ramu-Markham Fault, KKKF – Kia-Kaipito-Korigole Fault zone, NF – Nubara Fault, OSF – Owen Stanley Fault zone. Trenches (yellow): MKT – Manus-Kilinaillau Trench, NGT – New Guinea Trench, WWT – Wewak Trench, NBT – New Britain Trench, TT – Trobriand Trench, SCT – San Cristobal Trench. Spreading Centers (red): WSC – Willaumez Spreading Center, MSC – Manus Spreading Center, WLSC – Woodlark Spreading Center.

events are also found in the western tip of the Woodlark Basin and are most likely related to the rift propagating into the continental crust. The analysis highlights a stress regime that is dominated by a combination of left-lateral strike-slip faults, large-scale transcurrent motion, and less commonly nonrigid diffuse deformation at the tips of propagating rifts and spreading centers.

Because the region is dominated by postcollisional microplate rotation, the major deformation is oblique strike-slip, especially along arc-parallel faults. Examples include the giant Weitin Fault and, in the Solomon Island, the Kia-Kaipito-Korigole fault zone. A number of these faults have evolved into transform boundaries, including the Djaul Fault and Schouten Transform. The oblique slip has caused transtension on many of these structures and the beginning of rifting, such as the Extensional Transform Zone and Southern Rifts in the Manus Basin. The Willaumez Transform has become a large leaky transform. Elsewhere extreme rifting has given rise to structures such as the Moresby Detachment in the western Woodlark Basin. Numerous early subduction zone trench faults have become

inactive, such as the Trobriand Trough in the Solomon Sea and the Pocklington Trough south of the Woodlark Basin (now a passive margin fault). Others have become sutures between accreted terranes, such as the Ramu-Markham Fault along strike of the Wewak Trench. And, a number of the trench faults have become thrusts, including the Aure-Moresby Trough at the western continuation of the Pocklington Trough and the Papuan Thrust on land.

The Weitin Fault, along the northern margin of the South Bismarck Microplate, is among the largest active structures in the region, with a strike length of at least 600–700 km. Displacement at the eastern end of the fault on southern New Ireland is as much as 130 mm a^{-1} [160]. A M_w 7.5 earthquake in 2019 and a M_w 8.0 earthquake in 2020 ruptured the Weitin Fault over a distance of ~ 150 km, with observable slip of up to 5 m along a 30 km strike length [165]. The lithostratigraphic units exposed along the Weitin Fault correlate with the lower relict arc crust (IRac) of New Ireland and, in the New Britain Trench, with forearc crust (Fac1) of New Britain. In the trench, the fault exposes the basement of the Melanesian Arc (Jaulu volcanics). Along

TABLE 6: Bedrock areas (percent of total) for selected countries in southeast Asia and the western Pacific (after [98]).

Major lithology	Offshore PNG ¹	Onshore PNG	Indonesia	Philippines	Japan	S Korea	N Korea	China
Volcanic rocks	45	9.1	10.1	13.9	28.0	22.8	8.0	6.9
Plutonic rocks	<5	3.0	4.7	2.9	11.3	41.1	23.9	11.3
Ultramafic rocks	–	1.0	1.8	3.9	0.5	–	–	–
Sedimentary rocks	45	80.1	80.4	79.2	56.2	20.1	15.7	70.0
Metamorphic rocks	10	6.9	3.0	–	4.0	16.0	52.4	11.8

¹This study.

most of its length, it cuts 40 Ma old arc crust, except at the thinned portion of New Ireland where it is intercepted by the Southeast Rifts of the eastern Manus Basin [160]. A lack of seismicity on the Weitin Fault north of the Southeast Rifts (Figure 8) indicates that spreading in the backarc basin is now accommodating the southward migration of New Britain.

4.4.4. Preservation of Backarc Basin Crust

The map data from the marginal basins can be compared to regional geological maps of continental areas elsewhere in the Western Pacific (e.g. [98]) to better understand crustal growth by accretion of island arcs. Because most of the mapped assemblages are fault-bounded, area–age relationships cannot be interpreted in the same way as in other regions (e.g. [55]). Instead, the mapped areas are a record of the preservation of different crustal types during collision.

Many of the microplates will be erased during amalgamation, owing to the erosional nature of the accretion processes. This is illustrated by the very different evolution of the Manus Basin, Solomon Sea, and Woodlark Basin. In the Woodlark Basin, the backarc crust is being subducted along the San Cristobal Trench and consumed at a rate of 52 mm a⁻¹ [160]. The Solomon Sea Plate is bound by three trenches and is now mostly lost. Prior to subduction, the Solomon Sea Plate may have been similar in size to the Caroline Plate (~1,000 km across: [8]), compared to the 400 km basin width remaining today. Tomographic data show how much of the Solomon Sea Plate has already been subducted [15, 166, 167]. The Manus Basin is bound by an active arc and more than 1,500 km of inactive trench and strike-slip faults.

Although there are significant non-volcanic formations offshore, there is much more volcanic rocks in the marginal basins than on land. The offshore map area is nearly 40% covered by volcanic rocks, whereas volcanic rocks account for only 9% of the land area on PNG (sedimentary rocks account for 80% and metamorphic and plutonic rocks account for 11%: Table 6). The average continental crust of southeast Asia is composed of 90% sedimentary and metamorphic rocks by area [98]. The percentage of basaltic formations represented by the three large offshore basins (Manus, Solomon, and Woodlark) is therefore way out of proportion to the abundance of mafic rocks preserved in the accreted terranes.

The comparison suggests that large areas of mafic crust offshore in the Mesozoic were also not preserved in the

continental crust. Only 10% of the map area of Indonesia is volcanic (Table 6). By contrast, subduction-related volcanic and plutonic rocks dominate the bedrock of Japan, similar to the marginal basins of PNG today. The volcanic bedrock on land is distinctly bimodal (felsic and mafic), whereas mafic volcanic rocks dominate the marginal basins. The lack of mafic volcanic rock exposed on land must reflect a fundamental difference related to preservation of small oceanic basins in collisional settings, with the backarc basin assemblages most likely to be subducted. In the marginal basins of eastern PNG today, this may be nearly 50% of the total crust by area. If most of the mafic volcanic rocks are returned to the mantle, the expectation would be an overall more felsic composition of the accreted terranes, unless the mafic crust is somehow emplaced at midcrustal depths and simply not exposed. The preservation of the more mafic backarc assemblages requires that the boundaries of the microplates are dominated by structures where subduction will not occur, such as the major strike-slip faults bordering the Manus Basin. Thicker, more buoyant crust (up to 20 km thick) associated with multiple subduction zones also might be better preserved when the basins close (e.g. [168]).

4.4.5. Regional Metallogeny

The area mapped in this study is a prolific porphyry-epithermal Cu–Au province with uniquely fertile sources of metal and optimal structural control on the rise of melts and fluids. The islands of Manus, New Ireland, Bougainville, and the Tabar-Feni island chain comprise a >800 km permissive tract that dominates the Eocene to Pliocene Outer Melanesian magmatic arc [9, 22]. The northernmost islands, Manus and New Ireland, host Miocene porphyry Cu prospects. The Tabar-Feni-Lihir Islands (New Ireland offshore islands) host Pliocene to Holocene alkaline porphyry-epithermal Au systems, including the giant Ladolam Au deposit on Lihir. Bougainville hosts giant Pliocene porphyry Cu deposits associated with calc-alkaline diorite to granodiorite stocks at Panguna (online Supplementary Table S3 in the online Supplementary Material 1). A major cause of the regional mineral endowment is thought to be enhanced crustal permeability and fertilization of the mantle at the intersection of orogen-parallel, translithospheric corridors and similar-scale orthogonal structures (e.g. [169–171]).

Holm et al. [9] described the geodynamic setting of Cenozoic intrusion-related Cu–Au deposits, including fifty mines, deposits and prospects (nineteen porphyry

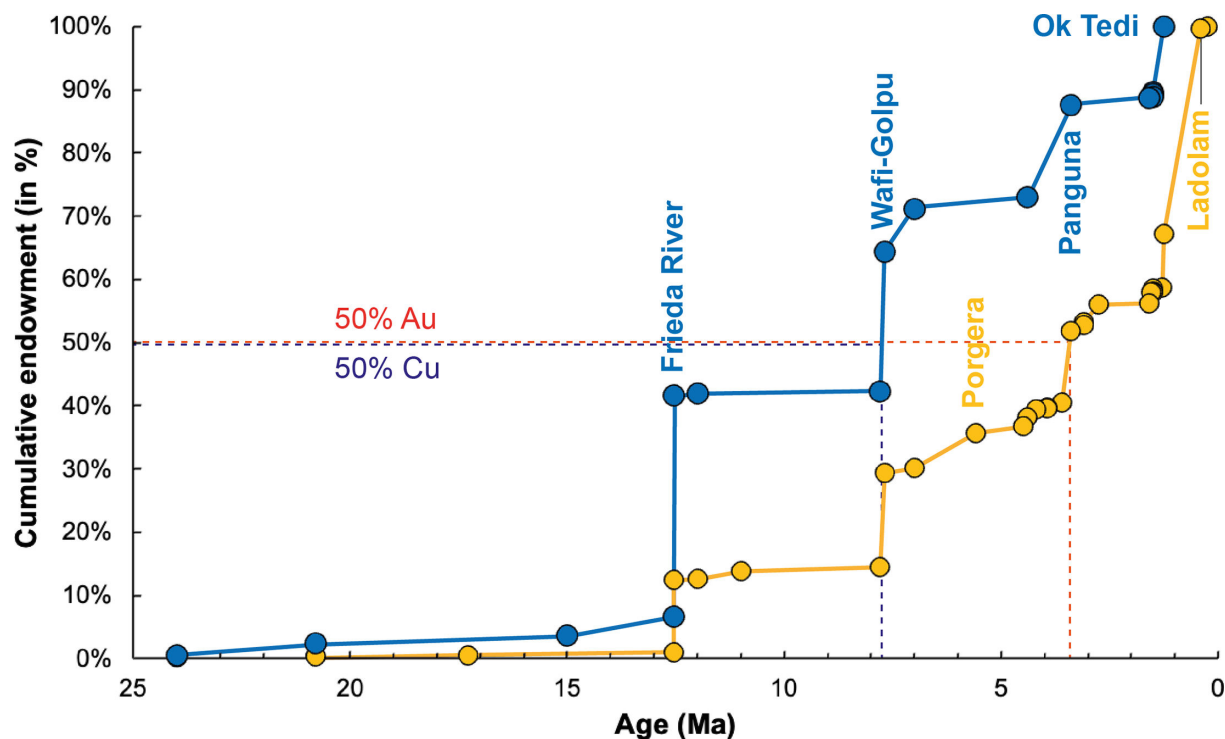


FIGURE 9: Cumulative endowment in Cu (blue) and Au (orange) of the crust in eastern PNG and the Solomon Islands in % relative to the total contained Cu (37.2 Mt) and Au (192 Moz; Table 7) after [9]. Mineral deposits include porphyry-epithermal and skarn deposits as well as few volcanogenic massive sulfide deposits.

Cu deposits, thirteen epithermal deposits, nine porphyry-epithermal hybrids, and two porphyry-skarn deposits; online Supplementary Table S3). Collectively, these deposits account for about 192 Moz of contained Au and 37 Mt of Cu (Table 7), equivalent to the metal endowment of major orogenic belts elsewhere in the world (e.g. Abitibi and Yilgarn). A recent assessment of the undiscovered Cu metal in the region is at least 62 Mt Cu, with a total endowment of 95 Mt known and predicted resources (Table 8). The majority of this metal was emplaced within the last 25 Ma (Figure 9). This episode spans the pre-collision Oligocene–Miocene subduction of the Pacific Plate at the Manus–Kilinailau Trench to the current northward subduction of the Solomon Sea Plate under New Britain. The Ladolam Au deposit, associated with postcollisional alkaline magmatism in the New Ireland Basin, is the youngest known major Au deposit in the world, forming within the last 500 ka [172].

The major Cu and Au deposits in mainland Papua New Guinea (New Guinea Orogen) are porphyry-type deposits, including Ok Tedi, Frieda River, Porgera, and Wafi-Golpu: Figure 9). Hybrid epithermal and porphyry-type deposits, such as Hidden Valley, occur along the Papuan Peninsula and extend east into the Woodlark Basin (Umuna, Misima Island, and Woodlark deposits). Different deposit types are closely juxtaposed in time and space. For example, the Quaternary alkalic low-sulfidation epithermal mineralization at Ladolam is thought to be related to a major underlying porphyry system [173].

The offshore volcanic basins are also prolific for seafloor hydrothermal activity. More than thirty hydrothermal vent fields are known in the Bismarck Sea and Woodlark Basins, including five on the Willaumez Spreading Center and Transform, nine in the Manus Spreading Center, twelve in the Southeast Rifts of the eastern Manus Basin, and three in the Woodlark Basin: [174, 175]). These include the Solwara deposits in the eastern Manus Basin, Vienna Woods on the western Manus Spreading Center, and the La Scala deposit in the Woodlark Basin. Despite the current seafloor hydrothermal activity, VMS deposits are notably missing in the older accreted terranes. VMS and minor manganese deposits are restricted to a small area of some of the oldest rock in the region in the Paleocene–Eocene Astrolabe mineral field in the Eastern Fold Belt (Laloki and Federal Flag deposits: online Supplementary Table S3). They are not known anywhere else in PNG.

Four main crustal types host the majority of the Cu–Au deposits in the map area (Figure 10; online Supplementary Table S3 and S7): (1) exhumed (low-grade) metamorphic rocks of the PFTB (Orfb: Frieda River, Porgera, Ok Tedi), (2) exhumed metamorphic rocks of the Owen Stanley Ranges (Orme: Wafi-Golpu), (3) the active Solomon Arc (uAc: Panguna, Gold Ridge), and (4) rifted forearc crust of the New Ireland Basin (Rfc2: Ladolam and Simberi). These formations cover about 245,000 km² or about 11% of the map (Orfb: 78,700 km²; Orme: 47,900 km²; uAc: 57,300 km²; Rfc2: 61,600 km², volcanic rocks only). Other assemblages are less endowed; for example, the relict arc crust of New Britain, which contains numerous prospects

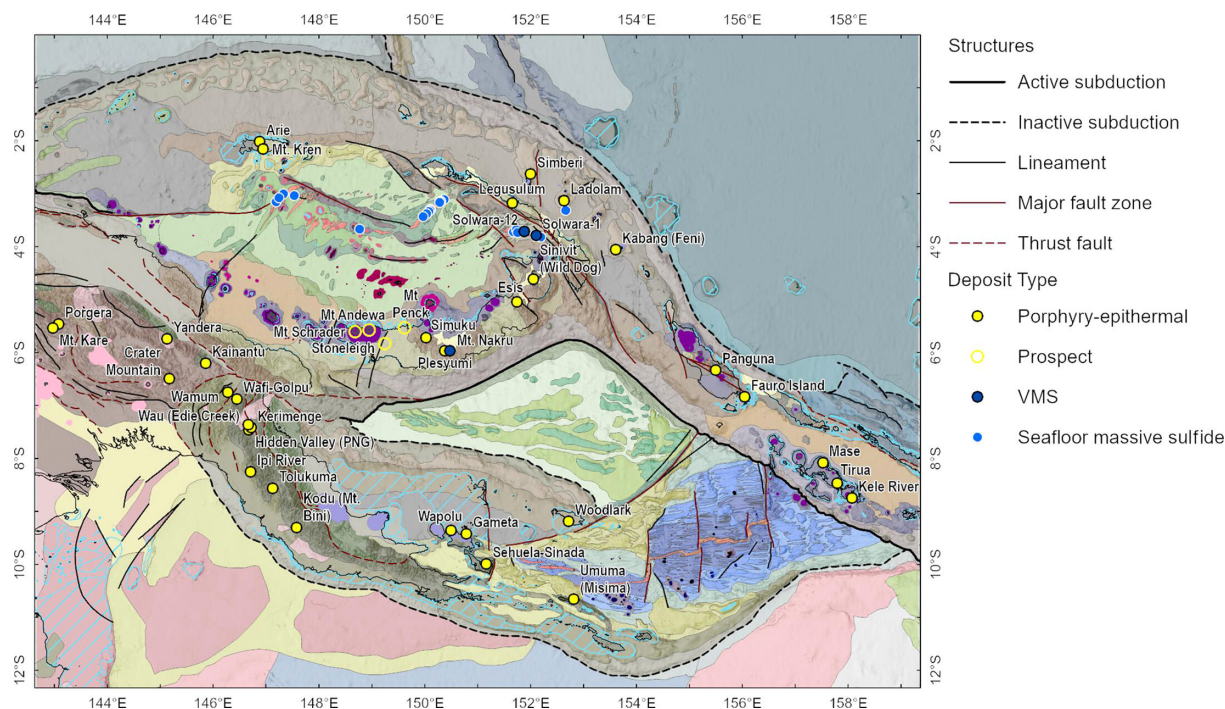


FIGURE 10: Main copper–gold deposits of eastern PNG and the Solomon Islands (after [9]) and seafloor massive sulfide deposits [174, 175] superimposed on the reduced version of the geological map on the formation level (Figure 5) (M1).

TABLE 7: Principal Cu and Au resources in eastern PNG and the Solomon Islands (after [9]) by assemblage and formation type as defined in this study and sorted by total Cu (Mt).

Assemblage	Host formation	Number of deposits	Number with resources	Total Au (Moz)	Total Cu (Mt)	Examples
Papuan Fold Belt	Orfb	9	9	57.1	21.1	Frieda River, Porgera, Ok Tedi
Owen Stanley	Orme	9	9	38.4	9.0	Wafi-Golu
Solomon	uAc	6	2	25.4	5.6	Panguna, Gold Ridge
New Britain	mRac	9	3	1.0	0.9	–
New Ireland-Manus	lRac	3	1	–	0.5	–
Eastern Fold Belt	Orfs	2	1	0.2	0.1	–
New Ireland Basin	Rfc2	3	3	69.8	–	Ladolam, Simberi
Total		41	28	192	37.2	

but few established resources. The wide range of different assemblages hosting the mineral deposits confirms that endowment is more closely linked to tectonic triggers than formation and assemblage type. The largest Cu–Au deposits and mineral districts formed at 12.5 Ma (Frieda River), 7.7 Ma (Wafi-Golpu), 3.4 Ma (Panguna), 1.1–1.4 Ma (Ok Tedi), and 0.15–0.70 Ma (Ladolam). Holm et al. [9] showed the cumulative addition of Au, with a steady increase in the first 20 Ma of crustal growth and then a jump in the last 5 Ma corresponding to the regional microplate breakout and postcollisional adjustments; 50% of the gold was introduced in the last 3.5 Ma, and most in the last 1 Ma, with a general increase in gold endowment associated with younger events (Figure 9). There are no large deposits known to be associated with the proto-Melanesian Arc and subduction at the Manus-Kilnailau Trench before

~25 Ma. Rather, the greatest endowment is where the same assemblage has been affected by repeated tectonic events, repeatedly introducing new melts and fluids at the same locations (e.g. 50 Moz combined gold resources in the PFTB related to three different episodes: 12.5 Ma at Frieda River, 5.6 Ma at Porgera, and 1 Ma at Ok Tedi; Figure 9). However, the distribution of known deposits raises a number of questions. Why are there so few mineral deposits in the Eocene and Oligocene rocks of the Papuan margin and proto-Melanesian Arc? With so much submarine volcanism, why are there so few VMS deposits? The lack of old deposits may simply reflect the low preservation of rocks from the precollisional history of the region. Similarly, the lack of VMS deposits in the accreted terranes reflects the especially low preservation of backarc basin crust.

TABLE 8: Estimated total Cu endowment in eastern PNG (after [174]) sorted by total Cu (Mt).

Tract	Area (km ²)	Known Cu resources (Mt)	Estimated Cu (Mt) ¹	Total Cu (Mt)
Medial PNG	67,400	17.5	25.1	42.6
Bismarck–New Ireland–Manus	16,830	7.1	17	24.1
Maramuni Arc	38,970	8.5	9.9	18.4
New Britain	17,990	0.7	8.5	9.2
SE Papuan Peninsula	1640	n/a	1.2	1.2
Northern PNG	29,140	n/a	n/a	n/a
Total	156,823	33.8	61.7	95.5
Offshore equivalent formations	105,240	–	–	–

¹Undiscovered resources; – not estimated; n/a data not available.

Holm et al. [9] pointed out that in approximately 20 Ma, when the OJP eventually collides with the Australian Craton, many of the Miocene and younger deposits will become part of a major new metallogenic province along northeast Australia. The 2013 USGS resource assessment for the islands of Bougainville, New Ireland, Manus, and New Britain (34,820 km² of permissive tracts) predicted 33 Mt Cu in known and undiscovered resources [176]. However, these land-based resource assessments provide only a partial view of the regional metal endowment. The equivalent offshore formations cover 105,240 km² and could reasonably be expected to contain at least the same amount of Cu (Table 8). Rocks that contain 97% of the upper crustal endowment of Au in the map area (including 57.1 Moz in Orfb, 38.4 Moz in Orme, 69.8 Moz in Rfc2, and 25.4 Moz in uAc: Table 7) cover only 156,823 km² on land where the assessment took place. The offshore area of these formations to a water depth of 1,000 m is about two-thirds of the land area (Table 8). Taking into consideration the total (onshore and offshore) area of permissive formations, the amount of Au that may eventually be added to the Australian Craton could be almost double that currently estimated from known and undiscovered resources.

5. CONCLUSIONS

In a previous study, we showed crustal accretion and hydrothermal activity in intraoceanic arc–backarc systems is strongly dependent on extension at many simultaneously active spreading centers that may span an entire basin [55]. The PNG model presents a very different style of growth where crustal thickening is highly episodic and controlled by pre-, syn-, and post-collisional interactions of fault-bounded microplates. Some of the basins have evolved from dominantly volcanic to sedimentary in less than 5 Ma, and in others, young volcanic centers have erupted where more than 7 km of sediment had previously accumulated (e.g. in the New Ireland Basin). As a result, diverse volcanic, sedimentary, and mineralizing systems have been closely juxtaposed in time and space.

The region is characterized by the presence of both the former Pacific Plate and the Solomon Sea Plate under New Britain, which is at least partly responsible for a globally

significant geoid anomaly surrounding the study area. Among other consequences, the long history of paleo-subduction increased both the fertility of the mantle and the likelihood of preservation of the supra-subduction crust. The recent history is dominated by collision with the OJP and tectonic triggers, such as microplate rotation, that have contributed to the high crustal permeability and mineral endowment. Rates of crustal accretion are less than that of the major intra-oceanic arc–backarc systems (66,000 km² Ma⁻¹ total for the Bismarck Sea and Woodlark basins, compared to 95,000 km² Ma⁻¹ in the Lau Basin: Table 5). However, crustal thickening at the plate margins is greatly enhanced by the overlapping subduction zones.

A grid-based analysis of the map gives an unbiased view of the structure and composition of the crust prior to its eventual accretion to the continent. One observation is that the proportion of backarc basin crust offshore is much greater than that found in the accreted terranes, confirming significant volumes of mafic crust are lost during continental growth or at least not exposed because they are emplaced at midcrustal depths. In the standard model, continental crust is more felsic in composition because of differentiation resulting from reworking and addition of new arc magmas (e.g. [177, 178]). However, selective preservation also appears to play a role. A significant fraction of Phanerozoic continental crust appears to have formed by island arc accretion and is mostly felsic, whereas the marginal basins before they are accreted to the continents are mostly basaltic, the latter being recycled into the mantle or hidden beneath the seismic Moho [179]. The amount of backarc basin crust that is preserved during closure appears to be only a small fraction of what was present prior to collision. The forearc basins, which are underlain by thicker and stronger lithosphere, survive collision. The best chance of preserving backarc basin crust is to isolate the basin in a microplate mosaic where all of the pre-accretion plate boundaries are strike-slip faults. The Manus Basin may be in a unique position for survival as it is surrounded by an active arc and nearly 600–700 km of strike-slip faults at its northern margin. The Woodlark Basin has a low probability of survival, as it is surrounded by three trenches, and the Solomon Sea Plate is already largely subducted at the New Britain Trench. This contrasts with typical

intra-oceanic arc–backarc systems, such as the Lau Basin, where spreading centers account for ~45% of the plate boundaries.

The major boundaries of displacive strain in easternmost PNG are arc-parallel shear zones that formed as a result of microplate rotation following collision and subduction reversal. These faults become transfer zones for basin opening and accommodate extension by continually growing along strike (cf. [177, 180]), terminating where they are intercepted by backarc spreading centers. The microplate boundaries of the marginal seas of PNG illustrate how these lithosphere-scale structures initiate and how they may be preserved in the geological record. In many cases, the faults likely originated from older structures in pre-existing arc basement underlying the younger rocks and therefore may have a range of behaviors during the pre-, syn- and post-collisional history of the basins. They are frequently reactivated to control melt and fluid pathways such as during postcollisional microplate rotation [32]. Earlier fertilization of the mantle provides a long-lived source of metal-rich arc magmas that are repeatedly tapped—a key for the development of super-endowed terranes (e.g. [181–183]). In PNG, the fertilized source of metals is thought to have been accessed by different extensional and compressional events during subduction initiation, subduction reversal, and jumps in active arc magmatism [9, 32].

Data Availability

All data are included in this article either as data tables or as supplementary materials.

Conflicts of Interest

The authors declare that there is no conflict of interest regarding the publication of this article.

Funding Statement

This project was funded through the Marine Mineral Resources Group at the GEOMAR Helmholtz Centre for Ocean Research Kiel and the Canada First Research Excellence Fund (CFREF; Metal Earth) grant. This study was partially funded through grant BR5297/2-1 BISMARc of the German Research Foundation (DFG) and through grant 05G0299A of the German Federal Ministry of Education and Research (BMBF) to PAB.

Acknowledgments

The authors would like to thank the German Helmholtz Association for support within the Helmholtz Distinguished Professorship program. The Natural Sciences and Engineering Research Council of Canada (NSERC), and CFREF are acknowledged for the support of this work through research grants and project funding. The authors acknowledge two anonymous reviewers for their constructive input and the

associate editor Aleksandr S. Stepanov for the efficient handling of this manuscript. This is Metal Earth contribution MERC-ME-2024-30.

Supplementary Materials

Table S1: List of onshore geological maps used in this study.
Table S2: List of individual research cruises from which bathymetric data have been used.
Table S3: Mineral deposits by formation type.
Map M1: Full-scale (1:1 million) geological map of the marginal seas of Papua New Guinea and the Solomon Islands.

References

- [1] S. Kodaira, T. Sato, N. Takahashi, et al., “New seismological constraints on growth of continental crust in the Izu-Bonin intra-oceanic arc,” *Geology*, vol. 35, no. 11, 2007.
- [2] O. Jagoutz and P.B. Kelemen, “Role of arc processes in the formation of continental crust,” *Annual Review of Earth and Planetary Sciences*, vol. 43, no. 1, pp. 363–404, 2015.
- [3] S. Rino, T. Komiya, B. F. Windley, I. Katayama, A. Motoki, and T. Hirata, “Major episodic increases of continental crustal growth determined from zircon ages of river sands; Implications for mantle overturns in the early Precambrian,” *Physics of the Earth and Planetary Interiors*, vol. 146, nos. 1–2, pp. 369–394, 2004.
- [4] S. L. Baldwin, P. G. Fitzgerald, and L.E. Webb, “Tectonics of the New Guinea region,” *Annual Review of Earth and Planetary Sciences*, vol. 40, no. 1, pp. 495–520, 2012.
- [5] N. Mortimer, H. J. Campbell, A. J. Tulloch, et al., “Zealandia: Earth’s hidden continent,” *GSA Today*, 27–35, 2017.
- [6] R. Hall, “Cenozoic geological and plate tectonic evolution of SE Asia and the SW Pacific: Computer-based reconstructions, model and animations,” *Journal of Asian Earth Sciences*, vol. 20, no. 4, pp. 353–431, 2002.
- [7] K. C. Hill and R. Hall, “Mesozoic–Cenozoic evolution of Australia’s New Guinea margin in a West Pacific context,” *Internet in Geol Soc Aust Spec Publ 22 Geol Soc Am Spec Pap 372*, R.R. Hillis, and R.D. Müller, Eds., pp. 265–290, Geological Society of America, 2003.
- [8] C. Gaina and D. Müller, “Cenozoic tectonic and depth/age evolution of the Indonesian gateway and associated backarc basins,” *Earth-Science Reviews*, vol. 83, nos. 3–4, pp. 177–203, 2007.
- [9] R. J. Holm, S. Tapster, H. A. Jelsma, G. Rosenbaum, and D. F. Mark, “Tectonic evolution and copper–gold metallogenesis of the Papua New Guinea and Solomon Islands region,” *Ore Geology Reviews*, vol. 104, pp. 208–226, 2019.
- [10] C. J. Pigram and H.L. Davies, “Terranes and the accretion history of the New Guinea orogen,” *BMR J Aust Geol Geophys*, vol. 10, pp. 193–211, 1987.
- [11] C. J. Pigram and P.A. Symonds, “A review of the timing of the major tectonic events in the New Guinea orogen,” *Journal of Southeast Asian Earth Sciences*, vol. 6, nos. 3–4, pp. 307–318, 1991.
- [12] K. C. Hill and A. Raza, “Arc-continent collision in Papua New Guinea: Constraints from fission track thermochronology,” *Tectonics*, vol. 18, no. 6, pp. 950–966, 1999.

- [13] MS. Norwick, "New palaeogeographic maps of the Northern margins of the Australian plate," 2003
- [14] HL. Davies, "The geology of New Guinea - the cordilleran margin of the Australian continent," *Episodes*, vol. 35, no. 1, pp. 87–102, 2012.
- [15] R. J. Holm, G. Rosenbaum, and SW. Richards, "Post 8 ma reconstruction of papua New Guinea and Solomon islands: Microplate tectonics in a convergent plate boundary setting," *Earth-Science Reviews*, vol. 156, pp. 66–81, 2016.
- [16] C. Bulois, M. Pubellier, N. Chamot-Rooke, and M. Delescluse, "Successive rifting events in marginal Basins: The example of the coral sea region (papua New Guinea)," *Tectonics*, vol. 37, no. 1, pp. 3–29, 2018.
- [17] B. Taylor, "The single largest oceanic plateau: Ontong java–manihiki–hikurangi," *Earth and Planetary Science Letters*, vol. 241, nos. 3–4, pp. 372–380, 2006.
- [18] H. L. Davies and AL. Jaques, "Emplacement of ophiolite in papua New Guinea," *Geological Society, London, Special Publications*, vol. 13, no. 1, pp. 341–349, 1984.
- [19] C. Gaina, R. D. Müller, J. Royer, and P. Symonds, "Evolution of the lousiade triple junction," *Journal of Geophysical Research*, vol. 104, no. B6, pp. 12927–12939, 1999.
- [20] C. Klootwijk, J. Giddings, C. Pigram, et al., "North sepik region of papua New Guinea: Palaeomagnetic constraints on arc accretion and deformation," *Tectonophysics*, vol. 362, nos. 1–4, pp. 273–301, 2003.
- [21] E. Honza, H. L. Davies, J. B. Keene, and D. L. Tiffin, "Plate boundaries and evolution of the Solomon sea region," *Geo-Marine Letters*, vol. 7, no. 3, pp. 161–168, 1987.
- [22] S. Garwin, R. Hall, and Y. Watanabe, "Tectonic setting, geology, and gold and copper mineralization in cenozoic magmatic arcs of Southeast Asia and the West pacific," *Economic Geology and the Bulletin of the Society of Economic Geologists*, vol. 100th Anniversary Volume, pp. 891–930, 2005.
- [23] M. G. Petterson, T. Babbs, C. R. Neal, et al., "Geological–tectonic framework of Solomon islands, SW pacific: Crustal accretion and growth within an intra-oceanic setting," *Tectonophysics*, vol. 301, nos. 1–2, pp. 35–60, 1999.
- [24] P. Mann and A. Taira, "Global tectonic significance of the Solomon islands and ontong java plateau convergent zone," *Tectonophysics*, vol. 389, nos. 3–4, pp. 137–190, 2004.
- [25] J. A. Tarduno, W. V. Sliter, L. Kroenke, et al., "Rapid formation of ontong java plateau by aptian mantle plume volcanism," *Science (New York, N.Y.)*, vol. 254, no. 5030, pp. 399–403, 1991.
- [26] M. Seton, N. Mortimer, S. Williams, et al., "Melanesian backarc Basin and arc development: Constraints from the Eastern coral sea," *Gondwana Research*, vol. 39, pp. 77–95, 2016.
- [27] DB. Dow, "A geological synthesis of papua New Guinea," *BMR Bull*, vol. 201, pp. 1–58, 1977.
- [28] J. Woodhead, J. Hergt, M. Sandiford, and W. Johnson, "The big crunch: Physical and chemical expressions of arc/continent collision in the Western bismarck arc," *Journal of Volcanology and Geothermal Research*, vol. 190, nos. 1–2, pp. 11–24, 2010.
- [29] ID. Lindley, "Extensional and vertical tectonics in the New Guinea islands: Implications for island arc evolution," in *Ann Geophys [Internet]*, G. Scalera, and G. Lavecchia, Eds., pp. 403–426, 2006.
- [30] J. K. Weissel, B. Taylor, and G. D. Karner, "The opening of the woodlark Basin, subduction of the woodlark spreading system, and the evolution of Northern melanesia since mid-pliocene time," *Tectonophysics*, vol. 87, nos. 1–4, pp. 253–277, 1982.
- [31] B. Taylor, A. Goodliffe, F. Martinez, and R. Hey, "Continental rifting and initial sea-floor spreading in the woodlark Basin," *Nature*, vol. 374, no. 6522, pp. 534–537, 1995.
- [32] P. A. Brandl, M. D. Hannington, J. Geersen, S. Petersen, and H.-H. Gennerich, "The submarine tectono-magmatic framework of cu-au endowment in the tabar-to-feni island chain, PNG," *Ore Geology Reviews*, vol. 121, p. 103491, 2020.
- [33] Stevens C, McCaffrey R, Silver EA, et al. Mid-crustal detachment and ramp faulting in the Markham Valley, Papua New Guinea. *Geology*. 1998;26:847.
- [34] C. DeMets, R. G. Gordon, D. F. Argus, and S. Stein, "Effect of recent revisions to the geomagnetic reversal time scale on estimates of current plate motions," *Geophysical Research Letters*, vol. 21, no. 20, pp. 2191–2194, 1994.
- [35] P. Bird, "An updated digital model of plate boundaries," *Geochemistry, Geophysics, Geosystems*, vol. 4, no. 3, p. 1027, 2003.
- [36] P. Tregoning, "Plate kinematics in the Western pacific derived from geodetic observations," *Journal of Geophysical Research*, vol. 107, no. B1, pp. 7–1, 2002.
- [37] P. Tregoning and A. Gorbatov, "Evidence for active subduction at the new Guinea trench," *Geophysical Research Letters*, vol. 31, no. 13, 2004.
- [38] R. Hall and W. Spakman, "Subducted slabs beneath the Eastern Indonesia–tonga region: Insights from tomography," *Earth and Planetary Science Letters*, vol. 201, no. 2, pp. 321–336, 2002.
- [39] L. M. Wallace, C. Stevens, E. Silver, et al., "GPS and seismological constraints on active tectonics and arc-continent collision in papua New Guinea: Implications for mechanics of microplate rotations in a plate boundary zone," *Journal of Geophysical Research*, vol. 109, no. B5, 2004.
- [40] L. M. Wallace, R. McCaffrey, J. Beavan, and S. Ellis, "Rapid microplate rotations and backarc rifting at the transition between collision and subduction," *Geology*, vol. 33, no. 11, 2005.
- [41] S. L. Baldwin, B. D. Monteleone, L. E. Webb, P. G. Fitzgerald, M. Grove, and E. June Hill, "Pliocene eclogite exhumation at plate tectonic rates in eastern papua New Guinea," *Nature*, vol. 431, no. 7006, pp. 263–267, 2004.
- [42] V. Bailly, M. Pubellier, J.-C. Ringenbach, J. de Sigoyer, and F. Sapin, "Deformation zone 'jumps' in a young convergent setting: The lengguru fold-and-thrust belt, New Guinea island," *Lithos*, vol. 113, nos. 1–2, pp. 306–317, 2009.
- [43] E. J. Phinney, P. Mann, M. F. Coffin, and T. H. Shipley, "Sequence stratigraphy, structural style, and age of deformation of the malaita accretionary prism (solomon arc–ontong java plateau convergent zone)," *Tectonophysics*, vol. 389, nos. 3–4, pp. 221–246, 2004.
- [44] B. Taylor, "Bismarck sea: Evolution of a backarc Basin," *Geology*, vol. 7, no. 4, 1979.

- [45] T. A. Little, S. L. Baldwin, P. G. Fitzgerald, and B. Monteleone, "Continental rifting and metamorphic core complex formation ahead of the woodlark spreading ridge, D'Entrecasteaux islands, Papua New Guinea," *Tectonics*, vol. 26, no. 1, 2007.
- [46] P. Tregoning, R. J. Jackson, H. McQueen, et al., "Motion of the South Bismarck Plate, Papua New Guinea," *Geophysical Research Letters*, vol. 26, no. 23, pp. 3517–3520, 1999.
- [47] J. J. Rytuba, E. H. McKee, and D. P. Cox, "Geochronology and geochemistry of the Ladolam gold deposit, Lihir Island, and gold deposits and volcanoes of Tabar and Tatau, Papua New Guinea," *US Geol Surv Bull*, vol. 2039, pp. 119–126, 1993.
- [48] P. Hollings, M. J. Baker, E. Orovan, and M. Rinne, "A special issue devoted to porphyry and epithermal deposits of the South West Pacific: An introduction," *Economic Geology*, vol. 113, no. 1, pp. 1–6, 2018.
- [49] N. J. Dyriw, S. E. Bryan, S. W. Richards, J. M. Parianos, R. J. Arculus, and D. A. Gust, "Morphotectonic analysis of the East Manus Basin, Papua New Guinea," *Frontiers in Earth Science*, vol. 8, pp. 43–23, 2021.
- [50] A. Vishiti, S. Petersen, C. E. Suh, and C. W. Devey, "Texture, mineralogy and geochemistry of hydrothermally altered submarine volcanics recovered South East of Cheshire Seamount, Western Woodlark Basin," *Marine Geology*, vol. 347, pp. 69–84, 2014.
- [51] P. J. Boulton, "A review of the petroleum potential of Papua New Guinea with a focus on the Eastern Papuan Basin and the pale sandstone as a potential reservoir fairway," *Geological Society, London, Special Publications*, vol. 126, no. 1, pp. 281–291, 2000.
- [52] A. D. Owen and J. C. Lattimore, "Oil and gas in Papua New Guinea," *Energy Policy*, vol. 26, no. 9, pp. 655–660, 1998.
- [53] M. O. Anderson, W. W. Chadwick, M. D. Hannington, et al., "Geological interpretation of volcanism and segmentation of the Mariana Back-Arc spreading center between 12.7°N and 18.3°N: GEOLOGY OF THE MARIANA BACK-ARC," *Geochem Geophys Geosystems*, vol. 18, pp. 2240–2274, 2017.
- [54] M. O. Anderson, M. D. Hannington, K. Haase, et al., "Tectonic focusing of voluminous basaltic eruptions in magma-deficient backarc rifts," *Earth and Planetary Science Letters*, vol. 440, pp. 43–55, 2016.
- [55] M. S. Stewart, M. D. Hannington, J. Emberley, et al., "A new geological map of the Lau Basin (South Western Pacific Ocean) reveals crustal growth processes in arc-backarc systems," *Geosphere*, vol. 17, p. 34, 2022.
- [56] D. T. Sandwell, R. D. Müller, W. H. F. Smith, E. Garcia, and R. Francis, "Marine geophysics. New global marine gravity model from Cryosat-2 and Jason-1 reveals buried tectonic structure," *Science (New York, N.Y.)*, vol. 346, no. 6205, pp. 65–67, 2014.
- [57] W. H. F. Smith and D. T. Sandwell, "Global sea floor topography from satellite altimetry and ship depth soundings," *Science*, vol. 277, no. 5334, pp. 1956–1962, 1997.
- [58] W. B. F. Ryan, S. M. Carbotte, J. O. Coplan, et al., "Global multi-resolution topography synthesis," *Geochemistry, Geophysics, Geosystems*, vol. 10, no. 3, pp. Q03014–n, 2009.
- [59] "NASA/METI/AIST/Japan Space Systems, U.S./Japan ASTER Science Team. ASTER Global Digital Elevation Model V003," *NASA EOSDIS Land Processes Distributed Active Archive Center*, 2019.
- [60] N. F. Exon and D. L. Tiffin, "Geology of offshore New Ireland Basin in Northern Papua New Guinea, and its petroleum prospects," *Trans Third Circum-Pac Energy Miner Resour Conf. Honolulu*, 623–630, 1984.
- [61] D. L. Tiffin, E. Honza, and J. Keene, "A multi-national, multi-parameter marine study of the Western Solomon Sea and region," *Geo-Marine Letters*, vol. 6, no. 4, pp. 175–180, 1986.
- [62] A. M. Goodliffe, B. Taylor, and F. Martinez, "Data report: Marine geophysical surveys of the Woodlark Basin region," *Ocean Drilling Program*, vol. vol, 1999.
- [63] W. Tufar, "Sonne 68 - OLGA II research cruise April 29 to June 25, 1990, preliminary cruise report," PANGAEA, Bremerhaven, 1990.
- [64] P. Herzig, M. Hannington, P. Stoffers, et al., "Tectonics, petrology and hydrothermal processes in areas of alkaline island-arc volcanoes in the South West Pacific: The Tabalhir-Tanga-Feni Island Chain, Papua New Guinea," *Cruise Report SONNE*, vol. 94, p. 27, 1994.
- [65] P. Herzig, et al., "Volcanism, hydrothermal processes and biological communities at shallow submarine volcanoes of the New Ireland fore-arc (Papua New Guinea)," *Cruise Report SONNE-133*, (BMBF FK 03G0133A). Vol. 10-August 10, PANGAEA, Manila - Kavieng - Rabaul - Suva. Bremerhaven, 1998.
- [66] P. M. Herzig, T. Kuhn, and S. Petersen, "Detailed investigation of the magmatic-hydrothermal gold mineralization at conical seamount (New Ireland Basin) and of massive sulfides at PACMANUS (Eastern Manus Basin), Papua New Guinea by shallow drilling: Cruise report - SO-166 CONDRILL -; [research cruise with R/V Sonne, cruise no. SO-166, Aug. 22, 2002 (San Francisco) - Sept. 13 (Rabaul/PNG) - Oct. 03 (Rabaul) - Oct. 11, 2002 (Suva/Fiji)]," 2024.
- [67] C. Devey, *FS Sonne Fahrtbericht / Cruise Report SO203: WOODLARK: Magma Genesis, Tectonics and Hydrothermalism in the WOODLARK Basin*, Townsville, Australia - Auckland, New Zealand, 2009.
- [68] W. Bach, *Report and Preliminary Results of RV SONNE Cruise SO 216, Townsville (Australia) - Makassar (Indonesia)*, Berichte Fachbereich Geowiss Univ Brem, 2011.
- [69] C. Berndt, S. Muff, I. Klauke, et al., "RV SONNE 252 cruise report / fahrtbericht, Yokohama: 05.11.2016 - Nouméa: 18.12.2016," in *SO252: RITTER ISLAND Tsunami potential of volcanic flank collapses [Internet]*, ARRAY(0x55df05d70910), Kiel, Germany, 2017.
- [70] F. Martinez and B. Taylor, "Backarc spreading, rifting, and microplate rotation, between transform faults in the Manus Basin," *Marine Geophysical Researches*, vol. 18, nos. 2–4, pp. 203–224, 1996.
- [71] N. P. Fofonoff, "Physical properties of seawater: A new salinity scale and equation of state for seawater," *Journal of Geophysical Research*, vol. 90, no. C2, pp. 3332–3342, 1985.
- [72] R. L. Carlson and G. S. Raskin, "Density of the ocean crust," *Nature*, vol. 311, no. 5986, pp. 555–558, 1984.
- [73] S. J. MacLeod, S. E. Williams, K. J. Matthews, R. D. Müller, and X. Qin, "A global review and digital database of large-scale extinct spreading centers," *Geosphere*, vol. 13, no. 3, pp. 911–949, 2017.
- [74] B. Meyer, A. Chulliat, and R. Saltus, "Derivation and error analysis of the Earth magnetic anomaly grid at 2 arc min

- resolution version 3 (emag2v3),” *Geochemistry, Geophysics, Geosystems*, vol. 18, no. 12, pp. 4522–4537, 2017.
- [75] B. Taylor, A. M. Goodliffe, and F. Martinez, “How continents break up: Insights from Papua New Guinea,” *Journal of Geophysical Research*, vol. 104, no. B4, pp. 7497–7512, 1999.
- [76] M. Joshima, Y. Okuda, F. Murakami, K. Kishimoto, and E. Honza, “Age of the Solomon sea Basin from magnetic lineations,” *Geo-Marine Letters*, vol. 6, no. 4, pp. 229–234, 1986.
- [77] J. K. Weissel and R.N. Anderson, “Is there a Caroline plate?,” *Earth and Planetary Science Letters*, vol. 41, no. 2, pp. 143–158, 1978.
- [78] G. Ekström, M. Nettles, and A.M. Dziewoński, “The global CMT project 2004–2010: Centroid-moment tensors for 13,017 earthquakes,” *Physics of the Earth and Planetary Interiors*, vols. 200–201, pp. 1–9, 2012.
- [79] A. M. Dziewoński, T. -A. Chou, and J. H. Woodhouse, “Determination of earthquake source parameters from waveform data for studies of global and regional seismicity,” *Journal of Geophysical Research*, vol. 86, no. B4, pp. 2825–2852, 1981.
- [80] C. Frohlich, “Triangle diagrams: Ternary graphs to display similarity and diversity of earthquake focal mechanisms,” *Physics of the Earth and Planetary Interiors*, vol. 75, nos. 1–3, pp. 193–198, 1992.
- [81] W.B. Hamilton, Internet, *Tectonics of the Indonesian Region*, United States Government Printing Office, Washington, 1979.
- [82] C. Ravenne, C. E. Broin, and F. Aubertin, “Structure et histoire de la région Salomon nouvelle-irlande. symp int Géodynamique sud-ouest pac.,” *Nouméa*, 1976.
- [83] N. F. Exon and M.S. Marlow, “Geology and offshore resource potential of the new Ireland-manus region—A synthesis,” in *Geol Offshore Resour Pac Isl Arcs - New Irel Manus Reg Papua N Guin [Internet]*, M.S. Marlow, S.V. Dadisman, and N.F. Exon, Eds., pp. 241–262, Circum-Pacific Council for Energy and Mineral Resources, Houston, 1988.
- [84] H.H. Gennerich, *Der Tabar-Feni-Inselbogen Und Sein Plattentektonisches Regime Oder Wie Entsteht Ein Inselbogen Ohne Eine Aktive Subduktionszone*, Bremen, 2001.
- [85] B. Ott and P. Mann, “Late miocene to recent formation of the aure-moresby fold-thrust belt and foreland Basin as a consequence of woodlark microplate rotation, Papua New Guinea,” *Geochem Geophys Geosystems*, vol. 16, pp. 1988–2004, 2015.
- [86] G. Francis, J. Lock, and Y. Okuda, “Seismic stratigraphy and structure of the area to the SouthEast of the trobriand platform,” *Geo-Marine Letters*, vol. 7, no. 3, pp. 121–128, 1987.
- [87] G. Fitz and P. Mann, “Tectonic uplift mechanism of the Goodenough and Ferguson island gneiss domes, eastern Papua New Guinea: Constraints from seismic reflection and well data,” *Geochemistry, Geophysics, Geosystems*, vol. 14, no. 10, pp. 3969–3995, 2013.
- [88] T. R. Bruns, J. H. Vedder, and A.K. Cooper, “Geology of the Shortland Basin region, central Solomons trough, Solomon Islands—review and new findings,” in *Geol Offshore Resour Pac Isl Arcs - Solomon Isl Bougainville Papua N Guin Reg [Internet]*, J.G. Vedder, and T.R. Bruns, Eds., Available from: pp. 125–144, Circum-Pacific Council for Energy and Mineral Resources, Earth Science Series, Houston, 1989.
- [89] S. Cowley, P. Mann, M. F. Coffin, and T. H. Shipley, “Oligocene to recent tectonic history of the Central Solomon intra-arc Basin as determined from marine seismic reflection data and compilation of onland geology,” *Tectonophysics*, vol. 389, nos. 3–4, pp. 267–307, 2004.
- [90] A. Taira, P. Mann, and R. Rahardiawan, “Incipient subduction of the Ontong Java plateau along the North Solomon trench,” *Tectonophysics*, vol. 389, nos. 3–4, pp. 247–266, 2004.
- [91] D. L. Erlandson, T. L. Orwig, G. Kiilgaard, J. H. Mussells, and L. W. Kroenke, “Tectonic interpretations of the East Caroline and Lyra Basins from reflection-profiling investigations,” *Geological Society of America Bulletin*, vol. 87, no. 3, 1976.
- [92] K. Shimizu, T. Sano, M. L. G. Tejada, et al, “Alkalic magmatism in the Lyra Basin: A missing link in the late-stage evolution of the Ontong Java plateau...,” *Internet Geological Society of America*, 2015.
- [93] R.W. Johnson, “Geotectonics and volcanism in Papua New Guinea: A review of the late Cenozoic,” *BMR J Aust Geol Geophys*, vol. 4, pp. 181–207, 1979.
- [94] E. M. A. Murphy and A. Salvador, *International Subcommission on Stratigraphic Classification of IUGS International Commission on Stratigraphy*, 1999.
- [95] A. Salvador, “International stratigraphic guide,” *The International Union of Geological Sciences*, 1994.
- [96] J. Thal, M. Tivey, D. Yoerger, N. Jöns, and W. Bach, “Geologic setting of Pacmanus hydrothermal area — high resolution mapping and in situ observations,” *Marine Geology*, vol. 355, pp. 98–114, 2014.
- [97] P. Bouysse, *Geological Map of the World – Explanatory Notes*. 3e éd, CCGM/CGMW, Paris, 2014.
- [98] B. Peucker-Ehrenbrink and M.W. Miller, “Quantitative bedrock geology of East and SouthEast Asia (Brunei, Cambodia, Eastern and Southeastern China, East Timor),” *Geochem Geophys Geosystems*, vol. 5, 2004.
- [99] B. Peucker-Ehrenbrink and M.W. Miller, “Quantitative bedrock geology of Alaska and Canada,” *Geochem Geophys Geosystems*, vol. 4, pp. 1–10, 2003.
- [100] K. C. Hill, R. D. Kendrick, P. V. Crowhurst, and P. A. Gow, “Copper-gold mineralisation in New Guinea: tectonics, lineaments, thermochronology and structure,” *Australian Journal of Earth Sciences*, vol. 49, no. 4, pp. 737–752, 2002.
- [101] R. J. Arculus, R. W. Johnson, B. W. Chappell, C. O. McKee, and H. Sakai, “Ophiolite-contaminated andesites, trachybasalts, and cognate inclusions of Mount Lamington, Papua New Guinea: Anhydrite-amphibole-bearing lavas and the 1951 cumulo-dome,” *Journal of Volcanology and Geothermal Research*, vol. 18, nos. 1–4, pp. 215–247, 1983.
- [102] World Resources Institute, *Global Distribution of Coral Reefs*, 2024.
- [103] H. L. Davies, P. A. Symonds, and I.D. Ripper, “Structure and evolution of the Southern Solomon sea region,” *BMR J Aust Geol Geophys*, vol. 9, pp. 46–68, 1984.
- [104] E. J. Hill and S. L. Baldwin, “Exhumation of high-pressure metamorphic rocks during crustal extension in the D’Entrecasteaux region, Papua New Guinea,” *Journal of Metamorphic Geology*, vol. 11, no. 2, pp. 261–277, 1993.

- [105] S. L. Baldwin, L. E. Webb, and B. D. Monteleone, "Late miocene coesite-eclogite exhumed in the woodlark rift," *Geology*, vol. 36, no. 9, 2008.
- [106] R. Rogerson, D. B. Hilyard, E. J. Finlayson, et al, "The geology and mineral resources of bougainville and buka islands, papua new guinea," *Port Moresby: Geological Survey of Papua New Guinea*, 1989.
- [107] D. H. Blake and Y. Miezitis, "Geology of bougainville and buka islands, new Guinea," *Rec Bur Miner Resour Geol Geophys*, vol. 93, pp. 1–77, 1967.
- [108] D. Lindley, "Early cainozoic stratigraphy and structure of the gazelle peninsula, East new britain: An example of extensional tectonics in the new britain arc-trench complex," *Australian Journal of Earth Sciences*, vol. 35, no. 2, pp. 231–244, 1988.
- [109] PD. Hohnen, "Geology of new Ireland, papua new Guinea.," *BMR Bulletin*, vol. vol, 1978.
- [110] W. D. Stewart and MJ. Sandy, "Geology of new Ireland and djaul islands, NorthEastern papua new Guinea," in *Geol Offshore Resour Pac Isl Arcs - New Irel Manus Reg Papua N Guin [Internet]*, M.S. Marlow, S.V. Dadisman, and N.F. Exon, Eds., pp. 13–30, Circum-Pacific Council for Energy and Mineral Resources, Houston, 1988.
- [111] R. J. Wysoczanski, E. Todd, I. C. Wright, et al., "Backarc rifting, constructional volcanism and nascent disorganised spreading in the Southern havre trough backarc rifts (SW pacific)," *Journal of Volcanology and Geothermal Research*, vol. 190, nos. 1–2, pp. 39–57, 2010.
- [112] KC. Macdonald, "Mid-ocean ridge tectonics, volcanism and geomorphology," *Encyclopedia of Ocean Sciences*, vol. vol, pp. 1798–1813, 2001.
- [113] P. Llanes, E. Silver, S. Day, and G. Hoffman, "Interactions between a transform fault and arc volcanism in the bismarck sea, papua new Guinea," *Geochemistry, Geophysics, Geosystems*, vol. 10, no. 6, 2009.
- [114] ML. Cameron, "Rifting and subduction in the papuan peninsula, papua new guinea: the significance of the trobriand trough, the nubara strike-slip fault, and the woodlark \ldots.," Internet, 2014.
- [115] G. Zhang, J. Zhang, S. Wang, and J. Zhao, "Geochemical and chronological constraints on the mantle plume origin of the caroline plateau," *Chemical Geology*, vol. 540, 2020.
- [116] S. Altis, "Origin and tectonic evolution of the caroline ridge and the sorol trough, Western tropical pacific, from admittance and a tectonic modeling analysis," *Tectonophysics*, vol. 313, no. 3, pp. 271–292, 1999.
- [117] H. F. Ryan and MS. Marlow, "Multichannel seismic-reflection data collected at the intersection of the mussau and manus trenches, papua new guinea," in *Geol Offshore Resour Pac Isl Arcs - New Irel Manus Reg Papua N Guin [Internet]*, M.S. Marlow, S.V. Dadisman, and N.F. Exon, Eds., pp. 203–203, Circum-Pacific Council for Energy and Mineral Resources, Houston, 1988.
- [118] D. F. Argus, R. G. Gordon, and C. DeMets, "Geologically current motion of 56 plates relative to the no-net-rotation reference frame," *Geochemistry, Geophysics, Geosystems*, vol. 12, no. 11, 2011.
- [119] G. Zhang, J. Yao, F. Xu, T. Wu, C.-F. Li, and S. Wang, "Origin of the mussau trench in the Western pacific: Geochemical and mineralogical constraints from basalts and serpentinitized peridotites," *Chemical Geology*, vol. 642, 2023.
- [120] K. A. Hegarty, J. K. Weissel, and DE. Hayes, *Convergence at the Caroline- Pacific Plate Boundary: Collision and Subduction. Tecton Geol Evol Southeast Asian Seas Isl Part 2*, American Geophysical Union (AGU), 1983.
- [121] R. Speckbacher, J. H. Behrmann, T. J. Nagel, M. Stipp, and J. Mahlke, "Fluid flow and metasomatic fault weakening in the moresby seamount detachment, woodlark basin, offshore papua new Guinea," *Geochemistry, Geophysics, Geosystems*, vol. 13, no. 11, 2012.
- [122] J. Chadwick, M. Perfit, B. McInnes, et al., "Arc lavas on both sides of a trench: Slab window effects at the Solomon islands triple junction, SW pacific," *Earth and Planetary Science Letters*, vol. 279, nos. 3–4, pp. 293–302, 2009.
- [123] T. P. Gladchenko, M. F. Coffin, and O. Eldholm, "Crustal structure of the ontong java plateau: Modeling of new gravity and existing seismic data," *Journal of Geophysical Research*, vol. 102, no. B10, pp. 22711–22729, 1997.
- [124] J. G. Fitton, J. J. Mahoney, P. J. Wallace, and A. D. Saunders, "Origin and evolution of the ontong java plateau: Introduction," *Geological Society, London, Special Publications*, vol. 229, no. 1, pp. 1–8, 2004.
- [125] M. L. G. Tejada, K. Shimizu, K. Suzuki, et al, "Isotopic evidence for a link between the lyra basin and ontong java plateau," *Geological Society of America*, 2015.
- [126] T. Hanyu, M. L. G. Tejada, K. Shimizu, et al., "Collision-induced post-plateau volcanism: Evidence from a seamount on ontong java plateau," *Lithos*, vols. 294–295, pp. 87–96, 2017.
- [127] J. J. Mahoney, M. Storey, R. A. Duncan, et al, "Geochemistry and geochronology of leg 130 basement lavas: Nature and origin of the ontong java plateau," *Proc Sci Results ODP Leg 130 Ontong Java Plateau*, vol. vol, pp. 3–22, 1993.
- [128] A. S. Furumoto, D. M. Hussong, J. F. Campbell, et al, "Crustal and upper mantle structure of the Solomon islands as revealed by seismic refraction survey of november-december 1966," *Pac Sci*, vol. 24, pp. 315–332, 1970.
- [129] S. Tapster, N. M. W. Roberts, M. G. Petterson, A. D. Saunders, and J. Naden, "From continent to intra-oceanic arc: Zircon xenocrysts record the crustal evolution of the Solomon island arc," *Geology*, vol. 42, no. 12, pp. 1087–1090, 2014.
- [130] R. J. Holm, C. Spandler, and SW. Richards, "Continental collision, orogenesis and arc magmatism of the miocene maramuni arc, papua new Guinea," *Gondwana Research*, vol. 28, no. 3, pp. 1117–1136, 2015.
- [131] P. Mann, F. W. Taylor, M. B. Lagoe, A. Quarles, and G. Burr, "Accelerating late quaternary uplift of the new georgia island group (Solomon island arc) in response to subduction of the recently active woodlark spreading center and coleman seamount," *Tectonophysics*, vol. 295, nos. 3–4, pp. 259–306, 1998.
- [132] E. T. Baker, G. J. Massoth, C. E. J. de Ronde, J. E. Lupton, and B. I. A. McInnes, "Observations and sampling of an ongoing subsurface eruption of kavachi volcano, Solomon islands, may 2000," *Geology*, vol. 30, no. 11, 2002.
- [133] R. J. Holm and SW. Richards, "A re-evaluation of arc-continent collision and along-arc variation in the bismarck sea region, papua new Guinea," *Australian Journal of Earth Sciences*, vol. 60, no. 5, pp. 605–619, 2013.
- [134] S.-M. Lee and E. Ruellan, "Tectonic and magmatic evolution of the bismarck sea, papua new Guinea: Review and new

- synthesis,” in *Geophys Monogr Ser 166 [Internet]*, D.M. Christie, C.R. Fisher, and S.-M. Lee, Eds., pp. 263–286, American Geophysical Union, Washington, D. C, 2006.
- [135] J. Karstens, C. Berndt, M. Urlaub, et al., “From gradual spreading to catastrophic collapse – reconstruction of the 1888 ritter island volcanic sector collapse from high-resolution 3D seismic data,” *Earth and Planetary Science Letters*, vol. 517, pp. 1–13, 2019.
- [136] J. D. Woodhead, S. M. Eggins, and RW. Johnson, “Magma genesis in the new britain island arc: Further insights into melting and mass transfer processes,” *Journal of Petrology*, vol. 39, no. 9, pp. 1641–1668, 1998.
- [137] RW. Johnson, “Potassium variation across the new britain volcanic arc,” *Earth and Planetary Science Letters*, vol. 31, no. 1, pp. 184–191, 1976.
- [138] J. D. Woodhead and RW. Johnson, “Isotopic and trace-element profiles across the new britain island arc, papua new Guinea,” *Contributions to Mineralogy and Petrology*, vol. 113, no. 4, pp. 479–491, 1993.
- [139] R. W. Johnson, J. C. Mutter, and RJ. Arculus, “Origin of the willaumez-manus rise, papua new Guinea,” *Earth and Planetary Science Letters*, vol. 44, no. 2, pp. 247–260, 1979.
- [140] G. P. Whitmore, K. A. W. Crook, and D. P. Johnson, “Sedimentation in a complex convergent margin: The papua new Guinea collision zone of the Western Solomon sea,” *Marine Geology*, vol. 157, nos. 1–2, pp. 19–45, 1999.
- [141] E. Honza, T. Miyazaki, and J. Lock, “Subduction erosion and accretion in the Solomon sea region,” *Tectonophysics*, vol. 160, nos. 1–4, pp. 49–62, 1989.
- [142] D. L. Tiffin, H. L. Davies, E. Honza, J. Lock, and Y. Okuda, “The new britain trench and 149° embayment, Western Solomon sea,” *Geo-Marine Letters*, vol. 7, no. 3, pp. 135–142, 1987.
- [143] LD. Abbott, “Neogene tectonic reconstruction of the adelbert-finisterre-new britain collision, Northern papua new Guinea,” *Journal of Southeast Asian Earth Sciences*, vol. 11, no. 1, pp. 33–51, 1995.
- [144] R. W. Johnson and IE. Smith, “Volcanoes and rocks of st andrew strait, papua new Guinea,” *Journal of the Geological Society of Australia*, vol. 21, no. 3, pp. 333–351, 1974.
- [145] K. Brooks and C. Tegner, “Affinity if the leg 180 dolerites of the woodlark Basin: Geochemistry and age,” *Proc Ocean Drill Program Sci Results*, vol. 180, pp. 1–18, 2001.
- [146] B. Monteleone, S. L. Baldwin, T. R. Ireland, et al, “Thermo-chronological constraints for the tectonic evolution of the moresby seamount, woodlark Basin, papua new Guinea,” *Proceeding Ocean Drill Progrm Sci Results*, vol. 180, pp. 1–35, 2001.
- [147] W. Y. Lus, I. McDougall, and HL. Davies, “Age of the metamorphic sole of the papuan ultramafic belt ophiolite, papua new Guinea,” *Tectonophysics*, vol. 392, nos. 1–4, pp. 85–101, 2004.
- [148] V. S. Kamenetsky, A. V. Sobolev, S. M. Eggins, A. J. Crawford, and R. J. Arculus, “Olivine-enriched melt inclusions in chromites from low-ca boninites, cape vogel, papua new Guinea: Evidence for ultramafic primary magma, refractory mantle source and enriched components,” *Chemical Geology*, vol. 183, nos. 1–4, pp. 287–303, 2002.
- [149] IEM. Smith, “The chemical characterization and tectonic significance of ophiolite terrains in SouthEastern papua new Guinea,” *Tectonics*, vol. 32, no. 2, pp. 159–170, 2013.
- [150] L. E. Webb, S. L. Baldwin, and PG. Fitzgerald, “The early-middle miocene subduction complex of the lousiade archipelago, Southern margin of the woodlark rift,” *Geochemistry, Geophysics, Geosystems*, vol. 15, no. 10, pp. 4024–4046, 2014.
- [151] J. Galewsky and E. A. Silver, “Tectonic controls on facies transitions in an oblique collision: The western Solomon sea, papua new Guinea,” *Geological Society of America Bulletin*, vol. 109, no. 10, pp. 1266–1278, 1997.
- [152] M. S. Marlow, N. F. Exon, H. F. Ryan, et al, “Offshore structure and stratigraphy of new Ireland Basin in Northern papua new Guinea,” in *Geol Offshore Resour Pac Isl Arcs - New Irel Manus Reg Papua N Guin [Internet]*, M.S. Marlow, S.V. Dadisman, and N.F. Exon, Eds., pp. 137–155, Circum-Pacific Council for Energy and Mineral Resources, Houston, 1988.
- [153] T. A. Little, B. R. Hacker, S. M. Gordon, et al., “Diapiric exhumation of earth’s youngest (UHP) eclogites in the gneiss domes of the D’Entrecasteaux islands, papua new Guinea,” *Tectonophysics*, vol. 510, nos. 1–2, pp. 39–68, 2011.
- [154] M. Pubellier, C. Monnier, R. Maury, and R. Tamayo, “Plate kinematics, origin and tectonic emplacement of supra-subduction ophiolites in SE Asia,” *Tectonophysics*, vol. 392, nos. 1–4, pp. 9–36, 2004.
- [155] H. L. Davies and I. E. Smith, “Geology of Eastern papua,” *Geological Society of America Bulletin*, vol. 82, no. 12, 1971.
- [156] S. A. Whattam, J. Malpas, J. R. Ali, and I. E. M. Smith, “New SW pacific tectonic model: Cyclical intraoceanic magmatic arc construction and near-coeval emplacement along the Australia-pacific margin in the cenozoic,” *Geochemistry, Geophysics, Geosystems*, vol. 9, no. 3, 2008.
- [157] P. V. Crowhurst, R. Maas, K. C. Hill, D. A. Foster, and C. M. Fanning, “Isotopic constraints on crustal architecture and permotriassic tectonics in new Guinea: Possible links with Eastern Australia,” *Australian Journal of Earth Sciences*, vol. 51, no. 1, pp. 107–124, 2004.
- [158] A. McCarthy, L. Magri, I. Sauermilch, et al, “The lousiade ophiolite: A missing link in the Western pacific,” *Terra Nova*, vol. 34, no. 2, pp. 146–154, 2022.
- [159] H. Doust and RA. Noble, “Petroleum systems of Indonesia,” *Marine and Petroleum Geology*, vol. 25, no. 2, pp. 103–129, 2008.
- [160] P. Tregoning, F. Tan, J. Gilliland, H. McQueen, and K. Lambeck, “Present-day crustal motion in the Solomon islands from GPS observations,” *Geophysical Research Letters*, vol. 25, no. 19, pp. 3627–3630, 1998.
- [161] J. Biemiller, C. Boulton, L. Wallace, et al., “Mechanical implications of creep and partial coupling on the world’s fastest slipping low-angle normal fault in SouthEastern papua new Guinea,” *Journal of Geophysical Research*, vol. 125, no. 10, 2020.
- [162] A. Koulali, P. Tregoning, S. McClusky, R. Stanaway, L. Wallace, and G. Lister, “New insights into the present-day kinematics of the Central and Western papua new Guinea from GPS,” *Geophysical Journal International*, vol. 202, no. 2, pp. 993–1004, 2015.

- [163] P. Tregoning, H. McQueen, K. Lambeck, et al., "Present-day crustal motion in Papua New Guinea," *Earth, Planets and Space*, vol. 52, no. 10, pp. 727–730, 2000.
- [164] L. M. Wallace, S. Ellis, T. Little, et al., "Continental breakup and UHP rock exhumation in action: GPS results from the Woodlark rift, Papua New Guinea," *Geochem Geophys Geosystems*, vol. 15, pp. 4267–4290, 2014.
- [165] K. Chen, C. Milliner, and J.-P. Avouac, "The Weitin fault, Papua New Guinea, ruptured twice by Mw 8.0 and Mw 7.7 earthquakes in 2000 and 2019," *Geophysical Research Letters*, vol. 46, pp. 12833–12840, 2019.
- [166] Y. Liu, S. Li, S. Jiang, et al., "Origin of microplates under oblique subduction system in New Guinea: Inferences from gravity and magnetic data," *Gondwana Research*, vol. 120, pp. 175–189, 2023.
- [167] Y. Yu, F. Tilmann, S. S. Gao, K. H. Liu, and J. Xi, "Insights into initial continental rifting of marginal seas from seismic evidence for slab relics in the mid-mantle of the Woodlark rift, southwestern Pacific," *Geology*, vol. 51, no. 12, pp. 1117–1121, 2023.
- [168] I. M. Artemieva, "Backarc Basins: A global view from geophysical synthesis and analysis," *Earth-Science Reviews*, vol. 236, p. 104242, 2023.
- [169] P. Billingsley and A. Locke, "Structure of ore deposits in the continental framework," *Trans Am Inst Min Eng*, vol. 144, pp. 9–64, 1941.
- [170] E. O'Driscoll, "Observations of the lineament-ore relation," *Philosophical Transactions of the Royal Society of London. Series A, Mathematical and Physical Sciences*, vol. 317, no. 1539, pp. 195–218, 1986.
- [171] J. P. Richards, A. J. Boyce, and M. S. Pringle, "Geologic evolution of the Escondida area, Northern Chile: A model for spatial and temporal localization of porphyry Cu mineralization," *Economic Geology*, vol. 96, no. 2, pp. 271–305, 2001.
- [172] G. D. Carman, "Geology, mineralization, and hydrothermal evolution of the Ladolam gold deposit, Lihir Island, Papua New Guinea," in *Soc Econ Geol Spec Publ*, S. F. Simmons, and I. Graham, Eds., pp. 247–284, Littleton, 2003.
- [173] D. R. Cooke, S. Sykora, E. Lawlis, et al., "Lihir alkalic epithermal gold deposit, Papua New Guinea," *Soc Econ Geol Spec Publ*, vol. Available from, 2020.
- [174] M. D. Hannington, C. Ronde, and S. Petersen, "Sea-floor tectonics and submarine hydrothermal systems," *Economic Geology and the Bulletin of the Society of Economic Geologists*, vol. 100th Anniversary Volume, pp. 111–141, 2005.
- [175] T. Monecke, S. Petersen, M. D. Hannington, et al., "The minor element endowment of modern sea-floor massive sulfides and comparison with deposits hosted in ancient volcanic successions. Rare earth critical element ore deposits," *Society of Economic Geologists*, 2016.
- [176] J. M. Hammarstrom, A. A. Bookstrom, and C. L. Dicken, "Chapter D in global mineral resource assessment," Internet in *Porphyry Copper Assessment of Southeast Asia and Melanesia*, 2013.
- [177] J. F. Dewey and B. F. Windley, "Growth and differentiation of the continental crust," *Philosophical Transactions of the Royal Society of London. Series A, Mathematical and Physical Sciences*, vol. 301, no. 1461, pp. 189–206, 1981.
- [178] C. J. Hawkesworth, P. A. Cawood, and B. Dhuime, "The evolution of the continental crust and the onset of plate tectonics," *Frontiers in Earth Science*, vol. 8, 2020.
- [179] C.-T. A. Lee, D. M. Morton, R. W. Kistler, and A. K. Baird, "Petrology and tectonics of Phanerozoic continent formation: From island arcs to accretion and continental arc magmatism," *Earth and Planetary Science Letters*, vol. 263, nos. 3–4, pp. 370–387, 2007.
- [180] D. E. Karig, "Physical properties and mechanical state of accreted sediments in the Nankai Trough, Southwest Japan arc. Geol Soc Am Mem.," *Geological Society of America*, 1986.
- [181] J. M. A. Hronsky, D. I. Groves, R. R. Loucks, and G. C. Begg, "A unified model for gold mineralisation in accretionary orogens and implications for regional-scale exploration targeting methods," *Mineralium Deposita*, vol. 47, no. 4, pp. 339–358, 2012.
- [182] R. H. Sillitoe, "Special paper: Major gold deposits and belts of the North and South American Cordillera: Distribution, tectonomagmatic settings, and metallogenic considerations," *Economic Geology*, vol. 103, no. 4, pp. 663–687, 2008.
- [183] J. P. Richards, "Postsubduction porphyry Cu-Au and epithermal Au deposits: Products of remelting of subduction-modified lithosphere," *Geology*, vol. 37, no. 3, pp. 247–250, 2009.
- [184] M. Seton, J. M. Whittaker, P. Wessel, et al., "Community infrastructure and repository for marine magnetic identifications," *Geochemistry, Geophysics, Geosystems*, vol. 15, no. 4, pp. 1629–1641, 2014.